MULTIVARIABLE FEEDBACK DESIGN BY SHAPING SINGULAR VALUES

by

Christophe Jacques Pagezy

Diplôme d'Ingenieur de l'Ecole Supèrieure d'Electricitè
(1981)

SUBMITTED TO THE DEPARTMENT OF
ELECTRICAL ENGINEERING AND COMPUTER SCIENCE
IN PARTIAL FULFILLMENT OF THE REQUIREMENTS
FOR THE DEGREE OF

MASTER OF SCIENCE

at the

MASSACHUSETTS INSTITUTE OF TECHNOLOGY

May 1982

Signature redacted

Signature of Author.....
Department of Electrical Engineering and Computer Science,
May 7, 1982

Signature redacted

Certified by.....
Thesis Supervisor

Signature redacted

Accepted by.....
Arthur C. Smith
Chairman, Department Graduate Committee

MULTIVARIABLE FEEDBACK DESIGN BY

SHAPING SINGULAR VALUES

by

Christophe Jacques Pagezy

Submitted to the Department of Electrical Engineering and Computer Science on May 7, 1982 in partial filfillment of the requirements for the Degree of Master of Science

ABSTRACT

Singular value analysis plays an essential role in linear multivariable feedback design. In addition to the closed-loop stability, the design requirements can be expressed in terms of the singular values of the loop transfer function. Some existing frequency domain diagonalization design methods are evaluated in terms of the design requirements and are shown to be restricted in their applicability. By using the properties of the singular value decomposition of a system, a new frequency domain diagonalization design method is derived. This method is simple and can be used to meet the design requirements. An example shows the applicability of this design method.

The satisfaction of the design requirement by using the linear quadratic methodology is discussed. By considering specific choices of frequency dependent quadratic weights, a systematic way of shaping the singular values of the loop transfer function is described.

Thesis Supervisor: Dr. Bernard C. Levy

Title: Assistant Professor of Electrical Engineering

ACKNOWLEDGEMENTS

I would like to thank my advisor, Professor Bernard Levy for his guidance throughout the course of this research. His thorough and painstaking reading and rereading of several drafts of this thesis and his valuable suggestions for its improvement are gratefully acknowledged.

I am also grateful to the Ecole Superieure d' Electricite for allowing me to complete my third year of studies at MIT.

My deepest thanks goes to all members of my family, particularly my parents for their moral support. Last, but not least, I wish to say thanks to Dom for all of her understanding. Without her unfailing encouragement, the completion of this work would have been impossible.

TABLE OF CONTENTS

TABLE OF CONTENTS (cont'd)

TABLE OF CONTENTS (cont'd)

LIST OF FIGURES

LIST OF FIGURES (cont'd)

CHAPTER 1: INTRODUCTION

1.1 Motivation

The importance of using feedback in control system engineering has long been recognized by designers as a way of achieving some of the following design objectives:

(i) Stabilization of an unstable system

(ii) Achievement of performance criteria such as a specified transient response and/or frequency response characteristics.

(iii) Reduction of the system response to noise.

However, an important issue in feedback control system design is the presence of model uncertainties. Indeed, any model is at best an approximation of reality and the relatively low order linear time invariant models most often used for controller synthesis are bound to be rather crude approximations. More precisely, there is a certain range of inputs typically bounded in amplitude and in frequency for which the model is a reasonable approximation of the given system. Outside this range, due to neglected nonlinearities and dynamic effects, the model and the true system may behave in drastically different ways. The principal danger occuring is that the design operating with the true system may become unstable. In the language of control theory, we must design a robust feedback control system where the term robustness refers to the extent to which variations from the nominal design model can occur without destabilizing the overall closed-loop feedback system.

In classical single-input single-output design, robustness issues

are well understood and are often specified in terms of gain margin and phase margin requirements. However, for multiple-input multiple-output (MIMO) systems, similar robustness measures are not straightforward. A major progress in the study of these problems was the work of Lethomaki [3], which introduces various robustness tests defined in terms of the singular values of the nominal open-loop system transfer function, when the nominal closed-loop system is stable. However, the robustness properties of feedback systems cannot be optimized without considering the deterministic and stochastic performance objectives of the control system. For open-loop stable systems, this is clearly demonstrated since the most robust control system is the open-loop system with no feedback. Of course, for this open-loop system the transient response to a step input command or the response to disturbances may not meet the performance specifications. This underscores the fact that there exists a fundamental tradeoff between robustness and deterministic and stochastic performance.

For single-input single-output (SISO) control systems these issues are well understood. The classical frequency domain techniques for SISO design naturally handle the robustness characterization. These techniques employ various graphical means (e.g. Bode, Nyquist, Nichols diagrams) for displaying the system model in terms of its frequency response. From these plots, it is easy to determine the minimum change in model frequency response that leads to instability and also to estimate the system transient response for various inputs. Thus,

classical control system designers can observe the fundamental tradeoffs that must be made from these plots.

This is in contrast to the multiple-input multiple-output (MIMO) case where these tradeoffs are not clear. Many design techniques for MIMO systems such as pole placement, state-space or frequency domain methods ignore partially or even completely the robustness issue. This is merely due to the fact that these design techniques do not use analytical tools for which robustness tests are available; in particular, they do not use the singular values of the open-loop transfer function [1], [3]. However, the classical SISO formulation of the feedback design problem in the face of uncertainties can be generalized easily to multiple-input multiple-output (MIMO) systems. Considering the singular value decomposition of the open-loop transfer function, we can obtain some MIMO generalizations of the classical Bode gain/phase constraints which limits ultimate performance of feedback in the face of uncertainties. More specifically, as shown in [1], the fundamental tradeoff between robustness and deterministic and stochastic performance imposes design constraints on the singular values of the open-loop transfer function. Thus, a useful perspective for the design of multivariable feedback systems will be to

(i) stabilize the nominal closed-loop system

(ii) shape the singular values of the open-loop transfer function as function of the frequency, in order to satisfy the robustness/performances tradeoff.

This will constitute the multivariable feedback design approach taken in this thesis. This approach is very similar in nature to that of Doyle and Stein in [1]. Design constraints on the singular values requires sound engineering judgement about the nature of modelling errors based on the physics of the controlled system. This is far from trivial in practical applications. However, it is hoped that practical experience with physical systems may provide further insight into how to specify design constraints since engineering knowledge about modelling errors is not always easily interpreted in terms of singular values.

Our multivariable design approach gives us a way to evaluate MIMO - design procedures. Indeed, engineers who design multivariable control system can use several methods. Depending on the problem they want to solve, they use "their engineering good sense" to select the design method that seems the most appropriate. However, this choise of design method is not perfectly rational. This motivates the need for a clearer view of what is common to existing design methods and what makes them different. A significant part of this thesis is devoted to evaluating several MIMO design procedures and their ability to meet design requirements.

In addition, a useful approach to multivariable feedback design corresponds to methods that diagonalize MIMO systems. This allows to employ classical SISO design techniques and thus to simplify the MIMO design problem. Unfortunately, existing frequency domain MIMO diagonalization techniques do not ensure stability for a sufficiently large

class of modelling errors. This motivates the need for a more satisfactory frequency domain diagonalization technique that allows the singular values to be shaped as a function of frequency.

1.2 Thesis Organization

This thesis is organized as follows:

In Chapter 2 we first review some preliminary definitions and properties of the singular values of a matrix. Then we show the importance of singular values in control by introducing a design perspective in terms of the singular values of the loop transfer function. We also give some special attention to how closed loop stability can be achieved. This presentation exposes what are the desirable features of multivariable feedback design methods. We then turn our attention on some presently available design methods. We first discuss frequency-domain based design methods which diagonalize MIMO systems, i.e. the "Characteristic Loci" and the "Inverse Nyquist Array" methods. Then we present the time-domain based design methods by exposing the main features of the Linear Quadratic approach. Since these design methods are well known to control designers, our presentation will be concise and we will focus mainly on the design philosophy used for each of these methods.

In Chapter 3, we study frequency-domain diagonalization techniques. We first evaluate existing diagonalization methods in terms of their ability to shape the singular values of the open loop transfer function. It is shown that this will be the case only for a restricted class of systems. This leads us to consider an alternative compensator structure

based on the singular value decomposition of the nominal plant model which allows the singular values of the open loop transfer function to be shaped at the plant input as well as at the plant output. Further results on the singular value decomposition of the plant model allows us to develop a Nyquist stability criterion for the closed loop system with our compensator structure. The implementation of the compensator is then considered. It reduces to an approximation problem. A trivial approximation algorithm is introduced and leads to the development of a design procedure appropriate to meet the design requirements. However, this design procedure may be limited by its approximating scheme. The approximation problem is then discussed in more detail. An approximation scheme consisting of an interpolation algorithm followed by an optimal model order reduction technique is developed. This leads to an alternative design procedure.

In Chapter 4, we study the time-domain based design methods. A review of the Linear Quadratic methodology shows how the quadratic weights can be chosen for shaping the singular values. However, it appears that the flexibility in the choice of the singular values of the loop transfer function is constrained by the lack of dynamics in the Linear Quadratic feedback loop. This motivates an alternative method of design [29] derived from the systematic Linear Quadratic dynamic compensation by Gupta [12]. Special choices of the frequency dependent weight matrices are studied. This results in methods that allow to shape the singular values of the loop transfer function with frequency.

The Chapter 5 gives an application example of the design procedure described in Chapter 3. The successive steps of the design procedure are applied to the CH. 47 helicopter. Some comments on different issues (approximations, performance/robustness tradeoff) arising in this design approach are presented. This gives an illustration of our design procedure and will show its applicability.

The Chapter 6 consists of conclusions and suggests directions for future research.

1.3 Thesis Contributions

The main contributions of this thesis are:

(1) The unification of existing multivariable feedback design methods by evaluating them under a common perspective of design.

(2) The development of a new diagonalization approach adequate to meet the design requirements and avoiding the basic flaws of existing frequency domain diagonalization techniques.

(3) A discussion of the impact of approximation problems on control systems design.

(4) A discussion of linear quadratic methods from the point of view of singular value shaping.

The results of this thesis summarize and extend the state of the art on multivariable feedback design by formulating the design problem as a singular value shaping problem.

1.4 Notation

SISO	single-input single-output
MIMO	multiple-input multiple-output
LQ	linear quadratic
LQG	linear quadratic gaussian
CL	characteristic loci
INA	inverse nyquist array
LTI	linear time invariant
SVD	singular value decomposition
A^H	complex conjugate transpose of the matrix A
A^T	transpose of the matrix A
A^{-1}	inverse of the matrix A
I	identity matrix
det A	determinant of A
$\text{diag}[k_1,\ldots k_n]$	diagonal matrix of diagonal elements $k_1,\ldots,k_n$
C	the complex numbers
IR	the real numbers
$\|\cdot\|_p$	p^{th} order norm
$\lambda_i(A)$	i^{th} eigenvalue of A
$\sigma_i(A)$	i^{th} singular value of A
$\sigma_{max}(A)$	largest singular value of A
$\sigma_{min}(A)$	smallest singular value of A
$\underline{X}$	vector X
j	$\sqrt{-1}$

$\bar{a}$	complex conjugate of the scalar a
$\|a\|$	magnitude of the scalar a
$\prod_{i=1}^{n} \alpha_i$	the product $(\alpha_1 \alpha_2 \ldots \alpha_n)$
$\sum_{i=1}^{n} \alpha_i$	the sum $(\alpha_1 + \alpha_2 + \ldots + \alpha_n)$
$N(\Omega, f(s), C)$	the number of clockwise encirclement of the point Ω by the locus of f(s) as s goes around the closed contour C in the complex plane in a clockwise sense
D_R	Nyquist contour of Fig. 2.5

CHAPTER 2: BACKGROUND

2.1 Introduction

The purpose of this chapter is to introduce some basic results and concepts which will be necessary to understand the developments of later chapters. However, since these concepts are standard in the control area, our presentation will be brief. For further developments the reader can consult the references mentioned below.

We will begin by reviewing some preliminary definitions and properties of the singular values of a matrix. Then the importance of singular values in control will be shown by introducing a practical design perspective for multivariable feedback control problems. This design perspective is expressed in terms of singular values of the loop transfer function and in terms of the closed-loop system stability. Special attention will be given on how the stability can be achieved. This presentation will expose what are the desirable features of a multivariable feedback design methodology.

We will present two categories of design methods. We will first discuss frequency domain-based design methods and more particularly the "Characteristic Loci" (CL) and the "Inverse Nyquist Array" (INA) design methods. Then we will turn to time domain-based design methods and expose the main features of the Linear Quadratic (LQ) design methodology. Since a thorough discussion of all these design methodologies would be tedious, details will be skipped and we will rather focus our attention on the design philosophy used for each of these methods.

2.2 Mathematical Preliminaries: Singular Values of a Matrix.

The following definitions and properties are elementary concepts of matrix theory and can be found in many books on linear algebra [16].

The singular values of a complex n x m matrix A, denoted $\sigma_i(A)$, are the k largest non negative square roots of the eigenvalues of $A^H A$, where k = min (m,n), i.e.:

$$\sigma_i(A) = \lambda_i^{1/2}(A^H A) \quad i = 1,\ldots,k \tag{2.1}$$

where we have assumed that the σ_i's are ordered so that, $\sigma_i \geq \sigma_{i+1}$.

The maximum and minimum singular values may respectively by defined by:

$$\sigma_{max}(A) = \bar{\sigma}(A) = \max_{\underline{x}\neq 0} \frac{||A\underline{x}||_2}{||\underline{x}||_2} = ||A||_2 \tag{2.2}$$

$$\sigma_{min}(A) = \underline{\sigma}(A) = \min_{\underline{x}\neq 0} \frac{||A\underline{x}||_2}{||\underline{x}||_2} = ||A^{-1}||_2^{-1}, \text{ if } A^{-1} \text{ exists} \tag{2.3}$$

where $||\underline{x}||_2$ is the usual Euclidean norm of the vector $\underline{x}$ and where $||A||_2$ is called the spectral norm of the matrix A.

The smallest singular value $\sigma_{min}(A)$ measures how near the matrix A is to being singular or rank deficient (a matrix is rank deficient if its rows and columns are linearly dependent). To see this, consider the problem of finding a matrix E of minimal spectral norm that makes A+E rank deficient. Since A+E must be rank deficient, there exists a nonzero vector $\underline{x}$ such that, $||\underline{x}||_2 = 1$ and $(A+E)\underline{x} = \underline{0}$. Thus:

$$\sigma_{min}(A) \leq ||A\underline{x}||_2 = ||E\underline{x}||_2 \leq ||E||_2 = \sigma_{max}(E) \quad .$$

Therefore, E must have a spectral norm of at least $\sigma_{min}(A)$ otherwise A+E cannot be rank deficient. Assuming square matrices, we have the property:

$$\sigma_{min}(A) > \sigma_{max}(E) \rightarrow \text{A+E is non singular} \quad .$$

The smallest singluar value gives a notion of the "distance to singularity". This property turns out to allow the formulation of various robustness tests [3].

A convenient way of representing a matrix that exposes its internal structure is the singular value decomposition (SVD). For an nxm matrix, the SVD of A is given by:

$$A = U\Sigma V^H = \sum_{i=1}^{k} \sigma_i(A)\, \underline{u}_i\, \underline{v}_i^H \qquad (2.4)$$

where U and V are unitary matrices, i.e., $U^H U = V^H V = I$, with columns vectors denoted by:

$$U = [\underline{u}_1, \ldots, \underline{u}_n]$$
$$V = [\underline{v}_1, \ldots, \underline{v}_n]$$

and where Σ contains a diagonal non negative definite matrix Σ_1 of singular values arranged in descending order, i.e.

$$\Sigma = \begin{cases} \begin{bmatrix} \Sigma_1 \\ 0 \end{bmatrix}, & n \geq m \\ [\Sigma_1, \; 0] & m \geq n \end{cases}$$

with $\Sigma_1 = \text{diag}\,[\sigma_1,\ldots,\sigma_k]$; $k = \min(m,n)$. The columns of U and V are unit eigenvectors of AA^H and A^HA respectively and are called the left and right singular vectors of the matrix A.

When A is a square matrix, further properties hold. From the singular value decomposition, it is clear that the number of non-zero singular values gives the rank of A. Furthermore, the smallest non-zero singular value gives a notion of the distance to rank deficiency for A. The SVD gives a complete information on the structure of A. Let us now give other useful properties of singular values for square matrices [17].

$$- \text{(i)}\ \sigma_i(A) - \sigma_j(B) \underline{\leq} \sigma_{i+j-1}(A+B) \underline{\leq} \sigma_i(A) + \sigma_j(B) \qquad (2.5)$$

assuming that the singular values are arranged in descending order.

- (ii) $c(A) = \dfrac{\bar{\sigma}(A)}{\underline{\sigma}(A)}$ is called the condition number of A with respect to inversion. Unitary matrices have a unit condition number.

- (iii) Eigenvalue bound: the eigenvalues of A have magnitudes bounded by the spectrum norm of the matrix, i.e.

$$|\lambda_i(A)| \underline{\leq} \bar{\sigma}(A) \quad \forall i = 1,..,n \ .$$

The fact that singular values are associated to a matrix norm, namely the spectral norm, and that they give a notion of distance to singularity explains their usefulness in the study of multivariable feedback systems.

2.3 The General Feedback Design Problem

2.3.1 Design Requirements

The role of this section is to introduce typical design requirements

for linear multivariable feedback systems. The developments presented here rely heavily on the work of J.J. Doyle and G. Stein in [1].

We will consider a standard feedback configuration illustrated in Figure 2.1. An optional precompensator is used to achieve arbitrary command shaping. Disturbances are assumed to be reflected at the output. All signals are multivariable in general and the mathematical models for the plant and compensator are finite dimensional time-invariant systems with transfer function matrices G(s) and K(s). The configuration, when it is stable, has the following properties:

Input-output behavior

$$y = GK(I + GK)^{-1} (r-n) + (I+GK)^{-1} d \tag{2.6}$$

$$e = r-y = (I+GK)^{-1} (r-d) + GK(I+GK)^{-1} n \tag{2.7}$$

Transfer function sensitivity

When changes occur in the plant such that the plant becomes

$$G' = G + \Delta G$$

then:

$$\Delta H_u = (I + G'K)^{-1} \Delta H_{o\ell} \tag{2.8}$$

where

$$\Delta H_u = G'K(I + G'K)^{-1} - GK(I + GK)^{-1}$$

$$\Delta H_{o\ell} = G'K(I + GK)^{-1} - GK(I + GK)^{-1}$$

ΔH_u and $\Delta H_{o\ell}$ denote changes in the closed-loop transfer function and changes in a nominally equivalent open-loop transfer function respectively.

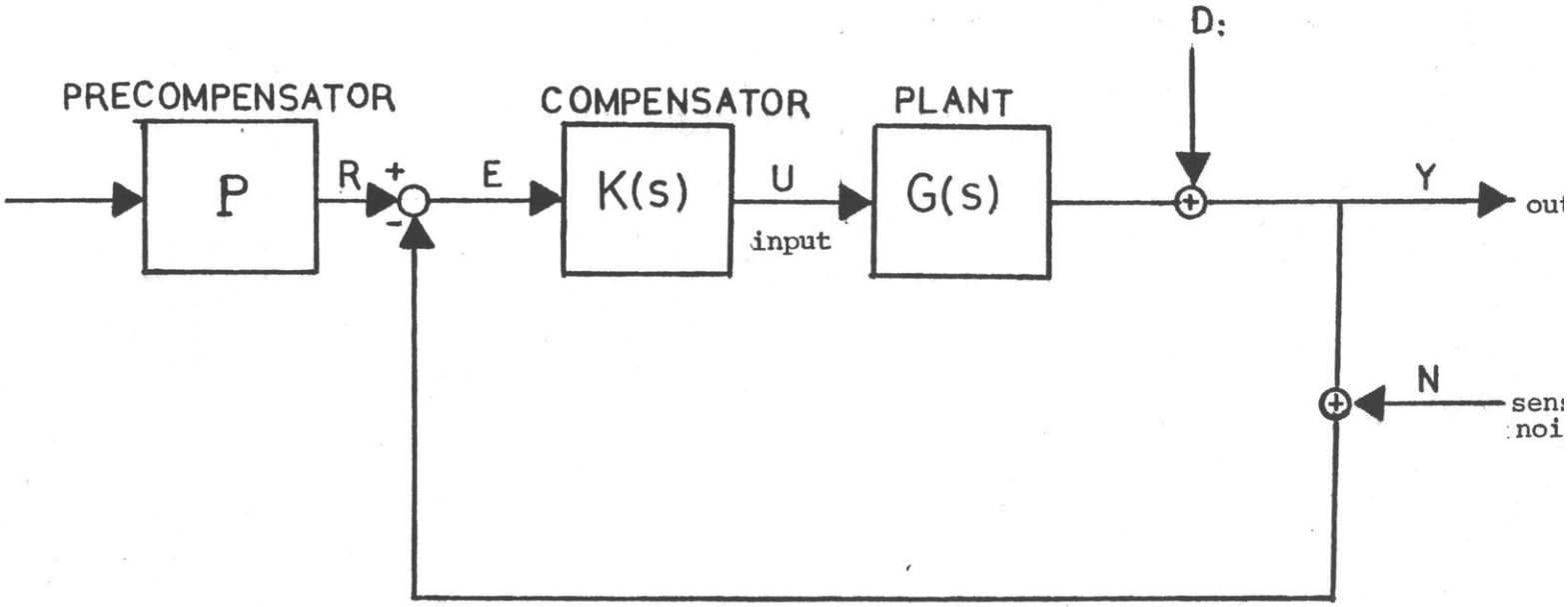

Figure 2.1: Standard feedback configuration

Equation (2.4) shows that good command following and disturbances rejection can be achieved by making the inverse return difference matrix $(I + GK)^{-1}$ "small" - Equation (2.8) shows that loop sensitivity is improved under the same condition provided that G' and G are not too different. The notion of size of a matrix can be captured in terms of singular values or, equivalently, in terms of matrix norms. The requirement that $(I + GK)^{-1}$ should be "small" means that we should have:

$\underline{\sigma}(I + G(j\omega)\ K(j\omega)]$ large for all frequencies ω where the commands, plant changes, disturbances are significant (2.9) say $o \leq \omega \leq \omega_o$.

From the inequality derived from (2.5), we have:

$$\underline{\sigma}(GK) - 1 \leq \underline{\sigma}\ (I + GK) \leq \underline{\sigma}\ (GK) + 1.$$

The condition (2.9) requires to achieve high loop gains, i.e., $\underline{\sigma}(GK)$ large for frequencies $o \leq \omega \leq \omega_o$.

But loop gains cannot be made arbitrarily large over an arbitrarily large frequency range [1]. Instead, they must satisfy certain performance tradeoffs and design limitations. A major performance tradeoff concerns the sensor noise attenuation.

From equation (2.6), the effect of sensor noise on the output is given by:

$$y = GK(I + GK)^{-1}\ n \simeq In \quad \text{when } \underline{\sigma}(GK) \text{ large} \quad .$$

Thus, sensor noise attenuation requires that $GK(I + GK)^{-1}$ should be "small" for frequencies where the sensor noise is significant. This yields the design requirement:

$\underline{\sigma}(I + GK^{-1}\ (j\omega))$ large a frequencies where $n(j\omega)$ is large . (2.10)

Since the requirement that $\underline{\sigma}(I + GK^{-1}(j\omega))$ be large can be approximated by the condition that $\bar{\sigma}(G(j\omega)\ K(j\omega))$ be small, the design requirements (2.9) - (2.10) clearly impose a tradeoff. But feedback designers would have little to complain if they had only to satisfy the tradeoff between command following - disturbance rejection and sensor noise attenuation. In practice, the requirement of tolerance of uncertainties on the plant G, most often overshadows any other loop gain limitation. Though a system may be designed using linear-time invariant models, the design must operate on a real physical system. The properties of physical systems, in particular the ways in which they deviate from finite-dimensional linear models put strict limitations on the frequency range over which the loop gains may be large.

To account for differences between the "true" system G'(s) and our nominal system G(s), several model uncertainties representations are available. Following J.J. Doyle and G. Stein in [1], we choose a multiplicative form, i.e.:

$$G'(s) = (I + L(s))\, G(s) \tag{2.11}$$

where L(s) is a perturbation operator which represents uncertainties reflected at the output of the plant. We assume that:

$$\bar{\sigma}(L(j\omega)) \leq \ell_m(\omega) \quad \forall\omega \geq 0 \ .$$

Typically, $\ell_m(\omega)$ will be small at low frequencies and increases to unity and above for higher frequencies as represented in Figure 2.2. The

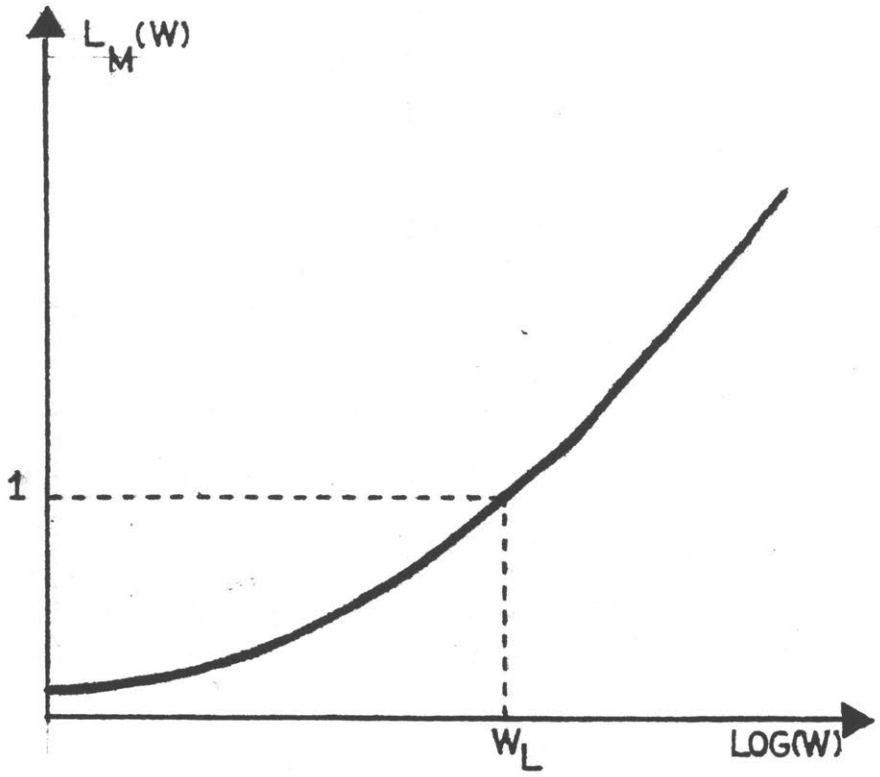

Figure 2.2: Typical uncertainty representation

determination of $\ell_m(\omega)$ may not be easy. A practical example can be found in [2]. Since our design operates on the "true" system $G'(s)$, performance objectives such as good command following and disturbance rejection are achieved under conditions analogous to (2.9) where $G'(s)$ replaces $G(s)$, so that we must have

$$\left| \begin{array}{l} \underline{\sigma}(I + G'(j\omega)\ K(j\omega)) \text{ large for a certain frequency} \\ \text{range } o \leq \omega \leq \omega_o \ . \end{array} \right. \tag{2.12}$$

Therefore, the problem of designing good feedback loops in the face of uncertainties requires a condition of the type:

$$ps(\omega) \leq \underline{\sigma}(I + G'(j\omega)\ K(j\omega)) \quad \forall \omega \leq \omega_o$$

where $ps(\omega)$ is large positive function of ω, specified over the defined frequency range by performance objectives as good command following, disturbance rejection. Since

$$\underline{\sigma}(I + GK) - \bar{\sigma}(L)\ \bar{\sigma}(GK) \leq \underline{\sigma}(I + G'K) \ ,$$

This performance objective is satisfied if:

$$\frac{ps(\omega)}{1-\ell_m(\omega)\ C(\omega)} \leq \underline{\sigma}(G(j\omega)\ K(j\omega)), \quad \forall \omega \leq \omega_o \tag{2.13}$$

where $C(\omega) = \dfrac{\bar{\sigma}(G(j\omega)\ K(j\omega))}{\underline{\sigma}(G(j\omega)\ K(j\omega))}$ is the condition number of GK. Assuming that $C(\omega)$ is not too different from unity, this design equation is meaningful only when, $\ell_m < 1$. When ℓ_m approaches unity, we must worry in fact much more about stability than performance. Namely, the

stability of the nominal closed-loop system must be maintained under all possible perturbations L(s) such that:

$$\bar{\sigma}(L(j\omega)) < \ell_m(\omega) \quad .$$

When this is the case, the system is said to be robust against uncertainties by assuming that the nominal closed-loop system is stable and by using arguments based on the multivariable Nyquist criterion, J.J. Doyle and G. Stein have shown that the robustness property is satisfied if:

$$\underline{\sigma}(I + (GK)^{-1}(j\omega)) > \ell_m(\omega) \quad , \quad \forall\omega \quad . \qquad (2.14)$$

Since $\underline{\sigma}(GK^{-1}(j\omega)) - 1 \leq \underline{\sigma}((GK)^{-1}(j\omega) + I) \leq \underline{\sigma}(GK^{-1}(j\omega)) + 1$, this robustness requirement reduces when $\ell_m(\omega)$ becomes large to the high loop gains limitation:

$$\left| \begin{array}{l} \bar{\sigma}(G(j\omega)\ K(j\omega)) \leq \dfrac{1}{\ell_m(\omega)} \quad \text{for frequencies} \\ \text{where } \ell_m(\omega) \text{ is large .} \end{array} \right. \qquad (2.15)$$

Conditions (2.13) - (2.15) together summarize the multiple input-multiple output feedback control design problem with uncertainties. Given the plant G(s), given the bound $\ell_m(\omega)$ on uncertainties and given a performance objective ps(ω), we want to find a compensator K(s) such that:

(i) The nominal system $GK[I+GK]^{-1}$ is stable.

(ii) The "robustness" condition (2.15) is verified.

(iii) The "performance" condition (2.13) is satisfied as well as possible.

The restrictions imposed on performance are motivated by the fact that robustness is a prime design requirement. Condition (ii) and (iii) allow us to plot a typical design requirement as in Figure 2.3.

It is worth to point out that model uncertainties representation have been assumed to take a multiplicative form and that uncertainties have been assumed to be reflected at the output. Indeed, other types of model error structure could have been chosen and would have given some other robustness conditions similar to the one that we have obtained. As shown in [3], these different choices and their associated robustness conditions are summarized in Figure 2.4. Thus, when σ_{max} (L(s)) becomes large, i.e., $\ell_m(\omega)$ large, each of these robustness condition can be approximated by a condition on the singular values of G(s) K(s). On the other hand, plant uncertainties have been assumed to be reflected at the output. For multivariable systems, since GK is different from KG, tolerances for uncertainties at the plant input and output are generally not the same. For instance using the multiplicative perturbation form G'(s) = G(s) (I+L(s)), i.e., uncertainties reflected at the input, another "robustness" condition can be derived and will be such that G(jω) K(jω) will be replaced by K(jω) G(jω) in (2.14). This is also the case for other forms of perturbation, i.e., the "robustness" condition for uncertainties reflected at the input and output differ only in that KG replaces GK. Classical designers will recognize that the difference between those "robustness" conditions is simply that each uses a loop transfer function appropriate for the point in the loop where robustness

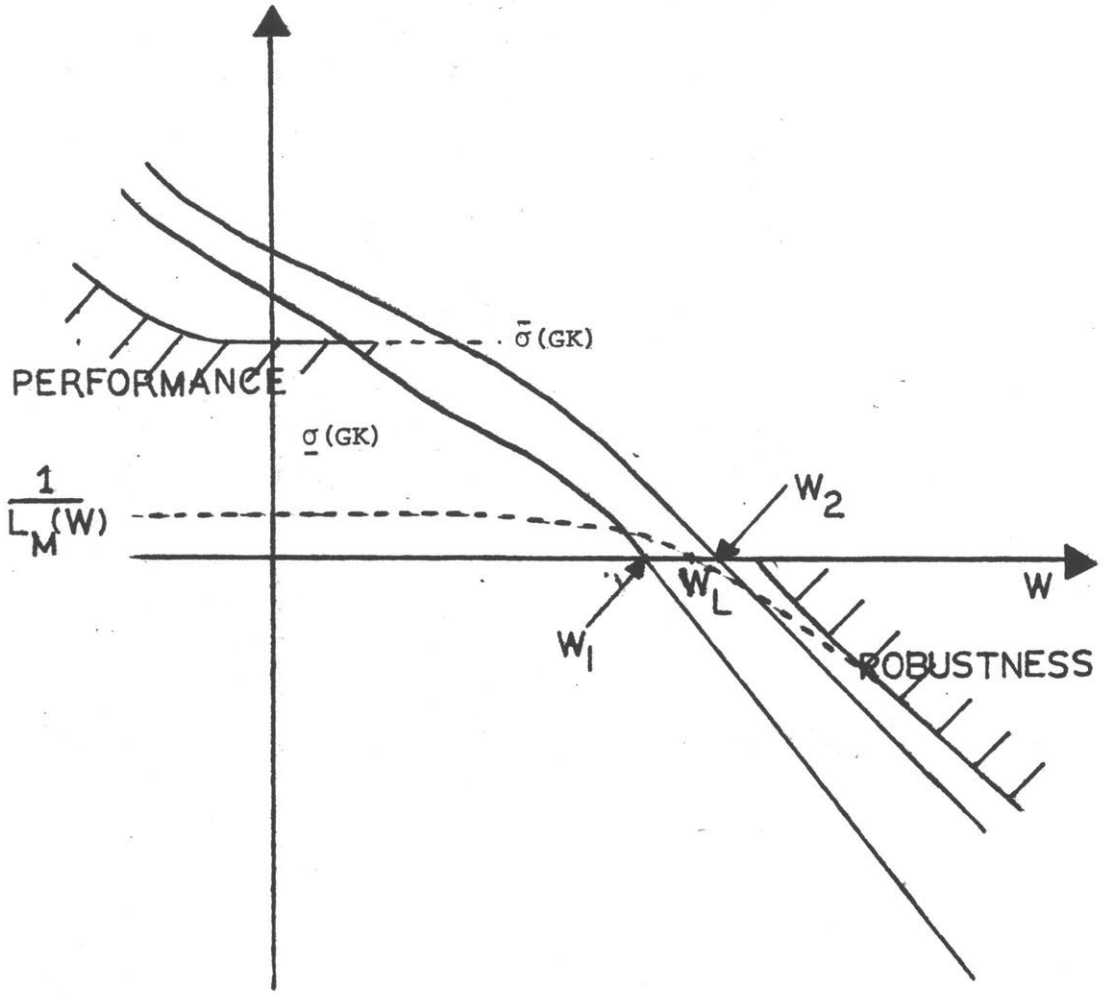

Figure 2.3: Typical design requirement

Block Diagram of Perturbed System	Perturbed Systems and Robustness Condition
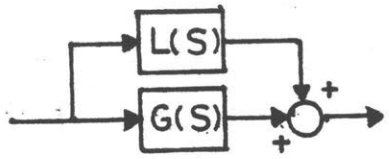 Feedforward (addition)	$G'(s) = G(s) + L(s)$ $\sigma_{min}(I + GK(s)) > \sigma_{max}(L(s))$
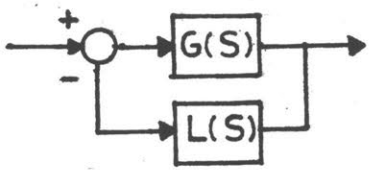 Feedforward (substraction)	$G'(s) = (G^{-1}(s) + L(s))^{-1}$ $\sigma_{min}(I + (GK)^{-1}(s)) > \sigma_{max}(L(s))$
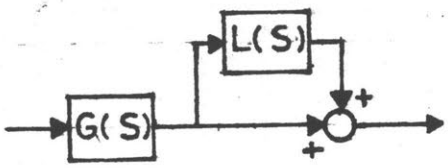 Multiplication	$G'(s) = (I + L(s)]\ G(s)$ $\sigma_{min}(I + (GK)^{-1}(s)) > \sigma_{max}(L(s))$
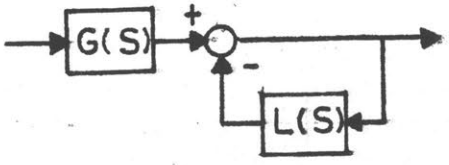 Division	$G'(s) = (I + L(s))^{-1}\ G(s)$ $\sigma_{min}(I + GK(s)) > \sigma_{max}(L(s))$

Figure 2.4: Physical representation of perturbed models corresponding to various error criteria and associated robustness conditions.

is being tested. It appears therefore that robustness tests at the plant input will impose bounds on the singular values of K(s) G(s) whereas robustness tests at the plant output impose bounds on the singular values of G(s) K(s).

Therefore a good multivariable linear feedback design method would be one that allows singular values $\sigma(G(j\omega)\ K(j\omega))$ (plant output) as well as $\sigma(K(j\omega)\ G(j\omega))$ (plant input) to be shaped as function of the frequency. This method should also allow us to meet the condition (i), i.e., to assess easily the nominal closed loop stability.

2.3.2 Study of the Closed Loop Stability

Let us denote by $N(\Omega, f(s), C)$ the number of clockwise encirclements of the point Ω by the locus of f(s) as s traverses the closed contour C in the complex plane in clockwise sense. The multivariable version of the Nyquist stability criterion can be stated as follows:

The closed loop configuration of Fig. 2.1 is stable if and only if for all R sufficiently large:

$$N(0, \det(I + G(s)\ K(s)), D_R) = -P \tag{2.16}$$

where P is the number of unstable open-loop poles an D_R is the Nyquist contour as represented in Figure 2.5.

Let us consider a SVD of $I + GK(s)$:

$$I + GK(s) = U^H(s)\ \Sigma(s)\ V(s) \tag{2.17}$$

where $\Sigma(s) = \text{diag}\ [\sigma_1(s), \ldots, \sigma_m(s)]$ with $\sigma_i(s) \geq \sigma_{i+1}(s)$, $\forall s$ and

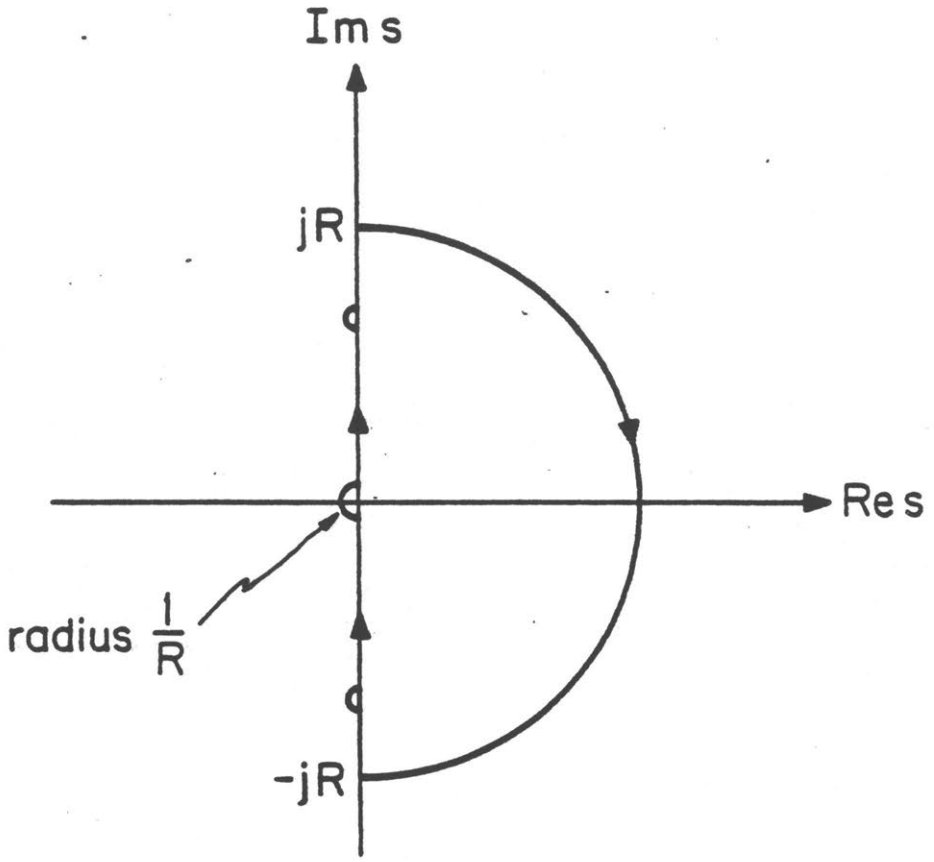

Figure 2.5: Nyquist contour D_R which encloses all unstable open loop poles, avoiding the open loop poles on the imaginary axis by identations of radius $\frac{1}{R}$

where $U(s)$, $V(s)$ are unitary matrices. We can rewrite the equation (2.17) and express $I+GK$ as the product of an hermitian matrix by a unitary matrix, so that we have:

$$I+G(s)\ K(s) = (U^H(s)\ V(s))\ (V^H(s)\ \Sigma(s)\ V(s))$$

$$\text{with} \quad \det\ (I+G(s)\ K(s)) = \det\ (\Sigma(s))\ \det\ (U^H(s)\ V(s)) \ . \tag{2.18}$$

$U^H(s)\ V(s)$ is a unitary matrix, its eigenvalues are complex numbers of modulus 1, $e^{j\theta_i(s)}$, $i = 1,\ldots,m$, and the arguments $\theta_i(s)$ are called principal phases. Thus, the determinant of $U^H(s)\ V(s)$ becomes:

$$\det\ [U^H(s)\ V(s)] = \prod_{i=1}^{m} e^{j\theta i(s)} = e^{j\theta(s)} \tag{2.19}$$

$$\text{with} \quad \theta(s) = \sum_{i=1}^{m} \theta_i(s)$$

$$\text{so that} \quad \det[I+G(s)\ K(s)] = \left(\prod_{i=1}^{m} \sigma_i(s)\right)\ e^{j\theta(s)} \ . \tag{2.20}$$

Theorem 2.1: The closed-loop configuration of Fig. 2.1 is stable if and only if for R sufficiently large

$$N(0,\ \sigma_m(s)\ e^{j\theta(s)},\ D_R) = -\ P$$

where P is the number of unstable open-loop poles and D_R is the Nyquist contour of fig. 2.5.

Proof: From the multivariable Nyquist stability criterion (2.16), we have the relation;

$$N(0,\ \det\ [I+G(s)\ K(s)),\ D_R) = N(0,(\prod_{i=1}^{m} \sigma_i(s))\ e^{j\theta(s)},\ D_R) = -\ P$$

let us consider

$$\gamma(s,\varepsilon) = \sigma_m(s)\left[\prod_{i=1}^{m-1} (1-\varepsilon)\ \sigma_i(s) + \varepsilon)\right] e^{j\theta(s)} \quad . \tag{2.21}$$

we have

$$\begin{cases} \gamma(s,1) = \sigma_m(s)\ e^{j\theta(s)} \\ \\ \gamma(s,0) = \det\ (I+G(s)ks)) \quad . \end{cases} \tag{2.22}$$

In order to prove the theorem, it is sufficient to show that the loci of $\sigma_m(s)\ e^{j\theta(s)}$ and $\det\ [I+G(s)\ K(s)]$ as s goes along D_R can be deduced from each other by a continuous deformation that does not pass through the critical point 0 as shown in Figure 2.6. Then we will have:

$$N(0,\ \det(I+G(s)\ K(s),\ D_R) = N(0,\ \sigma_m(s)\ e^{j\theta(s)},\ D_R) \quad .$$

$\gamma(s,\varepsilon)$ is a continuous function of ε for all $s \in D_R$ and thus from (2.22), appears to be a continuous deformation of the plot defined by $\det\ (I+G(s)\ K(s))$ for $\varepsilon \in [0,1]$. Since the singular values $\sigma_i(s)$ are non negative real numbers, for all $s \in D_R$ such that $\det(I+G(s)\ K(s) \neq 0$, $\gamma(s,\varepsilon)$ is nonzero for all $\varepsilon \in [0,1]$. The points s of D_R such that $\det[I+G(s)\ K(s)) = 0$ remain unchanged by the deformation $\gamma(s,\varepsilon)$ for all $\varepsilon \in [0,1]$ since, in this case, the smallest singular value $\sigma_m(s)$ is zero. There is no deformation for these points. Therefore we will have:

$$N(0,\ \det(I+G(s)\ K(s)),\ D_R) = N(0,\ \gamma(s,\varepsilon),\ D_R) \quad \forall\ \varepsilon \in [0,1] \quad .$$

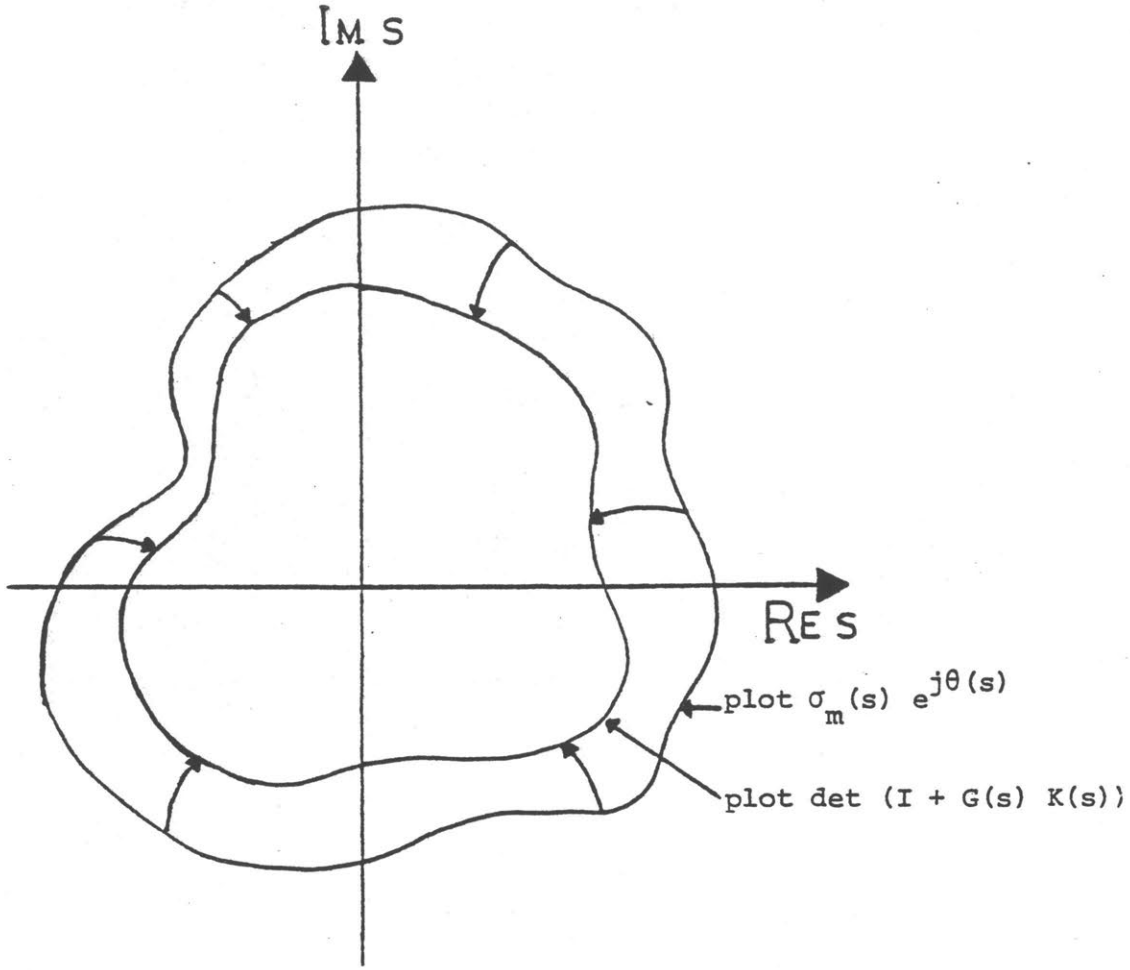

Figure 2.6: Continuous deformation of the plot defined by det [I + G(s) K(s)) into the plot defined by $\sigma_m(s)\ e^{j\theta(s)}$

To prove the theorem, we need only to set $\varepsilon = 1$ in this expression and take (2.22) into account. Q.E.D.

The stability criterion defined by theorem 2.1, gives us more insight on the conditions that need to be satisfied in order to assess the stability of the closed-loop system of Fig. 2.1. The number of encirclements of the critical point 0 by the plot defined by $\sigma_m(s)\, e^{j\theta(s)}$ as s goes along D_R will be determined by the values of $\theta(s)$. On the other hand, the closeness to the critical point depends on $\sigma_m(s)$.

This gives us a notion of margin of stability that will concern the frequency range where $\sigma_m(s)$ becomes small. But $\sigma_m(s)$ is the smallest singular value of $I + G(s)\, K(s)$; $\sigma_m(s)$ will be small in the frequency range where the loop gains $\sigma_i(G(s)\, K(s))$ are approximately equal to one. This range of frequencies is called the crossover frequency region and correspond to $[\omega_1, \omega_2]$ in the representation of Fig. 2.3.

In the same way as the singular values of the loop transfer function of multiple input-multiple output (MIMO) systems generalize the modulus of the loop transfer function for single-input single-output (SISO) systems, the phase angle $\theta(s)$ is a generalization for MINO systems of the phase argument of the loop transfer function for SISO systems. The behavior of the configuration 2.1 could be entirely determined by a plot as in Fig. 2.3 giving the singular values versus the frequency and a phase plot given $\theta(s)$ versus the frequency. Those two plots correspond for MIMO systems to the Bode plots of SISO systems. But the main problem of multivariable feedback design is that it is not clear how

the choice of K(s) affects the values of the loop gains $\sigma_i(G(s)\ K(s))$ $i = 1,\ldots,m$ and the values of $\theta(s)$. This makes the design of multivariable feedback systems a particularly difficult task.

2.4 Several Frequency Domain-Based Design Methods

The frequency domain design technqiues were developed originally by Bode, Nyquist, Evans, etc... For SISO systems, with these feedback design techniques, it was shown that the use of very simple compensators such as lead/lag compensators, P.I.D controllers, ...etc, was sufficient to meet design requirements (see any good classical control book, [5] for example). The simplicity of the design techniques in the case of SISO systems is due to the fact that the design requirements can be entirely defined in terms of the modulus and phase of the loop transfer function and, on the other hand, it is clear how the choice of the compensator will affect the loop transfer function. Unfortunately, this is not the case of MIMO systems, and SISO techniques cannot be generalized in a straightforward manner to deal with multivariable linear systems. This has generated a considerable amount of research over the past years.

D.H. Owens has developed in [5] a general framework for the study of frequency domain feedback design techniques for MIMO systems. Considering the unit feedback configuration of Fig. 2.1, standard SISO techniques can be used if we find a compensator K(s) such that the analysis of the closed-loop system can be reduced to a loop by loop analysis. More precisely, this is possible when for the plant G(s)

assumed for simplicity to be a m x m matrix, there exists some rational transfer matrices $U(s)$, $V(s)$ such that:

$$U(s)\ G(s)\ V(s) = \text{diag}[g_1(s),\ldots,g_m(s)],\quad \forall s\ . \tag{2.23}$$

Then, with a slight change of notation, we can choose the compensator $G_c(s)$ as:

$$G_c(s) = V(s)\ K(s)\ U(s) \tag{2.24}$$

where $V(s)$ and $U(s)$ are as in (2.23) and where $K(s)$ is a diagonal compensator:

$$K(s) = \text{diag}\ [k_1(s),\ldots,\ k_m(s)]\ . \tag{2.25}$$

The closed loop configuration is represented in Figure 2.7, where we have indicated several loop breaking points. The loop transfer function $G_1(s)$, for the loop broken at point (1) becomes:

$$G_1(s) = K(s)\ U(s)\ G(s)\ V(s) = \text{diag}\ [k_1(s)\ g_1(s),\ldots,k_m(s)\ g_m(s)]. \tag{2.26}$$

Thus at point (1) of the loop, the system appears to be equivalent to a sequence of totally decoupled SISO loops whose loop transfer functions are $k_i(s)\ g_i(s)$, $i=1,\ldots,m$ respectively. Therefore, a design can be performed in a loop by loop fashion, and standard SISO techniques can be applied to choose adequately the diagonal elements $k_i(s)$, $i=1,\ldots,m$. The compensator becomes easy to construct.

Since those nice features come merely from the existence of $U(s)$ and $V(s)$ which diagonalize the plant $G(s)$ as in (2.23), the design

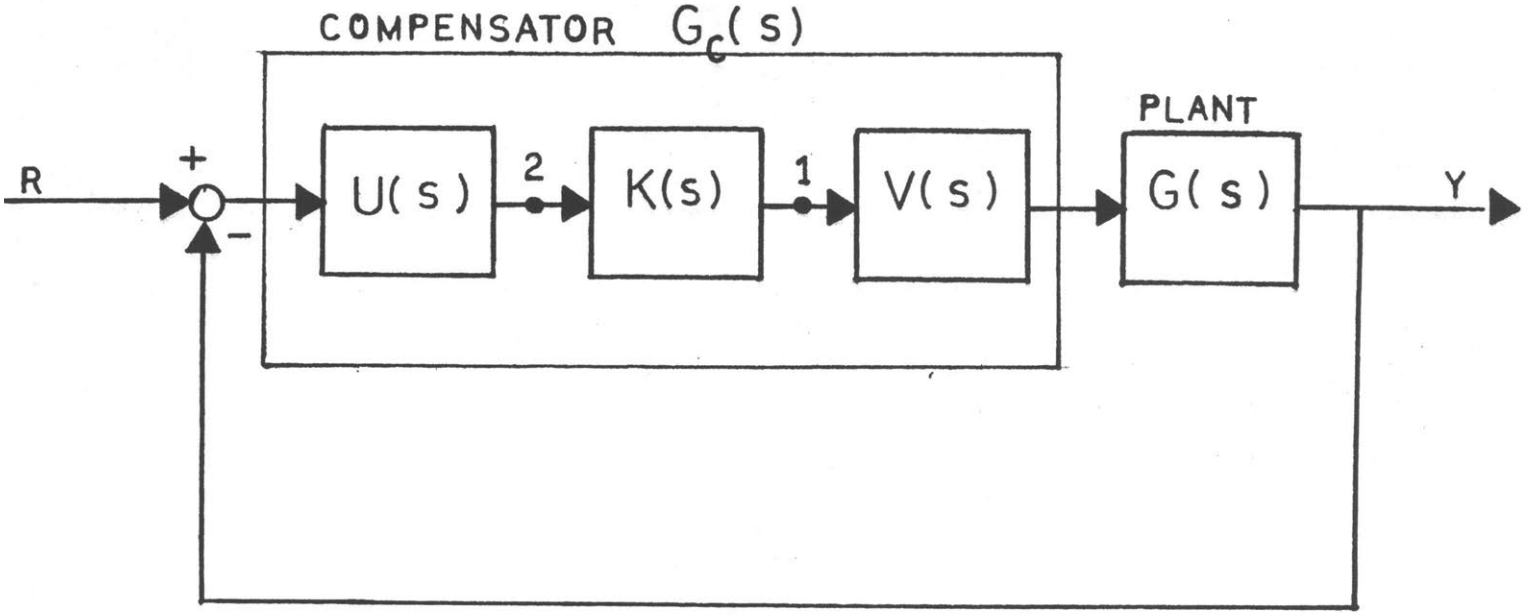

Figure 2.7; Configuration for loop by loop analysis

approach presented above is usually called a diagonalization method of design. One of the main problems of this diagonalization approach lies in the existence of matrices U(s) and V(s) as in (2.23). For some simple plant models G(s), those matrices may be easy to find by inspection. But when we consider more general cases, the identification of U(s) and V(s) becomes tedious, and a way of choosing them systematically is needed.

This has motivated the work of A.G.J. MacFarlane and al. that culminates in the eatablishment in [6] of a design method, the so called "Characteristic Loci" (CL) design method. They take advantage of the eigenvalues/eigenvectors decomposition of the plant model defined as

$$G(s) = V(s)\ \Lambda(s)\ U(s) \qquad (2.27)$$

where $\Lambda(s) = \text{diag}\,[\lambda_1(s),\ldots,\lambda_m(s)]$ is the matrix of eigenvalues and where U(s), V(s) $(= U^{-1}(s))$, are matrices whose column vectors are respectively the left and right eigenvectors associated to the eigenvalues $\lambda_i(s)$, i=1,...,m. Then,

$$U(s)\ G(s)\ V(s) = \Lambda(s) \quad .$$

That is, U(s) and V(s) satisfy the relation (2.23) and the diagonal elements $g_i(s)$, i=1,...,m are the eigenvalues of the plant. Then considering the configuration of Fig. 2.7, the loop transfer functions $G_1(s)$ and $G_2(s)$ for the loop breaking points (1) and (2) become

respectively:

$$G_1(s) = K(s)\,U(s)\,G(s)\,V(s) = \text{diag}\,[k_1(s)\,\lambda_1(s),\ldots,k_m(s)\,\lambda_m(s)]$$
$$G_2(s) = U(s)\,G(s)\,V(s)\,K(s) = \text{diag}\,[k_1(s)\,\lambda_1(s),\ldots,k_m(s)\,\lambda_m(s)]. \tag{2.28}$$

This suggests that a design can be constructed in a loop by loop fashion. Moreover the closed loop transfer function of the configuration is:

$$T(s) = (G(s)\,V(s)\,K(s)\,U(s)]\,(I+G(s)\,V(s)\,K(s)\,U(s)]^{-1}$$
$$= V(s)\,\text{diag}\left[\frac{k_1(s)\lambda_1(s)}{1+\lambda_1(s)k_1(s)},\ldots,\frac{k_m(s)\lambda_m(s)}{1+k_m(s)\lambda_m(s)}\right]u(s). \tag{2.29}$$

That is, the eigenvalues of the closed loop transfer function are the values $\{\frac{\lambda_i(s)k_i(s)}{1+\lambda_i(s)k_i(s)},\ i=1,..,m\}$. Thus $k_i(s)$, $i=1,\ldots,m$, can be chosen in order to confer desired properties to the closed-loop transfer function. But the choice of the $k_i(s)$, $i=1,\ldots,m$, must also be such that the closed-loop system is stable. The main difficulty arising is that the eigenvalues $\lambda_i(s)$, $i=1,\ldots,m$ are not simple mathematical entities. They are the solutions for each values of s of the characteristic equation:

$$\det[\lambda(s)I - G(s)] = 0\ , \tag{2.30}$$

For each value of s, $\lambda(s)$ solution of (2.30) is a multivalued function, each of these values being an eigenvalue of $G(s)$: $\lambda(s)$ is an algebraic function. However, the study in [7] of the properties of $\lambda(s)$ allowed Mac Farlane to derive a Nyquist stability criterion for the configuration

of Fig. 2.7 that can be satisfied by an adequate choice of the $k_i(s)$, $i=1,\ldots,m$. Thus, in the light of the relations (2.28) - (2.29) and of a Nyquist stability criterion, the CL method of design reduces to a sequential choice of the $k_i(s)$ $i=1,\ldots,m$.

A last difficulty in this method lies in the fact that the matrices U(s) and V(s) of the relation (2.27) are not in general rational transfer functions in s and thus cannot be implemented as L.T.I. systems. This is remedied in the CL method by approximating respectively U(s) and V(s) by rational transfer matrices $\hat{U}(s)$ and $\hat{V}(s)$. Provided that the approximations are accurate enough, the results of relations (2.28) - (2.29) and the stability insured by the Nyquist criterion will hold approximately when $\hat{U}(s)$ and $\hat{V}(s)$ are replaced respectively by U(s) and V(s) in the compensator of Fig. 2.7. Thus, with the actual implementation, the relation (2.23) becomes non longer exact, but:

$$\hat{U}(s)\ G(s)\ \hat{V}(s) \approx \Lambda(s) \quad . \tag{2.31}$$

That is, inherent to the approximation necessity, the CL method performs an approximate diagonalization of the plant. With this point of view, it is natural to ask if the approximation difficulty could not be avoided by choosing, a priori, to diagonalize the plant only approximately. This motivates the Inverse Nyquist array (INA) method of design introduced by H.H. Rosenbrock in [8]. The notion of approximate diagonalization is first of all, formalized by the concept of diagonal dominance.

A matrix $M = (m_{ij}, \ldots m,\ j=1,\ldots m]$ is said to be <u>diagonal dominant</u>

whenever one of the following properties is satisfied.

$$|m_{ii}| \geq \sum_{\substack{j=1 \\ j\neq i}}^{m} |m_{ij}| , \qquad \forall\ i=1,\ldots,m \tag{2.32a}$$

or

$$|m_{jj}| \geq \sum_{\substack{i=1 \\ i\neq j}}^{m} |m_{ij}| . \qquad \forall\ j=1,\ldots,m \tag{2.32b}$$

When this is the case, the eigenvalues of M are located in the union of the disk of center m_{ii} and radius R_i such that

$$R_i = \sum_{\substack{j=1 \\ j\neq i}}^{m} |m_{ij}| \quad \text{if (2.32.a) is satisfied,}$$

or (2.33)

$$R_i = \sum_{\substack{j=1 \\ j\neq i}}^{m} |m_{ij}| \quad \text{if (2.32.b) is satisfied.}$$

Thus, the location of the eigenvalues of a diagonal dominant matrix can be approximated in the complex plane. This lead H.H. Rosenbrock to the development of the following method of design. Let us assume the existence of two rational transfer matrices U(s) and V(s) such that U(s) G(s) V(s) is diagonal dominant. Then we have an approximate version of the relation (2.23):

$$U(s)\ G(s)\ V(s) \approx \text{diag}\ [g_1(s),\ldots,g_m(s)] \tag{2.34}$$

where U(s) and V(s) can be determined by a trial and error procedure. The diagonal elements $g_i(s)$, i=1,...,m constitute reasonable approximations of the eigenvalues of G(s) within bounds specified by the

off-diagonal elements of U(s) G(s) V(s). The extent to which this is true is visualized by the so-called Nyquist arrays which figure for each value of $g_i(s)$, i=1,...,m, the radius R_i corresponding to the admissible locations of the eigenvalues of G(s). (see [8] for further details). Therefore, if we consider the configuration of Fig. 2.7 where U(s) and V(s) are as in (2.34), the relations (2.28) - (2.29) developed for the CL method will hold approximately. This will allow to choose in a loop by loop fashion the diagonal elements $k_i(s)$, i=1,...,m in order to match approximately the desired properties of the closed-loop transfer function. Moverover, H.H. Rosenbrock showed in [8] that the closed-loop stability can be assessed in terms of a Nyquist stability criterion depending on the values of $k_i(s)$ and $g_i(s)$, i=1,...,m. Thus, the INA method of design reduces to a sequential choice of the diagonal elements $k_i(s)$ i=1,...,m.

The major achievement of the diagonalization approach, exact or approximate, is to reduce the MIMO design problem to a sequence of well defined SISO problems. At this stage our capabilities are greatly extended by our knowledge of simple design techniques. However, one should point out that these design simplifications are achieved at the expense of structural complexity. Precisely, the approach suggested by D.H. Owens relies on the critical existence of diagonalizing rational transfer matrices U(s) and V(s). The CL method of design presents inherent difficulties due to the introduction of algebraic functions and of the associated mathematical framework. And finally, the INA method of design relies only on a trial and error procedure to find the rational

transfer matrices U(s) and V(s). In spite of their attractive features, those design techniques may not be easy to apply to high order plants. Also, little mention has been made in our presentation of the requirements that will guide the sequential choice of the $k_i(s)$, i=1,...,m. We have just stated that this choice can be performed in order to satisfy the nominal closed loop stability and to confer desired properties to the closed loop transfer function. The later statement is unclear. Further attention should be given to the design requirements, and more particularly whether the diagonalization methods presented allows us to meet the design requirements as defined in section 2.3. In section 3.2, we will see that in fact the CL and INA methods do not guarantee robustness at the right point in the loop.

2.5 Time-Domain Design Methods

The time-domain approach uses the state space representation:

$$\begin{cases} \dot{\underline{x}} = A\underline{x} + B\underline{u} & \underline{x} \in \mathbb{R}^n, \ \underline{u} \in \mathbb{R}^m \\ \underline{y} = C\underline{x} & \underline{y} \in \mathbb{R}^p \end{cases} \tag{2.35}$$

where $G(s) = C(sI\ A)^{-1} B$ is the transfer function of the system. One of the main achievement of the time-domain approach for control design is the linear quadratic (LQ) design methodology. Consider the system:

$$\begin{cases} \dot{\underline{x}} = A\underline{x} + B\underline{u} \\ \underline{x}(0) = \underline{x}_o \end{cases} . \tag{2.36}$$

The problem is to bring a certain combination of states, say $C\underline{x}(t)$, to zero as quickly as possible. At the same time, we want the size of the input $\underline{u}(t)$ to remain bounded. This objective can be expressed

by a quadratic cost to be minimized:

$$J(u) = \int_0^\infty (\underline{x}^T(t)\ C^T C\ \underline{x}(t) + \underline{u}^T(t)\ Ru(t))\ dt \tag{2.37}$$

where $R = R^T > 0$ is a positive definite matrix and $Q = C^T C \geq 0$ is a non negative definite matrix. The LQ optimal control problem becomes then:

$$\begin{cases} \text{minimize} \quad J(u) = \int_0^\infty (\underline{x}^T(t)\ Q\underline{x}(t) + \underline{u}^T(t)\ R\underline{u}(t))\ dt \\ \text{given } \dot{\underline{x}}(t) = A\underline{x}(t) + Bu(t),\ \underline{x}(0) = \underline{x}_o \ . \end{cases} \tag{2.38}$$

Whenever (A,B) is stabilizable and (C,A) detectable, the problem is solved by a control law $\underline{u}(t) = - G\underline{x}(t)$ where G is given by:

$$G = + R^{-1}\ B^T\ K \tag{2.39}$$

and where K is the unique symmetric postive definite solution of the Algebraic Ricatti equation (ARE):

$$A^T K + KA + Q - KBR^{-1}\ B^T K = 0 \ . \tag{2.40}$$

Then, we have the following properties:

(i) The closed-loop system of figure 2.8 is stable.

(ii) The open-loop transfer function $L(s) = G(sI-A)^{-1}B$ satisfies the Kalman equality:

$$[I + G(-s)]^T\ R[I + G(s)] = R + B^T(-sI-A)^{-T}\ Q(sI-A)^{-1}B, \ \forall s \ . \tag{2.41}$$

The Kalman equality can be used to show [3], [13] that when R is diagonal, the LQ regulator of Fig. 2.8 has simultaneously in each feedback

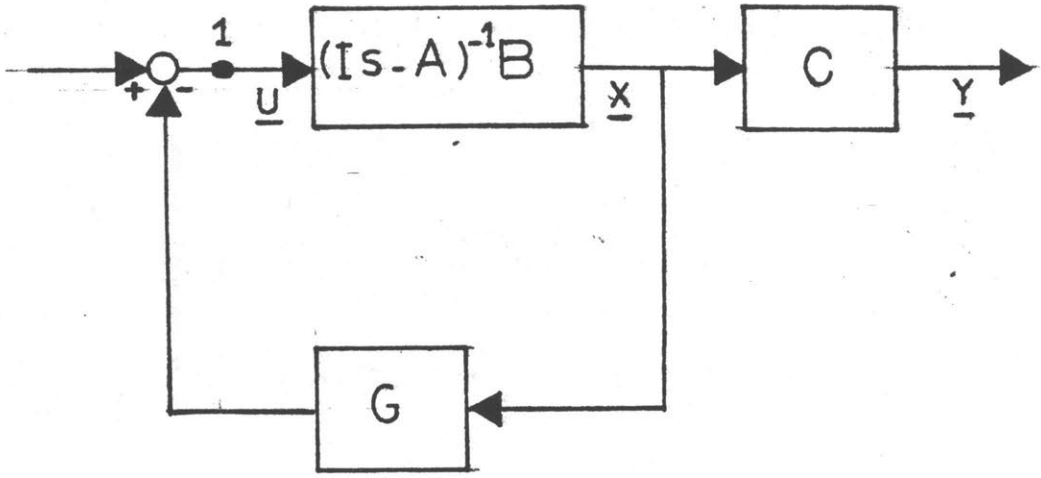

Figure 2.8: Linear quadratic Regulator

loop a quaranteed minimum gain and phase margins given by:

$$G_M \subset]\frac{1}{2}, +\infty[$$
$$PM \subset [-60°, +60°] \quad . \tag{2.42}$$

These quaranteed gain and phase margins hold at the plant input.

Root locus properties for the LQ regulator can also be derived from Kalman's equality when $R = \rho I$, $\rho > 0$

- As ρ becomes large, the closed-loop poles tend to the stable open-loop poles or the mirror image with respect to the imaginary axis of the unstable open-loop poles.

- As ρ becomes small, some of the closed-loop poles remain finite and tend to the stable zeroes of $B^T(-sI-A)^{-T} Q(sI-A)^{-1}B$. Others tend to infinity in Butterworth patterns [9]. LQ design methodologies use the insight given by the root locus in order to select adequately the weighting matrices Q and R. Properties (i) and (ii) will insure the closed-loop stability and robustness properties. Pole placement techniques developed in [10] and [11] provide ways of choosing Q and R in order to satisfy some desired properties of the closed-loop configuration of Fig. 2.8.

However, Kalman's equality shows that when ρ becomes large,

$$I_+ \; G(s) \simeq WC(sI-A)^{-1}B \tag{2.43}$$

where W is an orthonormal matrix. This means that loop shaping is badly constrained by the choice of Q and R as constant matrices. More

poles and zeroes need to be added in our root locus. This is also the case when the LQ methodology is used to solve control problems such as tracking, disturbance rejection, integral control, washout, multiple pole rolloff...etc. (see [13] for example).

This motivates the method proposed by K. Gupta in [12]; using Parseval's theorem, the cost criterion (2.37) can be written in the frequency domain as:

$$J(u) = \frac{1}{2}\int_{-\infty}^{+\infty} [x^H(j\omega)\ Qx(j\omega) + u^H(j\omega)\ Ru(j\omega)]\ d\omega \quad . \tag{2.44}$$

The quadratic weights Q and R are not functions of the frequency and one interpretation of this fact is that state and control excursions at all frequencies are considered equally bad. A natural generalization of (2.39) is to make Q and R functions of frequency;

$$J = \frac{1}{2}\int_{-\infty}^{+\infty} (\underset{\sim}{x}^H(j\omega)\ Q(j\omega)\ \underset{\sim}{x}(j\omega) + \underset{\sim}{u}^H(j\omega)\ R(j\omega)\ \underset{\sim}{u}(j\omega))d\omega \tag{2.45}$$

where $Q(j\omega)$ and $R(j\omega)$ are rational functions of squared frequency ω^2. We assume that

$$\begin{cases} Q(j\omega) = P_1{}^H(j\omega)\ P_1(j\omega) & (2.46.a) \\ R(j\omega) = P_2{}^H(j\omega)\ P_2(j\omega) & (2.46.b) \end{cases}$$

where P_1 is a p x n rational matrix of rank p and P_2 is a m x m rational matrix of rank m. By denoting

$$\begin{cases} \underset{\sim}{x}^1 = P_1(j\omega)\ \underset{\sim}{x} & (2.47.a) \\ \underset{\sim}{u}^1 = P_2(j\omega)\ \underset{\sim}{u} \quad , & (2.47.b) \end{cases}$$

The cost functional (2.45) becomes;

$$J = \frac{1}{2}\int_{-\infty}^{+\infty} (x^{1^H} x^1 + u^{1^H} u^1)\, d\omega \quad . \tag{2.48}$$

The next step is to define the following state space realization of (2.47.a) and (2.47.b).

$$\begin{cases} \dot{z}_1 = F_1 z_1 + G_1 x \\ x^1 = H_1 z_1 + D_1 x \end{cases} \tag{2.49.a}$$

$$\begin{cases} \dot{z}_2 = F_2 z_2 + G_2 u \\ u^1 = H_2 z_2 + D_2 u \end{cases} \tag{2.49.b}$$

Then the LQ optimal control problem (2.38) becomes;

$$\begin{cases} \text{minimize } J(u) = \int_0^\infty [x_1^T,\ z_1^T,\ z_2^T,\ u^T] \begin{bmatrix} D_1^T D_1 & D_1^T H_1 & 0 & 0 \\ H_1^T D_1 & H_1^T H_1 & 0 & 0 \\ 0 & 0 & H_2^T H_2 & H_2^T D_2 \\ 0 & 0 & D_2^T H_2 & D_2^T D_2 \end{bmatrix} \begin{bmatrix} x_1 \\ z_1 \\ z_2 \\ u \end{bmatrix} dt \\ \text{given } \begin{bmatrix} \dot{x}_1 \\ \dot{z}_1 \\ \dot{z}_2 \end{bmatrix} = \begin{bmatrix} A & 0 & 0 \\ G_1 & F_1 & 0 \\ 0 & 0 & F_2 \end{bmatrix} \begin{bmatrix} x_1 \\ z_1 \\ z_2 \end{bmatrix} + \begin{bmatrix} B \\ 0 \\ G_2 \end{bmatrix} u \quad . \end{cases} \tag{2.50}$$

The optimal control law is of the form $u(t) = C_1 x + C_2 z_1 + C_3 z_2$. A block diagram of the completed system is shown in Fig. 2.9. In contrast to the system of Fig. 28, we now have a dynamic compensator. Gupta's

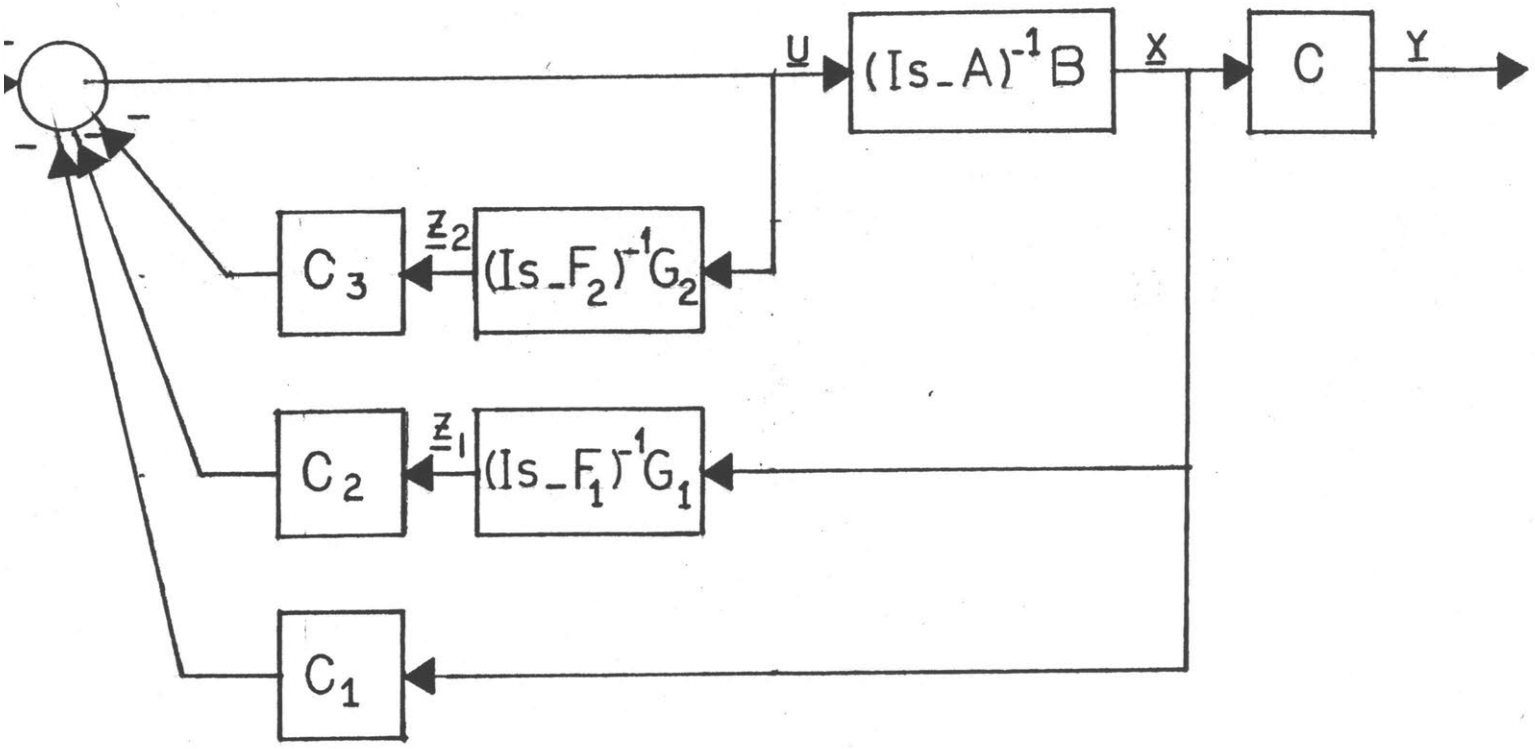

Figure 2.9: The LQ regulator with dynamic compensation

method does not eliminate the need to select quadratic weights. Instead of choosing Q and R is (2.38), we must choose H_1, D_1, H_2 and D_2 in (2.50). The approach he uses is to select $P_1(j\omega)$ and $P_2(j\omega)$ based on "qualitative considerations" and then, the quadratic weights are found automatically once a state space realization of P_1 and P_2 is found. Adequate choices of P_1 and P_2 allow Gupta to treat the tracking, disturbance rejection, integral control, washout, rolloff problems in a systematic way. On the other hand, the poles of $P_1(j\omega)$ and $P_2(j\omega)$ are respectively the poles and zeroes of the compensator. Thus poles and zeroes are added in the root locus by a proper choice of P_1 and P_2. The design if therefore done in the frequency domain. The compensator construction, however, is done in the time domain.

LQ design methodologies have been shown to be efficient to achieve nominal stability. They also provide good robustness guarantees at the plant input, even if that may not always be enough. But their major drawback comes from the fact that they assume that the state vector $\underline{x}$ of the system is available in order to apply the feedback control $\underline{u}(t) = - G\underline{x}(t)$. This assumption can be removed by using Linear Quadratic Gaussian (LQG) regulators.

The state of the system is first estimated by a Kalman filter (see [9] for example). Then a control law, $\underline{u}(t) = - G\hat{\underline{x}}(t)$, is applied where $\hat{\underline{x}}(t)$ is the state estimate of $\underline{x}(t)$ given by the Kalman filter and G is the standard LQ gain matrix. The most remarkable result is that the resulting closed-loop system is stable. Unfortunately, stability

margins for LQG regulators are the same as those for LQ state feedback regulators only at a point inside the LQG compensators. These margins cannot be automatically guaranteed at the physical input or output of the plant. However, when the open-loop plant model is minimum phase, two dual procedures developed in [14] and [15] allow us to recover the guaranteed LQ margins asymptotically at either the input or the output of the open loop plant. This is done in a way such that the loop transfer function at the input or at the output recovers asymptotically a loop transfer function that would be given by the LQ methodology. But the LQ stability margins cannot be generally recovered at both the plant input and output [3].

As for the frequency-domain based design methods, little mention has been made in our presentation of the time domain design methods of the requirements that will guide the choice of the weighting matrices. We just indicated that this choice would be conducted in order to confer desired properties to the root loci or according to some "qualitative considerations". Further attention should be given to this choice and in particular to what choices of weighting matrices will allow us to meet the design requirements defined in Section 2.3.

2.6 Concluding Remarks

The presentation of Section 2.3 has allowed us to derive typical design requirements for multivariable feedback systems. These design requirements are defined in terms of the singular values of the loop transfer function and of nominal closed-loop stability. Thus, an "ideal"

method of design requires that we should choose a compensator K(s) such that the loop gains $\sigma_i(G(s)\ K(s))$ and $\sigma_i(K(s)\ G(s))$ are shaped properly in function of the frequency and such that the closed-loop system of Fig. 2.1 is stable. Several frequency domain-based design methods have been presented in section 2.4. They reduce the MIMO feedback design problem to a sequence of SISO feedback design problems by diagonalizing the plant. But the loop by loop designs do not seem to address the design requirements as they were defined in section 2.3. Further attention should be given to this point and more particularly whether the diagonalization methods would allow us to meet the design requirements as defined in section 2.3. This will be done in Chapter 3.

We then turned our attention to time domain based design methods. We have seen that they achieve nominal stability for the closed-loop system. However, it appeared that we had little insight in the choice of weighting matrices in order to meet the design requirements as defined in section 2.3. Since the key element of time domain design methods is the LQ methodology, the scope of these methods would be enhanced if we knew how to apply LQ technqiues in order to meet the design requirements of section 2.3. More specifically, this motivates the need for obtaining systematic ways of choosing the quadratic weights so as to be able to shape the singular values of the open-loop transfer function. This problem will be examined in Chapter 4.

CHAPTER 3: DIAGONALIZATION METHODS

3.1 Introduction

The purpose of this chapter is to study multivariable feedback design methods based on diagonalization. The goal of these methods is to reduce the multivariable feedback design problem to a sequence of scalar design problems, for which a large body of well developed tools exist (e.g. "Classical Control"). The idea is therefore to transform the nominal plant G(s) into an exactly diagonal system or a diagonally dominant system. Classical SISO methods are then applied to each diagonal element treated as a separate SISO loop. In this chapter, we assume that the feedback design requirements are the same as in Section 2.3, i.e., given the nominal plant model G(s) and a multiplicative model error structure, we must obtain high loop gains at low frequencies, a loop gain reduction at high frequencies and ensure the nominal stability of the closed-loop system.

In section 3.2, existing diagonalization methods are evaluated in terms of their ability to satisfy these design requirements. It is shown that these methods work reliably only for a restricted class of systems, namely normal systems. However, their range of applicability would be enhanced if the transformation matrices involved in the diagonalization of the nominal plant were chosen to be unitary matrices. The discussion of this section is not original and relies heavily on the work of J.J. Doyle and G. Stein in [1].

In Section 3.3, we show that there exists a way to choose properly the transformation matrices by considering the singular value decomposition

of the nominal system. More precisely, the nominal system can be diagonalized by using the inverse of the right and left singular vectors matrices. This allows to consider a compensator structure for which the singular values of the open-loop transfer function can be shaped individually in function of the frequency. This can be done when the loop is broken at the plant input as well as at the plant output. Further results on the singular value decomposition of the plant model are obtained in Section 3.3.2.a). They allow us to develop in Section 3.3.2.b) a Nyquist stability criterion for the closed-loop system associated to our compensator structure.

The results of Section 3.3 enable us in Section 3.4 to obtain a design procedure which can be used to satisfy the design requirements. Since the right and left singular vectors matrices are non rational unitary matrices, we approximate them by real constant matrices in a certain frequency range. An approximation algorithm is presented in Section 3.4.1, and the overall design procedure is discussed in Section 3.4.2. The discussion of Section 3.4.3 shows that this design procedure may be limited by our approximation scheme.

In Section 3.5, the approximation problem for unitary tranformation matrices is considered. Some desirable features of the approximation scheme are discussed in Section 3.5.2. In Section 3.5.3 we present an approximation scheme which leads to an alternative design procedure.

The Section 3.6 contains some concluding remarks about the results of this chapter.

3.2 Characteristic Loci and Inverse Nyquist Array Methods

The CL and INA methodologies for the design of MIMO feedback control systems take advantage of the large amount of well developed tools for SISO control design by reducing the MIMO design problem to a sequence of independent SISO design problems. To make this precise, given the nominal plant model G(s), both the CL and INA methods assume the existence of matrices U(s) and V(s) such that $\hat{G}(s) = U(s)\, G(s)\, V(s)$ is bounded and is either diagonal or diagonal dominant for all $s \in D_R$, where D_R is the Nyquist contour of Fig. 2.5. If $\hat{G}(s)$ is diagonally dominant, then the diagonal matrix $\hat{G}_d(s)$ given by:

$$\hat{G}_d(s) = \text{diag}\,[\hat{g}_{11}(s),\ \hat{g}_{22}(s),\ldots,\hat{g}_{nn}(s)] \tag{3.1}$$

can be used as a good approximation to $\hat{G}(s)$ within bounds specified by the off-diagonal elements of $\hat{G}(s)$. For the purpose of this section, we will assume exact diagonalization of $\hat{G}(s)$ by U(s) and V(s) since all observations to be made will apply also when the system is only diagonal dominant. In this case, the diagonal elements $\hat{g}_{ii}(s)$ are eigenvalues $\lambda_i(G(s))$ of G(s) and U(s), V(s) are the matrices of its left and right eigenvectors. The fact that these matrices are not generally rational function in s is an issue which we will not discuss here.

The form of the compensator $G_c(s)$ proposed by the CL and INA methods is shown in Fig. 3.1 where K(s) is a diagonal matrix given by:

$$K(s) = \text{diag}\,[k_1(s),\ k_2(s),\ldots,k_n(s)] \quad . \tag{3.2}$$

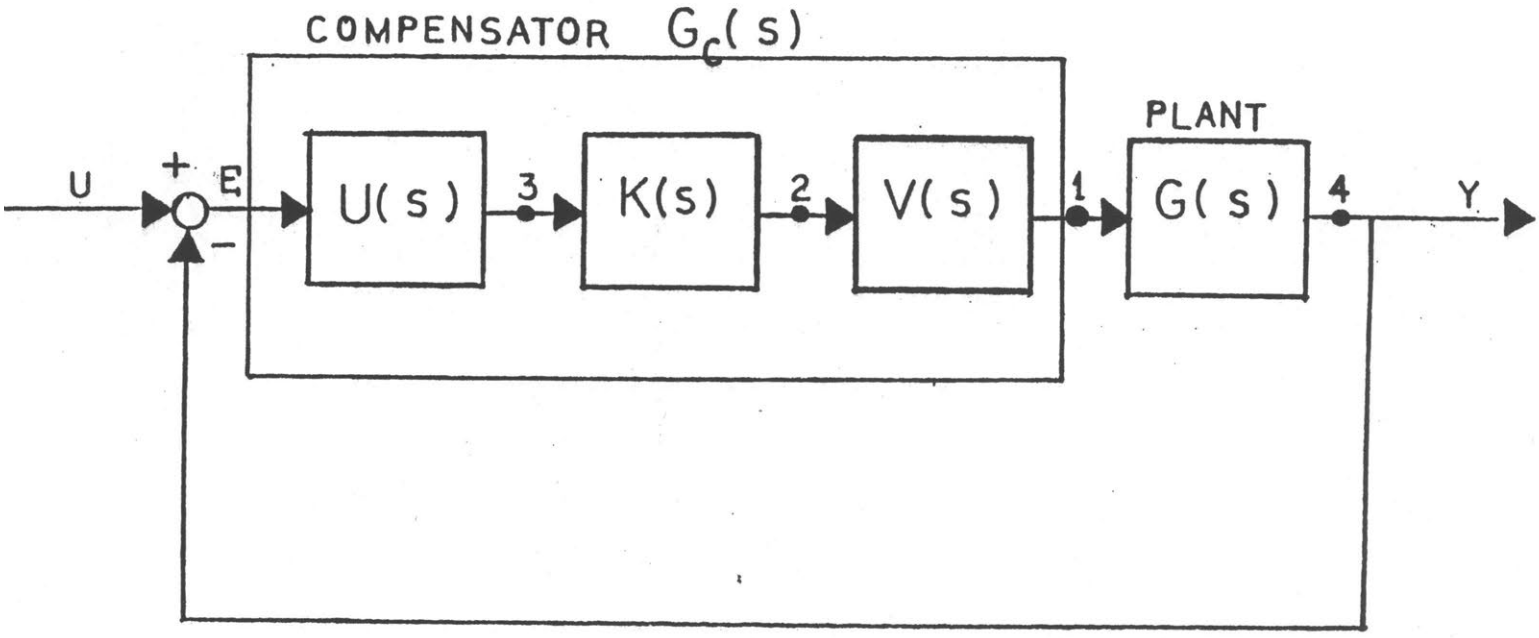

Fig. 3,1: Compensator used by INA and CL methods.

The loop transfer transfer function calculated at points i, $1 \leq i \leq 4$, is denoted by $G_i(s)$ where

$$I + G_1(s) = I + V(s)\, K(s)\, U(s)\, G(s) = V(s)\, \text{diag}\,[1 + k_i(s)\, \lambda_i(s)]\, U(s) \tag{3.3}$$

$$I + G_2(s) = I + G_3(s) = \text{diag}\,[1 + k_i(s)\, \lambda_i(s)] \tag{3.4}$$

$$I + G_4(s) = I + G(s)\, V(s)\, K(s)\, U(s) = V(s)\, \text{diag}\,[1 + \lambda_i(s)\, k_i(s)]\, U(s)\ . \tag{3.5}$$

As indicated in Section 2.4, the CL and INA methods use (3.4) to design the compensator $G_c(s)$, by selecting each $k_i(s)$ in $K(s)$ as the appropriate compensator for each of the SISO systems corresponding to the diagonal elements of $\hat{G}(s)$, namely $\lambda_i(s)$, i=1,...n.

From the fact that the smallest singular value of a matrix is bounded by the smallest magnitude of its eigenvalues, the relations (3.3) and (3.5) show that at the physically meaningful points 1 and 4 (plant input and plant output) we have:

$$\underline{\sigma}[I + G_1(s)] = \underline{\sigma}[I + G_c(s)\, G(s)] < |1 + \lambda_i(s)\, k_i(s)|_{\min} \tag{3.6}$$

and

$$\underline{\sigma}[I + G_4(s)] = \underline{\sigma}[I + G(s)\, G_c(s)] < |1 + \lambda_i(s)\, k_i(s)|_{\min}\ . \tag{3.7}$$

In the light of our design requirements, it is clear from (3.6) and (3.7) that the high loop gains requirement are met by the CL and INA methods

by considering $|1 + \lambda_i(s)\ k_i(s)|_{min}$ instead of $\underline{\sigma}[I + G_1(s)]$ or $\underline{\sigma}[I + G_4(s)]$. However, $\underline{\sigma}[I + G_1(s)]$ or $\underline{\sigma}[I + G_4(s)]$ could be very small and the performance poor even though $|1 + \lambda_i(s)\ k_i(s)|_{min}$ is large enough to indicate good performance.

The same problem occurs with the robustness conditions. The CL and INA methods yield by design good robustness margins at point (2) and (3), i.e. inside our compensator. The key question is whether these margins still hold at the plant input and output (points (1) and (4)). For the loop broken at points (1) and (4) respectively, we have

$$[I + G_1^{-1}(s)] = [I + G_4^{-1}(s)] = V(s)\ [I + \text{diag}\ (\frac{1}{\lambda_i(s)k_i(s)})]\ U(s)\ . \tag{3.8}$$

Hence,

$$\underline{\sigma}[I + (G_c(s)\ G(s))^{-1}] \leq |1 + \frac{1}{\lambda_i(s)k_i(s)}|_{min} \tag{3.9}$$

and

$$\underline{\sigma}[I + G(s)\ G_c(s))^{-1}] \leq |1 + \frac{1}{\lambda_i(s)\ k_i(s)}|_{min}\ . \tag{3.10}$$

from the relations (3.9) and (3.10), the CL and INA methods satisfy robustness requirements by considering

$$|1 + \frac{1}{\lambda_i(s)k_i(s)}|_{min} \quad \text{instead of } \underline{\sigma}[I + (G_c(s)\ G(s))^{-1}]$$

$$\text{or } \underline{\sigma}[I + (G(s)\ G_c(s))^{-1}]$$

However $\underline{\sigma}[I + (G_c(s)(G(s))^{-1}]$ or $\underline{\sigma}[I + (G(s)\ G_c(s))^{-1}]$ could be very small and the resulting design dangerously sensitive to uncertainties even though the term $\left|1 + \frac{1}{\lambda_i(s)k_i(s)}\right|_{min}$ is large enough to indicate good robustness.

From the previous discussion, the CL and INA design methods do not produce automatically controllers with good performance and with good robustness characteristics. However, this should not be perceived as a universal indictment of these methods. Our argumentation loses its strength when the singular value|eigenvalue bounds in relations (3.6) - (3.9) - (3.10) are tight. From relations (3.3) - (3.5) - (3.8), it is clear that the inequalities in (3.6) - (3.9) - (3.10) become equalities whenever the matrices U(s) and V(s) are unitary matrices, i.e. such that $U^H(s)\ U(s) = V^H(s)\ V(s) = I$. The class of systems G(s) for which the set of eigenvectors form an orthonormal basis is called <u>normal systems</u> and is characterized by the relation

$$G(s)\ G^H(s) = G^H(s)\ G(s)\ ,\ \forall s\ . \tag{3.11}$$

Therefore for these type of systems, the CL and INA design methods will prove to be efficient and reliable. Furthermore, the extent to which the relation $V^H(s) = U(s)$ is satisfied which indicates that U(s) and V(s) are unitary, can be used as a measure of the reliability of the CL and INA design methods.

From a more general point of view, the restrictions imposed on the validity of diagonalization methods point to the necessity of requiring

that the transformation matrices U(s) and V(s) should be unitary matrices as well as being exactly or approximately the left and right eigenvectors matrices of the plant model G(s). Since the designer has no control over G(s), only a special class of systems can be compensated with these diagonalization methods. However, it is clear that these restrictions would be avoided if we could choose in a systematic way for any plant G(s), the transformations U(s) and V(s) of our compensator in Fig. 3.1 such that:

- $\hat{G}(s) = U(s)\ G(s)\ V(s)$ is bounded and is either diagonal or diagonally dominant for all $s \in D_R$, where D_R is the Nyquist contour of Fig. 2.5,
- U(s) and V(s) are unitary.

The following discussion will show that this can be done.

3.3 Diagonalization via SVD Decomposition

3.3.1 Basic Structure Considered

The discussion which precedes has shown clearly that in order to meet the design requirements discussed in Section 2.3 with a diagonalization methods, it is mandatory that the transformation matrices be unitary or at least almost unitary. Furthermore, this unitarity property should not restrict the class of systems that can be considered. Therefore, the problem reduces to find for a plant G(s) some unitary matrices U(s), V(s) such that $\hat{G}(s) = U(s)\ G(s)\ V(s)$ is bounded and is either diagonal or diagonally dominant for all $s \in D_R$ where D_R is the Nyquist contour of Fig. 2.5. Our knowledge of matrix transformations tells us

that the singular value decomposition (SVD) of the plant G(s) will satisfy this objective. Indeed, if we consider a nxn transfer function G(s), the SVD of G(s) is given by

$$G(s) = U^H(s)\ \Sigma\ (s)\ V(s) \tag{3.12}$$

where $U(s) = [\underline{u}_1(s),\ldots,\underline{u}_n(s)]$ and $V(s) = [\underline{v}_1(s),\ldots,\underline{v}_n(s)]$ are unitary matrices, i.e. $U^H(s)\ U(s) = V^H(s)\ V(s) = I$ and where $\Sigma(s) = \text{diag}\ [\sigma_1(s),\ldots,\sigma_n(s)]$. Then, define $\hat{G}$ such that:

$$\hat{G}(s) = U(s)\ G(s)\ V^H(s)\ .$$

From the properties of U(s), V(s) we have $\hat{G}(s) = \Sigma(s)$ and therefore $\hat{G}(s)$ is exactly diagonal for all $s \in D_R$. Furthermore since G(s) corresponds to a well defined LTI system, G(s) is bounded for all $s \in D_R$. Since this property is conserved by pre-multiplication and post-multiplication by unitary matrices, $\hat{G}(s)$ is also bounded for all $s \in D_R$. Thus the SVD decomposition seems to provide a satisfactory diagonalization method. In the sequel, we will discuss in more details the properties of the diagonalization approach based on the SVD of G(s).

For the sake of simplicity, we will assume that G(s) is a nxn square matrix, the extension to the case of non square plant model being straightforward. The SVD of G(s) will be then $G(s) = U^H(s)\ \Sigma(s)\ V(s)$ with U(s), V(s) and $\Sigma(s)$ as in (3.12). The fact that U(s) and V(s) are not generally rational functions of s and therefore do not correspond to well-defined LTI systems is an issue that we will not consider yet.

Some attention will be given to this problem in Sections 3.4 and 3.5.

Let us consider the feedback configuration of Fig. 3.2 where the compensator is $G_c(s) = V^H(s)\, K(s)\, U(s)$ and where $K(s)$ is chosen diagonal, i.e. $K(s) = \text{diag}[k_1(s),\ldots,k_n(s)]$. If the loop transfer function calculated at point i, $1 \leq i \leq 4$, is denoted by $G_i(s)$, then:

$$G_1(s) = V^H(s)K(s)U(s)G(s) = V^H(s)\ \text{diag}\,[k_1(s)\sigma_1(s)\ldots,k_n(s)\sigma_n(s)]\ V(s) \tag{3.13}$$

$$G_2(s) = K(s)U(s)G(s)V^H(s) = \text{diag}\,[k_1(s)\sigma_1(s),\ldots,k_n(s)\sigma_n(s)] \tag{3.14}$$

$$G_3(s) = U(s)G(s)V^H(s)K(s) = \text{diag}\,[k_1(s)\sigma_1(s),\ldots,k_n(s)\sigma_n(s)] \tag{3.15}$$

$$G_4(s) = G(s)V^H(s)K(s)U(s) = U^H(s)\ \text{diag}\,[k_1(s)\sigma_1(s),\ldots,k_n(s)\ \sigma_n(s)]U(s) \tag{3.16}$$

This set of equations shows some important properties of our feedback configuration. First, the loop transfer functions at point (2) and (3) are exactly diagonal as expected from any exact diagonalization approach. But since the singular values of the loop transfer function calculated <u>either at the plant input or at the output</u> are equal to $\sigma_i(s)|k_i(s)|$, $i = 1,\ldots n$, the diagonal values of $G_2(s)$ and $G_3(s)$ give us an <u>exact knowledge</u> of the singular values at the plant input and output. This shows also that provided that our configuration is stable, it will have the same robustness at the plant input and output. Finally the loop gains $\sigma_i(s)|k_i(s)|$, $i=1,\ldots,n$, can be determined individually by choosing respectively the diagonal elements of $K(s)$ in a loop by loop fashion.

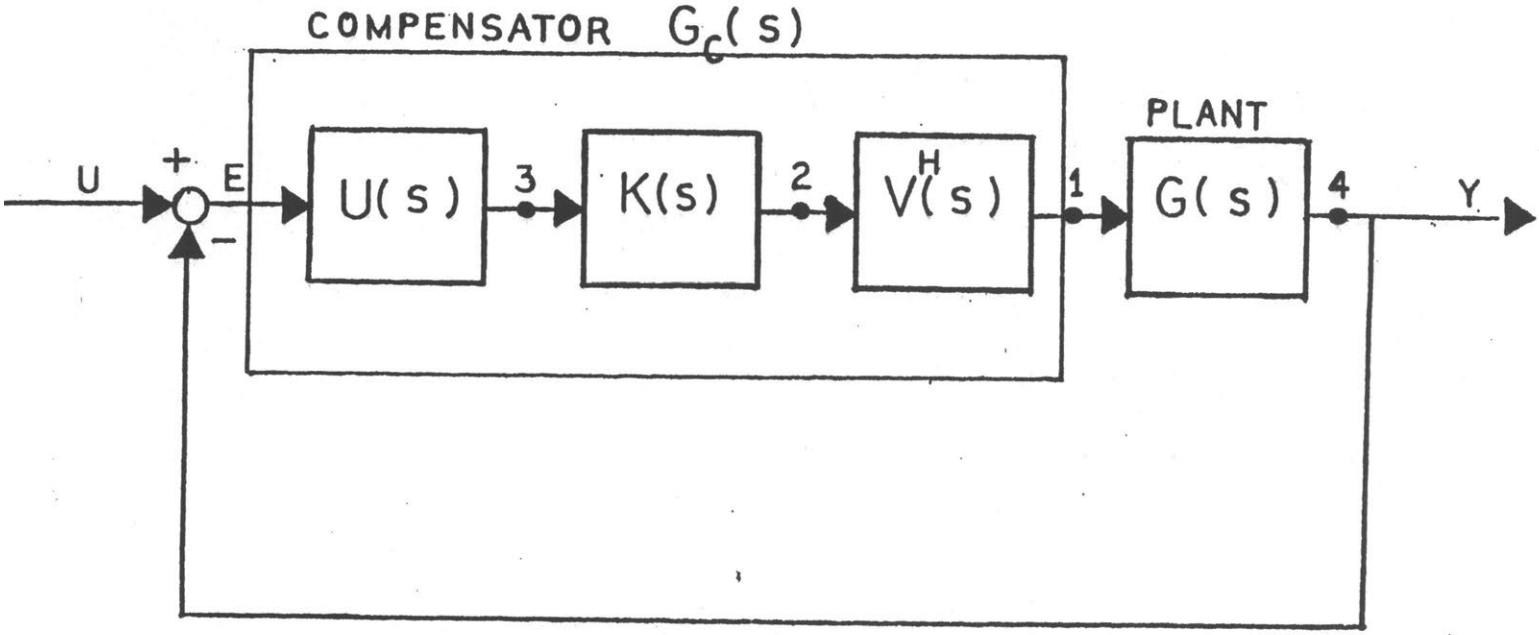

Fig. 3.2: Diagonalization via SVD: feedback configuration.

Assuming that the closed-loop system is stable, let us consider the robustness and performance measures that could be selected for our configuration.

performance measure $\underline{\sigma}[I + G_2(j\omega)] = \underline{\sigma}[I + G_3(j\omega)]$

$$= \left|1 + k_1(j\omega)\ \sigma_i(j\omega)\right|_{\min} . \qquad (3.17)$$

Robustness measure

plant input: $$\underline{\sigma}[I + G_i^{-1}(j\omega)] = \left|1 + \frac{1}{k_i(j\omega)\sigma_i(j\omega)}\right|_{\min} . \qquad (3.18)$$

plant output: $$\underline{\sigma}[(I + G_4^{-1}(j\omega)] = \left|1 + \frac{1}{k_i(j\omega)\sigma_i(j\omega)}\right|_{\min} . \qquad (3.19)$$

We see clearly that a loop by loop choice of the elements of K(s) will allow us to carry out exactly the performance|robustness tradeoff imposed by the design requirements. This is what was expected by choosing unitary transformation matrices in order to avoid the drawbacks of existing diagonalization methods. Therefore a diagonalization approach using the configuration of Fig. 3.2 seems adequate to meet design performance and robustness requirements. But these requirements make no sense if the closed-loop system is unstable. Thus we need to study under what conditions the configuration of Fig. 3.2 will be stable.

3.3.2 Nyquist Stability Criterion

In order to study the stability conditions for the configuration of Fig. 3.2, we will first discuss some further properties of the SVD

of G(s).

3.3.2a) Further Results on the SVD of G(s)

The singular values $\sigma_i(s)$, i=1,...,n, are the square roots of the eigenvalues of $G^H(s)\ G(s)$. For any complex frequency s, they are given by the positive solutions of the characteristic equation

$$\det\ [\sigma^2(s)\ I - G^H(s)\ G(s)] = \Delta_1(\sigma^2, s) = 0 \quad . \tag{3.20}$$

Here G(s) is a nxn square matrix values function of s whose entries are rational. Since G(s) is a transfer function matrix of a real LTI system, we have

$$G(\bar{s}) = \overline{G(s)} \text{ for all } s \ . \tag{3.21}$$

Therefore $G^H(s) = G^T(\bar{s})$ will be a nxn square matrix valued function of $\bar{s}$ whose elements are rational functions in $\bar{s}$. An alternative point of view is to consider the characteristic equation

$$\Delta_2(\Sigma, s, z) = \det\ (\Sigma I - G^T(z)\ G(s)) = 0 \tag{3.22}$$

where z and s are complex numbers. For the choice of $z = \bar{s}$, the solutions $\Sigma(s,z)$ given by (3.22) are the squared singular values of G(s):

$$\Delta_2(\Sigma, s, z)\Big|_{z=\bar{s}} = \Delta_1\ (\sigma^2, s) \ . \tag{3.23}$$

Since $G^T(z)$ is a rational transfer function in z, the elements of $G^T(z)\ G(s)$ are rational functions of s and z.

Since all observations to be made apply to each irreducible factor of $\Delta_2(\Sigma, s, z)$, we will assume for simplicity that $\Delta_2(\Sigma, s, z)$ is irreducible over the field of rational functions of s and z. Then Δ_2 (Σ, s, z) has the form:

$$\Delta_2 (\Sigma, s, z) = \Sigma^n + a_1(s, z)\, \Sigma^{n-1} + \ldots + a_n(s, z) \tag{3.24}$$

where the coefficients $a_i(s,z), i=1,\ldots,n$, are rational functions in s and z. If $b_o(s,z)$ is the least common denominator of these coefficients, equation (3.24) can be put in the form:

$$b_o(s,z)\, \Sigma^n + b_1(s,z)\, \Sigma^{n-1} + \ldots + b_n(s,z) = 0 \tag{3.25}$$

where the coefficients $b_i(s,z)$, $i = 1,\ldots,n$, are now polynomials in s and z. The function $\Sigma(s,z)$ defined by (3.25) is called an algebraic function [21]. Algebraic functions are generalizations of the concept of a simple function of complex variables. The theory of algebraic functions shows that $\Sigma(s,z)$ has for domain of definition a Riemann domain constructed by appropriately piecing together a number of copies of the domain C^2 equal to the order of the defining equation (3.25). Then $\Sigma(s,z)$ defines a single valued analytic function from the Riemann domain on to the set of complex numbers. Finite poles and zeroes of the algebraic function $\Sigma(s,z)$ are defined by the roots of the equations

$$b_o(s,z) = 0 \tag{3.26}$$

and

$$b_n(s,z) = 0 \tag{3.27}$$

respectively, and may be located on the Riemann domain. The algebraic function $\Sigma(s,z)$ has branch points wherever the defining equation (3.22) has repeated roots. They are determined by the discriminant equation

$$p(s,z) = 0 \tag{3.28}$$

where $p(s,z)$ is the polynomial in s and z obtained by eliminating Σ between $\Delta_2(\Sigma,s,z) = 0$ and $\frac{\partial}{\partial\Sigma}[\Delta(\Sigma,s,z)] = 0$. The collection of branch points may be viewed as a collection of branch sets. In every simply connected region of C^2 which does not contain any part of branch sets, the theory of algebraic functions shows that the values of the characteristic function $\Sigma(s,z)$ form a set of locally distinct analytic functions $\{\Sigma_i(s,z),\ i=1,...n\}$. Each of these locally distinct analytic functions is called a branch of the algebraic function $\Sigma(s,z)$. In particular for $\bar{s} = z$, the functions $\{\Sigma_i(s,z),\ i=1,...n\}$ will be analytic in s. Furthermore, since the branch sets given by (3.28) reduce to the points of the complex plane satisfying:

$$p(s,\bar{s}) = 0 \tag{3.29}$$

the functions $\{\Sigma_i(s,\bar{s}),\ i=1,...n\}$ form a set of locally distinct analytic functions in every region of the complex plane which does not contain solutions of (3.29).

It follows from this discussion and from the fact that for any square matrix G(s), the set of eigenvalues of $G^H(s)\ G(s)$ and $G(s)\ G^H(s)$ are identical, that at almost all points of the complex plane the nxn rational transfer function G(s) can be expressed as

$G(s) = U^H(s)\ \Sigma(s)\ V(s)$ where

(i) The functions $\sigma_i(s)$, i=1,...n are a set of analytic functions whose values at any specific complex frequency s are the square root of the eigenvalues of the matrix $G^H(s)\ G(s)$. These eigenvalues are the values for $\bar{s} = z$ of a complete set of branches for the algebraic function associated to the matrix $G^T(z)\ G(s)$ by the characteristic equation (3.22).

(ii) The vectors $\underline{y}_i(s)$, i=1,...n, (respectively $\underline{u}_i(s)$, i=1,..,n) consitute an orthonormal set of vector valued functions of s whose values at any specific complex frequency s are eigenvectors of the complex matrix $G^H(s)\ G(s)$ (respectively $G(s)\ G^H(s)$). The individual component functions of these vectors are analytic functions on the same domains as the appropriate singular value functions $\sigma_i(s)$.

(iii) The expression (3.12) is well defined at all points of the complex plane except at the branch points given by (3.29).

These results are a straightforward application to the eigenvalues of $G^H(s)\ G(s)$ and $G(s)\ G^H(s)$ of the theory of algebraic functions [21], [22]. But the structure of the characteristic equation (3.20) will allow us to obtain further properties.

Theorem 3.1: Consider the nxn square transfer function matrix G(s). For any value s_o of the complex plane, the set of singular values $\{\sigma_i(s_o),\ i=1,...,n\}$ is identical to the set of singular values $\{\sigma_i(\bar{s}_o),\ i=1,..,n\}$ where $\bar{s}_o$ denotes the complex conjugate of s_o.

Proof: Consider the characteristic equation (3.20) for the value $s = s_o$, i.e.

$$\Delta_1(\sigma^2, s_o) = \det [\sigma^2 I - G^H(s_o)\, G(s_o)] = 0.$$

Since for any square matrices A we have det A = det A^T, we get

$$\Delta_1(\sigma^2, s_o) = \det [\sigma^2 I - G^T(s_o)(G^H)^T(s_o)] = 0 \quad .$$

But for all complex values of s we have $G(s) = \overline{G(\bar{s})}$, so that

$$G^T(s_o) = G^H(\bar{s}_o) \text{ and } (G^H)^T(s_o) = G(\bar{s}_o).$$

Thus we find

$$\Delta_1(\sigma^2, s_o) = \det [\sigma^2 I - G^H(\bar{s}_o)\, G(\bar{s}_o)] = \Delta_1(\sigma^2, \bar{s}_o)$$

The characteristic equations giving the singular values at $s = s_o$ and $s = \bar{s}_o$ are identical. Therefore they yield the same solutions. Q.E.D.

The theorem 3.1 implies that the branch points given by equation (3.29) occur in complex conjugate pairs or are real.

Theorem 3.2 Consider the nxn square transfer function matrix G(s). There exists a singular value decomposition of G(s), $G(s) = U^H(s)\, \Sigma(s)\, V(s)$ such that the singular values $\sigma_i(s)$ for i = 1,...,n, satisfy the relation relation

$$\sigma_i(s) = \sigma_i(\bar{s}) \quad \forall s,\ i = 1,\ldots,n \tag{3.30}$$

A proof using only straightforward argments based on polynomial and matrix properties is given in appendix. For our purpose we will only try to show on a simple example why this theorem holds. Consider the case of a 2 x 2 matrix and let us examine its singular values for

$s = j\omega$. Since by theorem 3.1, the set of singular values for each $s_o = j\omega_o$ is identical to the set of singular values for $s = -j\omega_o$, a typical plot of singular values along the $j\omega$-axis can be represented as in Fig. 3.3. Obviously, the singular values $\sigma_a(j\omega)$ and $\sigma_b(j\omega)$ do not satisfy the relation (3.30). But a simple re-indexation

$$\begin{cases} \sigma_2(j\omega) = \sigma_a(j\omega) & \omega \geq -\omega_1 \\ \sigma_2(j\omega) = \sigma_b(j\omega) & \omega \leq -\omega_1 \end{cases} \qquad \begin{cases} \sigma_1(j\omega) = \sigma_b(j\omega) & \omega \geq -\omega_1 \\ \sigma_1(j\omega) = \sigma_a(j\omega) & \omega \leq -\omega_1 \end{cases}$$

is such that for every values of $s = j\omega$, $\sigma_1(j\omega)$ and $\sigma_2(j\omega)$ are the singular values of $G(j\omega)$ and $\sigma_1(j\omega)$, $\sigma_2(j\omega)$ satisfy the relation (3.30). Moreover the indexation $\sigma_1(j\omega)$, $\sigma_2(j\omega)$ corresponds to the singular values arranged in a descending order. Thus as in Desoer and Wang [20], for values along the imaginary axis, theorem 3.2 can be viewed as stating that there exists a proper indexation of the functions $\sigma_i^2(j\omega)$ between branch points, such that the relation (3.30) is satisfied for $s = j\omega$.

More generally, it can be seen that the indexation corresponding to the singular values arranged in descending order is such that the relation (3.30) is satisfied for values along the $j\omega$-axis. This turns out to be helpful for finding a SVD of $G(s)$ as in theorem 3.2 for values of s along the $j\omega$ axis since computer packages usually give the singular values arranged in descending order.

However, if we do not restrict our attention to the values of s along the imaginary axis, the relation (3.30) can be satisfied as shown

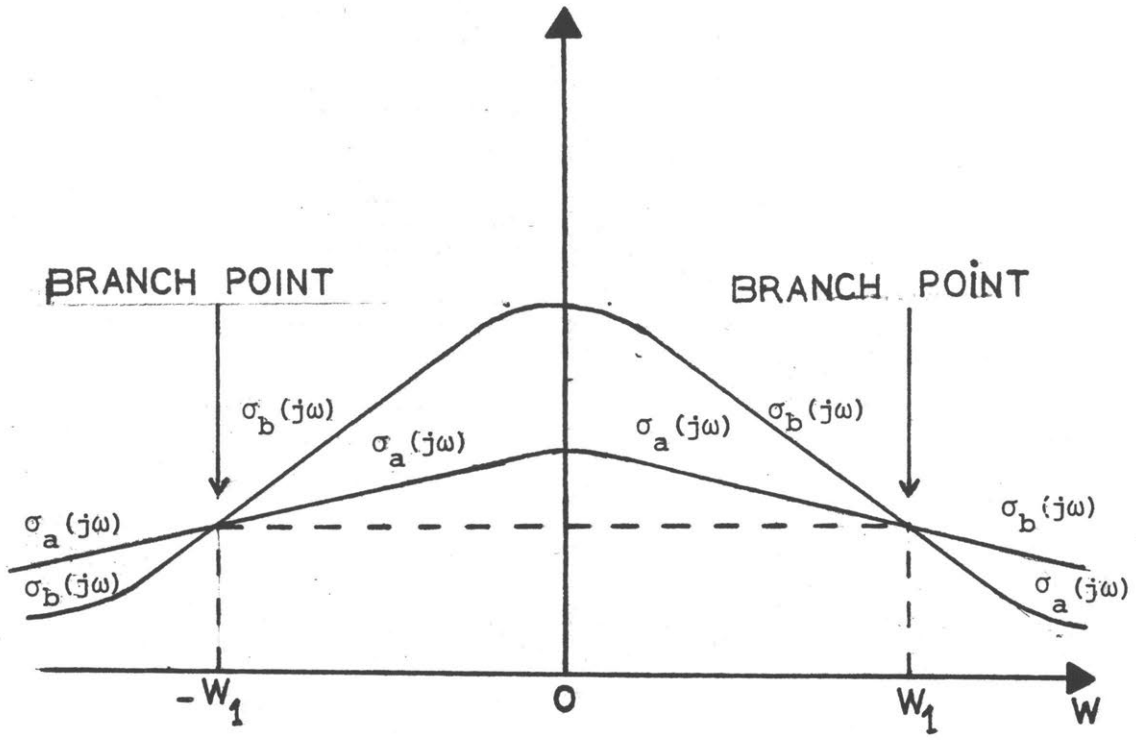

Fig. 3.3: Typical representation of singular values for $s = j\omega$ in 2 x 2 case.

in Appendix.

3.3.2.b Nyquist Stability Criterion Derivation

The result of theorem 3.2 allows us to assume that the configuration of Fig. 3.2 has been obtained from a particular SVD of G(s) satisfying the relation (3.30). Furthermore it will be assumed in the sequel that the diagonal compensator K(s) is a rational transfer function in s.

Let $N(\Omega, f(s), C)$ denote the number of clockwise encirclements of the point Ω by the locus f(s) as s goes around the closed contour C in the clockwise direction. Then the multivariable Nyquist theorem applied to the configuration of Fig. 3.2 states that:

- The system of Fig. 3.2 is closed loop stable if and only if for R sufficiently large

$$N(0, \det [I + G_c(s)\, G(s)], D_R] = - P \tag{3.31}$$

where P is the number of unstable open loop poles and D_R is the Nyquist contour of Fig. 2.5 which encloses all P unstable open loop poles.

Let us examine in more detail the relation (3.31) of the stability theorem. $I + G_c(s)\, G(s)$ is such that

$$\det [I + G_c(s)\, G(s)] = \det [I + V^H(s)\, K(s)\, \Sigma(s)\, V(s)]$$

$$= \det [V^H(s)\, (I + K(s)\, \Sigma(s))\, V(s)]$$

$$= \prod_{i=1}^{n} (1 + k_i(s)\, \sigma_i(s)) \tag{3.32}$$

since V(s) is unitary and $\Sigma(s)$, K(s) are diagonal matrices. Therefore,

the stability requirement (3.31) can be written as

$$N(0, \prod_{i=1}^{n} (1 + k_i(s)\ \sigma_i(s)),\ D_R) = -P \quad . \tag{3.33}$$

For all $i=1,\ldots,n$, we have by assumption $\sigma_i(s) = \sigma_i(\bar{s})$ and $k_i(s) = \overline{k_i(\bar{s})}$ for all s. Therefore since the singular values are real numbers, we have

$$1 + k_i(\bar{s})\sigma_i(\bar{s}) = \overline{1 + k_i(s)\ \sigma_i(s)} \quad i=1,\ldots,n,\ \forall s \ . \tag{3.34}$$

This equation tells us that the loci $(1 + k_i(s)\ \sigma_i(s))$ $i=1,\ldots,n$, as s follows the Nyquist contour D_R of Fig. 2.5 will be symmetric with respect to the real axis. Furthermore, from our choice of $K(s)$, $(1 + k_i(s)\ \sigma_i(s))$ $i=1,\ldots,n$ are strictly real for real values of s. As shown by Desoer and Wang in [20], this implies that the loci $1 + k_i(s)\ \sigma_i(s)$, $i=1,\ldots,n$ are closed and symmetric with respect to the real axis as s goes along D_R. This allows to reformulate the condition (3.33)

$$\begin{aligned} N(0, \prod_{i=1}^{n} (1 + k_i(s)\ \sigma_i(s)),\ D_R) &= \sum_{i=1}^{n} N(0,\ 1 + k_i(s)\ \sigma_i(s),\ D_R) \\ &= \sum_{i=1}^{n} N(-1,\ k_i(s)\ \sigma_i(s),\ D_R) = -P \end{aligned} \tag{3.35}$$

and to derive a Nyquist stability criterion for the configuration of Fig. 3.2.

Theorem 3.3: Nyquist Stability Criterion

Assuming that the configuration of Fig. 3.2 has been obtained from a

particular SVD of G(s) satisfying (3.30) and that K(s) is a rational transfer function in s, the system of Fig. 3.2 is closed-loop stable if and only if for R sufficiently large

$$\sum_{G-1}^{n} N(-1, k_i(s)\sigma_i(s), D_R) = -P$$

where P is the number of unstable open-loop poles and D_R is the Nyquist contour of Fig. 2.5.

Proof: This is a consequence of relations (3.31), (3.33), (3.35).

3.3.3 Concluding Remarks

Given that the assumptions of Theorem 3.3 are satisfied, by choosing the elements of K(s) loop by loop, we will be able

(i) to assess the stability of the configuraiton of Fig. 3.2 using the stability criterion of theorem 3.3,

(ii) to carry out a performance/robustness tradeoff with the exact design requirements described in Section 3.3.1.

Therefore our diagonalization approach using a particular SVD of the plant G(s) suggests a method of design well adapted to meet the design requirements defined in Section 2.3.

But we have assumed throughout this section a compensator $G_c(s)$ of the form, $G_c(s) = V^H(s)K(s)U(s)$. Unfortunately, the matrices U(s) and $V^H(s)$ are not generally rational function matrices in s and therefore

do not correspond to realizable LTI systems. Therefore, our method of design would yield compensators that cannot be physically implemented. Some attention will be given to this implementation problem in the following sections.

3.4. A Basic Design Procedure

The analysis of the previous section has shown that the behavior of the closed-loop system of Fig. 3.2 can be discussed in terms of the quantities $g_i(s) = \sigma_i(s)\, k_i(s)$, $i=1,\ldots,n$. This was achieved by assuming a special form of the compensator $G_c(s) = V^H(s)K(s)V(s)$ where $V(s)$ and $U(s)$ were the right and left singular vectors matrices of the SVD of $G(s)$. But as previously mentioned, it will not be normally possible to construct a realizable controller $G_c(s)$. Even in the rare cases when this might be possible, such a controller would be unnecessarily complicated. A more practical and valid approach is to investigate the possibility of using controllers $\tilde{G}_c(s)$ which are approximately equal to $G_c(s)$ at appropriately chosen frequency.

In the design technique proposed here the controller $\tilde{G}_c(s)$ will have the form

$$\tilde{G}_c(s) = B^T K(s)\, A \tag{3.36}$$

where $A = [\underline{a}_1,\ldots,\underline{a}_n]$, $B = [\underline{b}_1,\ldots,\underline{b}_n]$ are nxn matrices <u>with real ele-</u>

ments. Now suppose that at some specific complex frequency, say s_o, we could choose some $\underline{a}_i$'s and $\underline{b}_i$'s that would be good approximations of the singular vectors $\underline{u}_i(s_o)$ and $\underline{v}_i(s_o)$ so that

$$\underline{b}_i^T \simeq \underline{v}_i^H(s_o) \text{ and } \underline{a}_i \simeq \underline{u}_i(s_o). \tag{3.37}$$

Then, we can consider the effect of choosing the compensator $\tilde{G}_c(s)$ instead of $G_c(s)$. The problem of how to make such an approximation is considered in the next section. We have

$$\tilde{G}_c(s_o)G(s_o) = B^T K(s_o) A U^H(s_o)\Sigma(s_o)V(s_o)$$

$$\simeq G_c(s_o)G(s_o). \tag{3.38}$$

At the frequency s_o, the behavior of the closed-loop system of Fig. 3.2 using $\tilde{G}_c(s)$ instead of $G_c(s)$ is approximately unchanged. Moreover, one can expect that in general this result will hold over a band of frequencies around s_o. These considerations lead to the idea of manipulating the quantities $\sigma_i(s)k_i(s)$, i=1,...,n, into an appropriate form by choosing a controller $\tilde{G}_c(s) = B^T K(s) A$ approximately equal to $G_c(s)$

at some specific value fo complex frequency. Note that to be effective, this approach will depend on the degree of alignment in (3.37). Moreover, the range of frequencies over which the approximate equality (3.38) is valid depends on the rate of change of the singular vector directions.

3.4.1 The Alignment Procedure for Approximating V(s), U(s) by Real Matrices A,B

The alignment procedure used in this section is similar to the one presented in [6]. Further details on the alignment procedure can be found in this reference.

Let $V(s) = [\underline{v}_1(s),\ldots,\underline{v}_n(s)]$ and $U(s) = [\underline{u}_1(s),\ldots,\underline{u}_n(s)]$ be the singular vectors matrices. We will only discuss the case of U(s) since the alignment procedure for the columns of V(s) is obviously similar. If $\underline{x}_i(s)$ is any vector of unit length, then $\underline{x}_i(s)$ is exactly equivalent to $\underline{u}_i(s)$ if and only if

$$U^H(s)\ \underline{x}_i(s) = \underline{e}_i$$

where $\underline{e}_i$ denotes the i^{th} column vector of the unit matrix I_n. As $\underline{x}_i(s)$ and $\underline{u}_i(s)$ become misaligned, the magnitude of the i^{th} entry of the vector $U^H(s)\ \underline{x}_i(s)$ will decrease and all other entries will come into play. We can therefore use the relationship between the magnitude of the i^{th} entry of $U^H(s)\ \underline{x}_i(s)$ and the magnitude of all other entries

as a measure of the alignment of $\underline{x}_i(s)$ with $\underline{u}_i(s)$. This leads us to take as a measure of the misalignment between the pair of vectors $\underline{a}_i$ and $\underline{u}_i(s_o)$, the quotient

$$\Phi_i = \frac{|\underline{u}_i^H(s_o)\underline{a}_i|^2}{\sum_{\substack{j=1 \\ j\neq i}}^{n} |\underline{u}_j^H(s_o)\underline{a}_i|^2} . \tag{3.39}$$

Thus, the alignment between $\underline{a}_i$ and $\underline{u}_i(s_o)$ will be carried out by maximizing the quotient Φ_i, and the successive vectors $\underline{a}_i$, i=1,...,n, which achieve stationary maximum values of Φ_i can be viewed as generating a matrix $A = [\underline{a}_1,\ldots,\underline{a}_n]$ approximating $U(s_o)$.

Let $\underline{u}_j(s_o)$ be expressed in terms of a pair of real vectors $\underline{\alpha}_j$ and $\underline{\beta}_j$ as

$$\underline{u}_j(s_o) = \underline{\alpha}_j + j\,\underline{\beta}_j, \tag{3.40}$$

so that

$$|\underline{u}_j^H(s_o)\underline{a}_i|^2 = \underline{a}_i^T(\underline{\alpha}_j\underline{\alpha}_j^T + \underline{\beta}_j\underline{\beta}_j^T)\underline{a}_j. \tag{3.41}$$

If we now define $$C_i = \underline{\alpha}_i \underline{\alpha}_i^T + \underline{\beta}_i \underline{\beta}_i^T \tag{3.42}$$

and $$D_i = \sum_{\substack{j=1 \\ j \neq i}}^{n} (\underline{\alpha}_j \underline{\alpha}_j^T + \underline{\beta}_j \underline{\beta}_j^T) \tag{3.43}$$

the coefficients Φ_i becomes

$$\Phi_i = \frac{\underline{a}_i^T C_i \underline{a}_i}{\underline{a}_i^T D_i \underline{a}_i} \; . \tag{3.44}$$

To obtain a maximum, we can differentiate (3.44) and set the derivative to zero, so that

$$C_i \underline{a}_i = \Phi_i D_i \underline{a}_i . \tag{3.45}$$

Thus if λ_i is the relevant maximum value of Φ_i, it must be such that

$$C_i \underline{a}_i = \lambda_i D_i \underline{a}_i \tag{3.46}$$

and $\underline{a}_i$ will then be the associated vector for which such a maximum is obtained. But since we have

$$U^H(s_o)U(s_o) = I = \sum_{j=1}^{n} u_j(s_o)u_j^H(s_o) = D_i + C_i \tag{3.47}$$

the relation (3.46) becomes

$$C_i\underline{a}_i = \frac{\lambda_i}{1 + \lambda_i}\ \underline{a}_i. \tag{3.48}$$

Also, C_i from its definition is real, symmetric and non negative definite. Therefore its eigenvalues c_{ij} will be real non negative numbers and its associated eigenvectors $\underline{a}_{ij}$ are real. Thus, from (3.48), we see that the vector $\underline{a}_i$ maximizing the coefficient Φ_i will be the real eigenvector $\underline{a}_{ij}$ associated with the eigenvalue c_{ij} of C_i yielding the largest λ_{ij}, where

$$\lambda_{ij} = \frac{c_{ij}}{1-c_{ij}}\ . \tag{3.49}$$

If we denote $\lambda_i^* = \max\left\{\frac{c_{ij}}{1-c_{ij}}\ ,\ j=1,\ldots n,\right\}$, then the quotient Φ_i has λ_i^* for maximum value.

Therefore, from these results, the alignment procedure for the column vectors of the real matrix $A = [\underline{a}_1,\ldots,\underline{a}_n]$ with the column vectors of the matrix $U(s_o) = [\underline{u}_1(s_o),\ldots,\underline{u}_n(s_o)]$, denoted ALiGN (A, $U(s_o)$ takes the form:

ALiGN (A, U(s_o))

(i) compute the matrices C_i, i=1,...,n, as in (3.42).

(ii) compute the eigenvalues c_{ij}, j=1,...,n and their associated eigenvectors $\underline{a}_{ij}$, j=1,...,n for each C_i, i=1,...,n.

(iii) determine for each i=1,...,n the eigenvector $\underline{a}_{ij}$* corresponding to the eigenvalue c_{ij} yielding $\lambda_i^* = \max \left\{ \frac{c_{ij}}{1-c_{ij}}, \; j=1,...,n. \right\}$

(iv) set $\underline{a}_i = \underline{a}_{ij}^*$ i=1,...,n.

The vectors $\underline{a}_i$, i=1,...,n, will be real and will maximize respectively the quantities Φ_i. Applied successively to the matrices U(s) and V(s), the ALiGN procedure yields real approximating matrices A and B at a particular frequency $s = s_o$.

3.4.2 Basic Design Procedure

It is convenient before becoming involved in the details of the method to briefly summarize some results of the previous section. For the configuration of Fig. 3.2, the behavior of the closed-loop system can be discussed in terms of the quantities $g_i(s) = \sigma_i(s)k_i(s)$, i=1,...,n, in such a way that the design requirements becomes typically:

(i) The stability criterion $\sum_{i=1}^{n} N(-1, g_i(s), D_R) = -P$ must be satisfied. This merely concerns the intermediate frequency range where $|g_i(j\omega)| \simeq 1$, i=1,...,n, (crossover frequencies),

(ii) At low frequencies, the performance conditions will be achieved by making $|g_i(j\omega)|$, i=1,...,n, large (high loop gains),

(iii) At high frequencies, the "robustness condition" will be achieved by making $|g_i(j\omega)|$, i=1,...,n, small (gain reduction).

The main goal of our design method will be to construct some simple and realizable compensators such that the analysis of the configuration of Fig. 3.2 holds approximately in certain range of frequencies. Then we will seek to transform the quantities $g_i(s) = \sigma_i(s)k_i(s)$, $i=1,\ldots,n$, in order to satisfy the design requirements in the corresponding frequency range.

In order to satisfy this goal, at any given angular frequency $j\omega$ using the results of the previous section the following procedure may be adopted for the system $G(s) = U^H(s)\Sigma(s)V(s)$ as in theorem 3.2:

(i) Compute $V^H(j\omega)$ and $U(j\omega)$ at the angular frequency involved,

(ii) Compute real matrices A and B^T which approximate $U(j\omega)$ and $V^H(j\omega)$ using ALiGN(.),

(iii) Select $g_i(s)$, $1=1,\ldots,n$ via the compensating matrix $\tilde{G}_c(s) = B^T K(s) A$ where the diagonal elements of K(s) are chosen with the assumption that $\tilde{G}_c(j\omega) \simeq V^H(j\omega)K(j\omega)U(j\omega)$.

This procedure will be denoted for convenience COMP $(G(s),\omega)$ denoting that it yields an appropriate compensator $G_c(s)$ for the system G(s) for frequencies around ω. This leads to the following method of design.

<u>High frequency compensation</u>: Suppose that ω_h is a high frequency for the plant G(s). Then the "robustness condition" of our design requires some loop gain reduction. We can then apply COMP $(G(s), \omega_h)$ and choose the relevant diagonal matrix K(s) to be a real gain matrix achieving the desired gain reduction at the high frequency ω_h. We obtain an appropriate real compensator $\tilde{G}_h$ achieving good robustness properties

for frequencies around ω_h.

Intermediate frequency compensation: To construct a compensator in an intermediate frequency, we write

$$\tilde{G}_c(s) = G_h G_n(s) \tag{3.50}$$

where the dynamic term $G_m(s)$ is introduced to provide intermediate frequency compensation. The results of the high frequency compensation will remain approximately valid if

$$G_m(j\omega) \simeq W \quad \text{for} \quad \omega \geq \omega_h$$

where W is a unitary matrix. Then $\tilde{G}_c(s) \simeq G_h W$ for $\omega \geq \omega_h$ does not change the robustness properties obtained by G_h. An alternate point of view shows that the compensator $G_m(s)$ can be considered as controlling the transformed plant $G(s)G_h$ since $G(s)\tilde{G}_c(s) = [G(s)G_h][G_m(s)]$. But $G_m(s)$ plays a role only at intermediate frequencies. It will be merely selected to guarantee the stability of the configuration of Fig. 3.2 where the plant G(s) is replaced by $G(s)G_h$. We will therefore apply the procedure COMP $(G(s)G_h, \omega_m)$ where ω_m is an intermediate frequency for the plant $G(s)G_h$, and the diagonal elements of K(s) are chosen to be lead/lag compensators providing adequate phase advance or delay in order to satisfy the stability criterion applied to the transformed plant $G(s)G_h$.

Low frequency compensation: If the compensator $\tilde{G}_c(s) = G_h G_m(s)$ obtained by the first two stages does not satisfy the design requirements at low frequencies, the compensator can be updated to take the form

$$\tilde{G}_c(s) = G_h G_m(s) \left[I + \frac{G_\ell}{s} \right] \tag{3.51}$$

and if the integral gain G_ℓ is not too large, we have

$$G(s)\tilde{G}_c(s) \simeq G(s)G_h W \qquad (\omega \to \infty) \tag{3.52}$$

$$G(s)\tilde{G}_c(s) \simeq G(s)G_h G_m(s) \qquad \text{at intermediate frequencies} \tag{3.53}$$

$$G(s)\tilde{G}_c(s) \simeq G(s)G_h G_m(s)\frac{1}{s}G_\ell \qquad \text{at low frequencies.} \tag{3.54}$$

Since $G_m(s)$ acts only at intermediate frequencies, it is useful to remember that $G_m(s)$ will be approximately a constant matrix at low frequencies. Then, as for the previous stage, $\frac{1}{s} G_\ell$ can be considered as controlling the transformed plant $G(s)G_h G_m(s)$ at low frequencies. Therefore the term $\frac{1}{s} G_\ell$ can be constructed by applying the procedure COMP $[G(s)G_h G_m(s), \omega_\ell]$ where ω_ℓ is the low frequency.

3.4.3 Discussion

Our design proceeds in three stages corresponding respectively to high, intermediate and low frequencies. At each stage a controller G_h, $G_m(s)$ or G_ℓ is selected by applying the procedure COMP(,) to the successive plants $G(s)$, $G(s)G_h$, $G(s)G_hG_m(s)$. This design procedure yield a compensator $\tilde{G}_c(s)$ such that

$$\tilde{G}_c(s) = G_hG_m(s)\left[I + \frac{G_\ell}{s}\right].$$

With this approach, the compensator $\tilde{G}_c(s)$ will have simple elements and will be easily relizable. Therefore the design technique which has been introduced provides a complete and systematic way of satisfying the design requirements.

However, two major implicit assumptions must hold to apply the design procedure. First of all, the ALiGN procedure must provide at each stage sufficiently good approximants for the analysis of Section 3.3 to hold approximately. This is certainly the most critical part of our design approach. Indeed, one can imagine a unitary matrix $U(j\omega)$ that cannot be approximated accurately by a real matrix A. Then, the procedure COMP(,) applied at the frequency ω will yield an unsatisfactory compensator. Furthermore, assuming that a good approximation of $U(j\omega)$ and $V^H(j\omega)$ by constant real matrices can always be obtained, the effectiveness of our design approach will depend on the degree to which these approximations remain good, hence on the rate of change of

the singular vector directions. Thus it may turn out that the consideration of only three characteristic frequencies ω_ℓ, ω_m, ω_h at which adequate compensators are constructed is not sufficient. This could be remedied by considering additional frequencies in the overall frequency range but this would result in more complicated compensators.

Those remarks should not be understood as a universal indictment of our design procedure. The design approach may prove to be efficient and reliable in a lot of cases, but rather it has to be pointed out that there is no theoretical guarantee that the design approach can be applied to any plant G(s). Further insight on the detailed structure of the unitary matrices obtained from the SVD of a plant would be necessary to determine exactly when the design approach will be efficient.

3.5 The Approximation Problem

The development in the previous section of a method of design allowing us to meet the design requirements was shown to be limited in its applicability. These limitations come from the fact that the transformation matrices U(s) and $V^H(s)$ appearing in the compensator $G_c(s) = V^H(s)K(s)U(s)$ do not correspond to finite-dimensional LTI systems and thus cannot be implemented directly. This was remedied in our design procedure by approximating the matrices U(s) and $V^H(s)$ by constant real matrices at certain frequencies. Obviously our design method would be improved if we knew how to find some good rational approximations $\hat{U}(s)$, $\hat{V}^H(s)$ of the transformation matrices U(s) and $V^H(s)$, or alternatively an approximation $\hat{G}_c(s)$ of the compensator $G_c(s)$. This would al-

low us to use the following design technique: Perform a loop by loop design assuming that the matrices U(s) and $V^H(s)$ of our compensator can be implemented. Then implement the compensator as $\hat{V}^H(s)K(s)\hat{U}(s)$ or alternatively as $\hat{G}(s)$. Therefore the problem we are faced with reduced to find "suitable" approximation procedures of the non rational matrices U(s) and $V^H(s)$ or alternatively of $G_c(s)$ by rational transfer matrices corresponding to finite-dimensional LTI systems.

In this section, we will focus our attention on several issues associated with this approximation problem. Since this problem by itself is beyond the scope of our study, the following discussion does not aim to give a complete treatment of the subject. Rather, at a pragmatic level, we will merely discuss some procedures that could be used in order to improve the applicability of our design procedure.

3.5.1 Error Norm Selection

When speaking of approximation of a certain matrix H(s) by another matrix $\hat{H}(s)$, we need to know to what extent an approximant $\hat{H}_1(s)$ is better than another approximant $\hat{H}_2(s)$. This notion can be captured by defining an error norm

$$E(H(s), \hat{H}(s)) = ||\hat{H}(s)-H(s)||$$

where $||.||$ stands for some matrix norm. Then the best approximant will be the one yielding the smallest error norm and we will speak of a good approximation when the error norm is smaller than a preassigned value.

Since there is a wide variety of possible choices for the error norm, the questions of what norm to select arises. For our purpose, since the approximation scheme is used to find a physical implementation of our compensator, the approximation needs to hold only for values of s on the imaginary axis, i.e. for $s=j\omega$. Then, one can think of choosing between the widely used norms:

$$L_p \text{ norm:} \quad E_p[H(s), \hat{H}(s)] = \left[\int_0^\infty ||H(j\omega)-\hat{H}(j\omega)||_2^{\,p} d\omega\right]^{\frac{1}{p}} \text{ for } p \geq 1$$

$$L_\infty \text{ norm:} \quad E_\infty[H(s), \hat{H}(s)] = \sup_\omega ||H(j\omega)-\hat{H}(j\omega)||_2$$

where $||.||_2$ stands for the spectral norm of a matrix. Certainly other error norm selections could be made but since those proposed are the most straightforward we will rather restrict our discussion to them. The key questions are then: <u>what will dictate our choice</u>, <u>and among the possible choices</u> (E_p, $p \geq 1$, E_∞) <u>which is the best</u>?

As indicated before, the approximation procedure will be used to implement our compensator. Thus one can view the actual implementation $\hat{G}_c(s)$ of the compensation as being a perturbed form of the "ideal" compensator resulting from our design. The inherent risk appears to be that with the actual implementation of the compensator, the closed-loop system becomes unstable. Therefore our error norm criterion must

be such that in the approximation process all the errors affecting the compensator that destabilize the closed-loop system can be ruled out by the error norm criterion. Stated in this form, our problem offers a striking similarity with the problem of defining a norm allowing us to account for all the perturbations that destabilize the closed-loop system.

For the sake of simplicity, let us consider the case of the closed-loop SISO system of Fig. 3.4 which is assumed to be nominally stable. Let $\tilde{g}(s)$ denote the perturbed system. The problem is to define among the L_p, $p \geq 1$, L_∞ norms the one that would allow us to account for the "smallest" errors between $\tilde{g}(s)$ and $g(s)$ that destabilize the closed-loop system. Since the notion of smallness requires a norm definition we will rather speak of worst errors. In the SISO case these worst errors are illustrated in the Nyquist diagram of Fig. 3.5. At point A, the Nyquist locus of $g(s)$ is nearest to the critical point -1 and thus the worst error moves A to A' by "stretching" the Nyquist locus to pick up an extra encirclement of the critical point (A' is infinitesimally close to -1). Specific constructions of $\tilde{g}(s)$ can be found in [3] where $\tilde{g}(s)$ and $g(s)$ are different only in the frequency range $[\omega_o-\varepsilon, \omega_o+\varepsilon]$. In this case, the norm that will be the best adapted will be such that errors with infinetely small ε are taken into account. Francis showed in [23] that only the L_∞ norm satisfies this condition. The norms L_p, $p \geq 1$ do not account for the errors when ε is chosen sufficiently small.

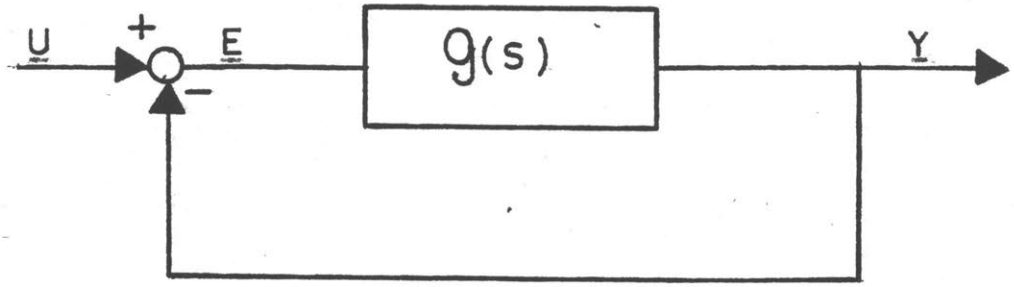

Fig. 3.4: SISO closed-loop system.

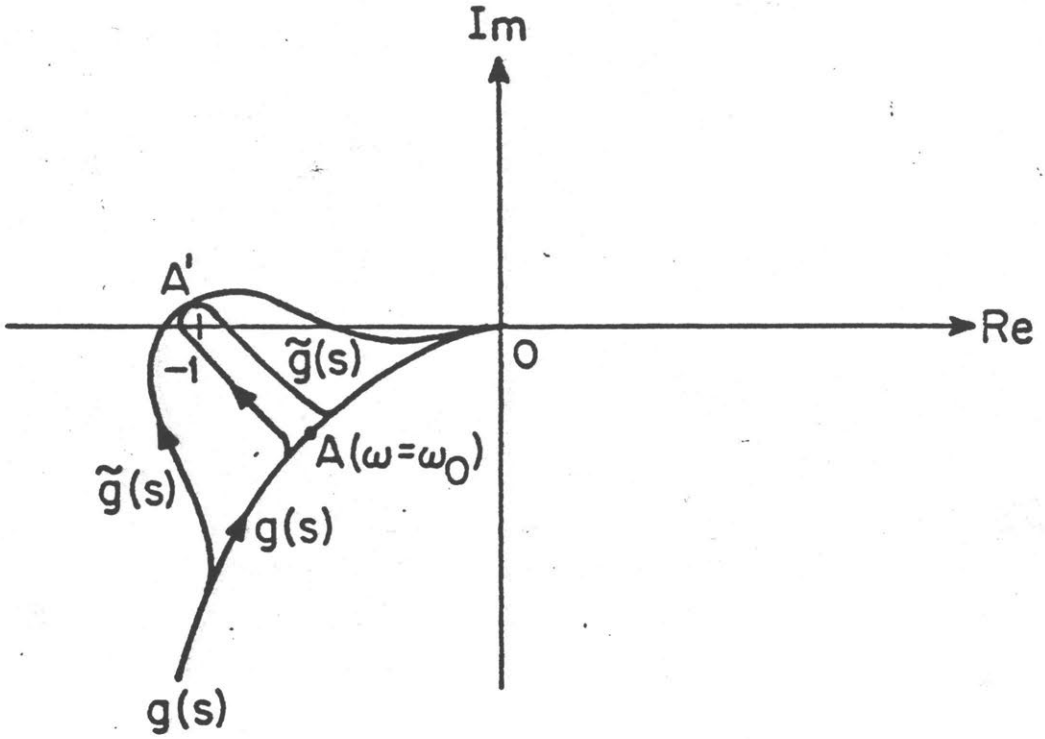

Fig. 3.5: Illustration of worst type of errors in SISO case on a Nyquist diagram.

The discussion in the MIMO case is not as simple for the simple reason that worst errors are not easy to define. Lethomaki presents in [3] a thorough discussion of this problem. However, one can conjecture from our present discussion that the L_∞ norm will be the best adapted to the approximation scheme. Further developments would show that in fact the L_∞ topology is the only topology in the space of transfer matrices strong enough to study the stability of feedback systems. This leads us to choose an error norm criterion of the form:

$$E_\infty[H(s), \hat{H}(s)] = \sup_\omega \left|\left|H(j\omega)-H(j\omega)\right|\right|_2 \tag{3.55}$$

The size of the allowable value of the error norm criterion in the approximation procedure would require a thorough study of the effects of perturbations occuring on the compensator $G_c(s)$, on the stability and the robustness of our original design.

We will conclude our discussion with an additional observation. Our choice of error norm criterion requires that the approximation should be performed equally well over the frequencies $0 \leq \omega \leq \infty$. However, it is well known that at high frequencies saturation phenomenas will occur and the physical system will be usually used in the low frequency range. Therefore, the approximation needs to be more accurate at low frequencies than at high frequencies. With this point of view, our error norm appears to be too restrictive and unrealistic. This can be corrected by introducing a "weight" function $W(j\omega)$ in our error norm criterion giving

more weight to low frequencies than high frequencies. Then, the error norm criterion will have the form:

$$E_{\infty}[H(s), \hat{H}(s)] = \sup_{\omega} W(j\omega) \left| \left| H(j\omega) - \hat{H}(j\omega) \right| \right|_2 . \qquad (3.56)$$

3.5.2 Issues in the Approximation Problem

For a given error norm criterion an approximant will be considered as "good" if a preassigned error tolerance is respected. The actual implementation of the compensator will preserve the stability and the robustness of the design to an extent related to the error tolerance. However, there may exist several "good" approximants; common sense tells us that we should choose the simplest one, i.e. the approximant of lowest order. On the other hand if we restrict ourselves to approximants of a fixed order, we should choose the one that minimizes the error norm criterion. Therefore, the following questions arise naturally;

- how to obtain the simplest possible model for a preassigned error tolerance (minimum degree solution)?

- for a given degree, what is the best possible model (minimum norm solution)?

- and finally, what is the complexity of the solution algorithm (if it exists)?

These approximation issues have been the object of an increasing amount of attention over the past few years. This has been motivated mainly by the desire to solve problems such as model reduction, identi-

fication, digital filter design where typically, a desired frequency response matrix has to be approximated by systems of lower order which are easier to implement. For these problems several approximation techniques have been obtained. Among various approaches, there are schemes using non linear optimization, polynomial recursion, Hankel matrix, etc... (for more details see [24], [25] and references therein). The most important feature of these approximation methods is that except for the Hankel matrix approach, optimality with respect to some error criterion is rarely considered and never established. In the particular case considered here, the only approach that would allow us to find either a minimal degree solution or a minimal norm solution with respect to some error norm criterion (i.e. the Hankel matrix approach) assumes that the system to be approximated is a finite-dimensional LTI system. Therefore we are led to the conclusion that in our case no approximation technique will be able to guarantee optimality with respect to the error criterion.

From a pragmatic point of view, this forces us to restrict the goal of our approximation scheme. This means that we will try to find an approximation scheme that is "reasonable" without necessarily being optimal. Since non rational transfer function matrices do not correspond to finite-dimensional LTI systems, the first step towards a reasonable solution will be to find a rational matrix that interpolates our original matrix at different values along the imaginary axis. Then if the desired accuracy of the interpolation yields a rational matrix of order which is too large, we will apply a standard model reduction

technique to this system. Thus our approximation method will follow the steps:

1. Interpolation by a rational matrix

2. Model order reduction procedure (if necessary).

Since this approximation method is not optimal, if we want to implement $\hat{G}_c(s)$ which approximates $G_c(s)$ by using this scheme, we will not know to what extent the stability and the robustness of our design is preserved. Instead, we will seek to approximate the matrices $U(s)$ and $V^H(s)$ by some rational matrices $\hat{U}(s)$ and $\hat{V}^H(s)$. The corresponding compensator will be of the form $\hat{V}^H(s)K(s)\hat{U}(s)$ and we will assume it preserves approximately the properties of the exact compensator of Fig. 3.2.

In the following sections we will propose some methods for implementing the two steps of the approximation scheme and discuss their application to the approximation of $U(s)$ and $U^H(s)$.

3.5.3 An Approximation Scheme: Interpolation and Model Reduction

3.5.3.a Presentation of an Interpolation Method: The Nevanlinna Algorithm

We will discuss briefly a slightly modified version the Nevanlinna algorithm. A complete presentation and derivation of the algorithm can be found in [26].

Let $s_o, s_1, \ldots, s_p$ be distinct complex numbers in the right half plane, that is $\mathrm{Re}[s_k] > 0$ for $k=0,\ldots p$. Also let $U_0, U_1, \ldots U_p$ be some nxn complex matrices. The Nevanlinna algorithm enables us to find recursively a matrix function $\Phi_o(s)$ such that:

(i) $\Phi_o(s)$ is rational analytic and satisfies $||\Phi_o(s)||_2 < 1$ in the domain $Re(s) > 0$

(ii) $\Phi_o(s_k) = U_k$ for $k = 0,1,\ldots,p$.

The algorithm has a solution if and only if the Pick matrix defined as

$$P = \left[\frac{(\bar{s}_\ell+1)(s_k+1)}{\bar{s}_\ell+s_k} \left[I-U_k^H U_\ell \right] : \quad 0 \leq k, \ \ell \leq p \right] \tag{3.57}$$

is non negative definite. In this case the algorithm goes as follows:

1st Step: Computation of the Fenyves Array

Given the values $\Phi_o(s_k) = U_k$ for $k=0,1,\ldots,p$ compute the matrix sequence $W_k = \Phi_k(s_k)$ for $k=0,1,\ldots,p$ by using the equations:

$$\begin{cases} \psi_k(s) = \dfrac{1}{y_k(s)} (I-W_k W_k^H)^{-1/2} (\Phi_k(s)-W_k)(I-W_k^H \Phi_k(s))^{-1} (I-W_k^H W_k)^{1/2} & (3.58) \\ y_k(s) = \left(\dfrac{\bar{s}_k^2-1}{s_k^2-1} \right)^{1/2} \left(\dfrac{s_k-s}{\bar{s}_k-s} \right) & (3.59) \\ \Phi_{k+1}(s) = (I-K_k K_k^H)^{-1/2} (\psi_k(s)-K_k)(I-K_k^H \psi_k(s))^{-1} (I-K_k^H K_k)^{1/2}. & (3.60) \end{cases}$$

The sequence $\{W_k, k=0,1,\ldots,p\}$ determines the so-called Fenyves array. From the set of equations (3.58)-(3.59)-(3.60), any $\Phi_{k+1}(s)$ rational analytic and bounded in the right half plane yields a $\Phi_k(s)$ rational

analytic and bounded in the right half plane with the prescribed value W_k at s_k. The transformation $\Phi_{k+1}(s) \to \Phi_k(s)$ gives the inductive step of the interpolation algorithm.

2nd Step: Determination of the Interpolating Matrix Function $\Phi_o(s)$

Let us consider the 2n x 2n matrix L,

$$L = \begin{bmatrix} A & B \\ C & D \end{bmatrix}.$$

With L is associated the following homographic transformation acting on n x n matrices:

$$X \to [X] = (AX+B)(CX+D)^{-1} \tag{3.61}$$

Now define

$$H(E) = \begin{bmatrix} (I-EE^H)^{-1/2} & (I-EE^H)^{-1/2}E \\ (I-E^HE)^{-1/2}E^H & (I-E^HE)^{-1/2} \end{bmatrix} \tag{3.62}$$

and

$$B(s_k,s) = \begin{bmatrix} y_k(s)I & 0 \\ 0 & I \end{bmatrix}. \tag{3.63}$$

Then the transformation $\Phi_{k+1}(s) \rightarrow \Phi_k(s)$ determined by equations (3.58)-(3.60) can be written as $\Phi_k(s) = L_k(s)\Phi k_{+1}(s)$ where

$$L_k(s) = H(W_k)B(s_k,s)H(K_k) \quad \text{for} \quad k=0,1,\ldots,p. \tag{3.64}$$

Therefore the solutions $\Phi_o(s)$ of the algorithm are of the form

$$\Phi_o(s) = L_o(s)L_1(s) \ \ldots \ L_p(s)\Phi(s) \tag{3.65}$$

where $\Phi(s)$ is any analytic function matrix satisfying $||\Phi(s)||_2 \leq 1$ for Re s > 0 (for instance $\Phi(s) = I$).

3.5.3.b Adaptation of the Algorithm to the Interpolation of U(s), $V^H(s)$

As previously seen, our goal is to find rational matrices $\hat{U}(s)$ and $\hat{V}^H(s)$ that approximate as accurately as possible U(s) and $V^H(s)$ for $s=j\omega$. We will only discuss the case of U(s) in the sequel since the case of $V^H(s)$ is obviously identical.

The interpolation algorithm presented in the previous section can only be used when the interpolation points are located in the right half plane. Thus, in order to apply the Nevanlinna algorithm we need to use the following procedure:

Step 1: Choose a sequence of points $s_o,\ldots,s_p$ such that $Re(s_k) = \varepsilon > 0$ for $k=0,\ldots,p$ and where ε is small.

Step 2: Compute the values $U_k=U(s_k)$ for $k=0,1,\ldots,p$.

Step 3: Apply the Nevanlinna algorithm with the data $[s_k,U_k]$.

This yields an interpolating matrix $\hat{U}(s)$ such that $\hat{U}(s_k) = U_k$ for $k=0,1,\ldots,p$.

The steps of our procedure require few comments. First, the result yielded by the Nevanlinna algorithm is a rational function matrix of s, analytic and bounded in the right-half plane. This means that $\hat{U}(s)$ corresponds to the transfer function matrix of a finite-dimensional LTI stable system. This stability property was not a formal requirement of our approximating scheme since we are not particularly interested in the stability of our compensator. But it can be useful in the choice of the diagonal compensator K(s). Secondly, the choice of the interpolating points s_k, $k=0,\ldots,p$ ε-close to the imaginary axis guarantees by continuity that the interpolation will be almost exact on the $j\omega$-axis.

Finally, a work of caution has to be given. In Step 3, we have implicitly assumed that the Nevanlinna algorithm could be applied without taking care of the solvability of the interpolation problem. The solvability criterion requires that the matrix P as in (3.57) be non negative definite. Since the matrices U_k, $k=0,\ldots,p$ are unitary matrices, the block diagonal elements of P are zero matrices. Therefore P is either a zero matrix or cannot be non negative definite; we are in a degenerate case of the Nevanlinna-Pick problem.

One way to get around this difficulty is to interpolate the matrix values $\frac{1}{\rho} U_k$ at point s_k for $k=0,1,\ldots,p$ with $|p| > 1$. Thus the Step 3 of our procedure have to be replaced by:

Step 3.a: Choose ρ, $|\rho| > 1$, such that the solvability criterion is satisfied for the data $[s_k, \frac{1}{\rho} U_k]$

Step 3.b: Apply the Nevanlinna algorithm to the data $[s_k, \frac{1}{\rho} U_k]$. This yields a solution $\frac{1}{\rho} \hat{U}(s)$ such that $\hat{U}(s_k) = U_k$ $k=0,1,\ldots,p$.

Without doubt, the Step 3.a will be the most critical part of the interpolation. At least, with our choice of data the Pick matrix P will not have zero block diagonal matrices and can eventually be non negative definite. We will not discuss this particular point any further since more insight on the properties of U(s) and on the consequences of our choice of interpolating points is necessary.

From the form of the Nevanlinna algorithm, it is clear that the more interpolating points we choose, the larger the order of $\hat{U}(s)$ (resp $\hat{V}^H(s)$) will be. Therefore, for an accurate approximation, the order of $\hat{U}(s)$ (resp $\hat{V}^H(s)$) will become large, resulting in high order compensators. Thus, in most cases, it will be necessary to apply a model reduction technique to the matrices $\hat{U}(s)$ and $\hat{V}^H(s)$.

3.5.3.c Multivariable Model Reduction Technique

As mentioned before, there exists several model reduction techniques. The most appealing is the one of Kung and Lin in [27]. They consider the case of a linear time-invariant, strictly casual system characterized by a transfer function matrix

$$H(s) = \sum_{i=1}^{\infty} H_i \, s^{-i}. \tag{3.66}$$

We can associate the this transfer function matrix an infinite block-Hankel matrix denoted $\Gamma[H(s)]$ as

$$\Gamma[H(s)] = \begin{bmatrix} H_1 & H_2 & H_3 \cdots \\ H_2 & H_3 & H_4 \cdots \\ H_3 & & \\ \vdots & & \end{bmatrix} \tag{3.67}$$

and a Hankel-norm

$$||H(s)||_H = ||\Gamma[H(s)]||_2. \tag{3.68}$$

Properties of the Hankel matrix allow Kung and Lin to develop an algorithm yielding minimal degree approximants with respect to the Hankel-norm error criterion

$$E[H(s), \hat{H}(s)] = ||H(s) - \hat{H}(s)||_H \tag{3.69}$$

(The reader is referred to [27] for further details). This algorithm consists of three steps:

(i) Compute the minimal basis solution of a polynomial matrix equation

(ii) Solve an algebraic Riccati equation

(iii) Find the partial fraction expansion of a rational matrix.

This algorithm is also very efficient computationally. However, the most attractive aspect of this model reduction method is that it is, as far as we know, the only closed form (Hankel norm) optimal solution for multivariable system reduction. Moreover, the choice of the error norm criterion can be justified by the fact that the Hankel norm lies in between the L_2 and L_∞ norms and appears as a sort of tradeoff of these norms. However, some caution should be exercised since it is shown in [28] that the Hankel norm induces a topology in the space of transfer matrices which is too weak for studying stability of feedback systems. As it was already mentioned, the only relevant topology is the L_∞ topology.

But since our approximation scheme does not aim to give an error analysis of the approximant, we will consider the model reduction algorithm introduced by Kung and Lin as an efficient algorithm. Its adaptation to our case is straightforward since it can be directly applied to a Laurent series expansion of the rational transfer matrix $\hat{U}(s)$ obtained by Step 3.b of our interpolation procedure.

3.5.3.d Concluding Remarks

In the discussion which precedes we have introduced an approximation scheme. It can be summarized as:

Step 1: Choose a sequence of points $s_o, s_1, \ldots, s_p$ such that $Re(s_k) = \varepsilon > 0$ for $k=0,1,\ldots,p$ and ε is small

Step 2: Compute the values $U_k = U(s_k)$ $k=0,1,\ldots,p$

Step 3: a) Choose, ρ, $|\rho| > 1$ such that the Pick matrix for the data $[s_k, \frac{1}{\rho} U_k]$ is non negative definite

b) Compute $\frac{1}{\rho} \tilde{U}(s)$ for the data $[s_k, \frac{1}{\rho} U_k]$ using the Nevanlinna algorithm

Step 4: If the order of $\tilde{U}(s)$ is not too large, $\hat{U}(s) = \tilde{U}(s)$. Otherwise apply the model reduction technique of King and Lin to $\tilde{U}(s)$. This yields $\hat{U}(s)$.

We have not attempted to derive an optimal approximation method. It is only believed that the previous scheme will yield "reasonable" approximants of $U(s)$ and $V^H(s)$ given our knowledge of approximation techniques. Indeed, we could have tried to apply directly to $U(s)$ and $V^H(s)$ one of the standard approximation techniques. This would have required, in a preliminary stage, to conduct a Laurent series expansion of $U(s)$ and $V^H(s)$ and then apply a standard model reduction technique to a truncated part of these Laurent series. Since these truncated Laurent series represent good rational approximations of $U(s)$ and $V^H(s)$ only in a presumably high frequency range, this approximation process would have been reasonable only for high frequencies in which we are less interested. Our scheme, at least until Step 4, does not have this undesirable feature. Also, the Laurent series expansion of $U(s)$ and $V^H(s)$ require to have an exact knowledge of $U(s)$ and $V^H(s)$ as matrix functions of s. From a practical point of view, computer SVD routines usually give us singular vector values only at specified values of s. An adequate choice of those values of s will allow to conduct

our approximation procedure, since only the data $[s_k, U_k]$ is necessary for the procedure to be applied whereas the exact knowledge of U(s) and $V^H(s)$ would require to perform by hand the computationally cumbersome SVD.

Provided our approximations are accurate enough, the basic properties of the feedback configuration of Fig. 3.2 where U(s) and $V^H(s)$ are replaced by their approximants are approximately preserved. This allows us to conduct a design where the diagonal elements of K(s) are chosen in loop by loop fashion in order to meet the design requirements.

3.6 Summary and Concluding Remarks

In this chapter, we have focused our attention on diagonalization methods of design. A brief review of the existing diagonalization methods, particularly the CL and INA methods has shown that these methods do not produce automatically a good performance and good robustness margins for the controlled system. This comes from the fact that the diagonalization approach is formulated in terms of eigenvalues/eigenvectors although the performance and robustness measures are expressed in terms of singular values. In order to remedy to this deficiency, we investigated an alternative diagonalization approach using a singular value decomposition of the plant. We found that the behavior of the configuration of Fig. 3.2 corresponding to a SVD of the plant could be studied as a sequence of equivalent SISO loop transfer functions. More precisely, given the plant G(s) and an existing SVD $G(s) = U^H(s)\Sigma(s)V(s)$ with $\Sigma(\bar{s})=\Sigma(s)$, the choice of a

controller

$$G_c(s) = V^H(s) \text{ diag } [k_i(s),\ i=1,\ldots,n]U(s)$$

allowed us:

(i) to find a stability criterion in terms of the equivalent SISO loop transfer functions $g_i(s) = \sigma_i(s)k_i(s)$, $i=1,\ldots,n$

(ii) to define the performance and the robustness measures of the controlled system in terms of $g_i(s) = \sigma_i(s)k_i(s)$, $i=1,\ldots,n$.

These results led us to the idea that an adequate choice of the $k_i(s)$, $i=1,\ldots,n$, will allow us to meet in a systematic way the design requirements. But the fact that the resulting compensator $G_c(s) = V^H(s)$ diag $[k_i(s),\ i=1,\ldots,n]U(s)$ does not correspond to a finite dimensional LTI system forced us to take an alternate point of view where the non rational elements of $G_c(s)$, namely $V^H(s)$ and $U(s)$, have to be approximated by rational transfer matrices.

In a first approach, we approximated $U(s)$ and $V^H(s)$ by real constant matrices at certain frequencies. A specific algorithm called ALiGN was obtained for this purpose. It allowed us to derive a design procedure where the compensator is constructed to provide the required compensation in several frequency ranges. But this design procedure, although efficient in some cases, cannot be applied to the most general plants $G(s)$, in particular when approximations by real constant matrices cannot be conducted accurately or when the rate of change in singular

vector directions is too large. Clearly, these restrictions come from the simplistic approximation procedure adopted. Thus, in a second approach, we tried to find more satisfactory approximation procedures for U(s) and $V^H(s)$. We found that this approximation should be conducted with respect to a frequency-weighted error norm criterion, corresponding to the L_∞ topology in the space of transfer function matrices. Unfortunately, current knowledge of approximation techniques does not allow us to find a closed form for approximants of U(s) and $V^H(s)$, not only with respect to the ideal error norm criterion but also to any error norm criterion. Thus, we were forced to restrict our objectives and suggested only a reasonable approximation scheme proceeding as follows:

(i) Interpolation of U(s), $V^H(s)$ by rational transfer matrices using the Nevanlinna algorithm

(ii) A multivariable model reduction technique applied to the results of (i).

This scheme allows accurate approximations at any set of preselected frequencies. Thus a design using these approximants can be performed provided that we assume that the results of the configuration of Fig. 3.2 hold approximately at the set of preselected frequencies.

Obviously, the main problem encountered in the development of a design method using a SVD of the plant is the approximation problem. On this point, our knowledge is still limited since no closed form approximation solutions with respect to an error norm criterion have yet

been found when the matrix to be approximated is not a rational transfer matrix. This is a problem that future research should address. Solution of this problem would yield an easy and systematic diagonalization method of design for MIMO systems.

On the other hand, the approximation problem arose from our desire to use the SVD properties of the plant in order to derive an exact diagonalization design method. This approach appears to be quite similar to what Mac Farlane and did for the CL method of design using the eigenvalues/eigenvectors properties of the plant. But, as Rosenbrock showed in the INA method of design, exact diagonalization may be too restrictive. Only an approximate diagonalization approach corresponding to the concept of diagonal dominance is in fact necessary to conduct a loop by loop design. Thus, using Rosenbrock's ideas, the approximation problem would be avoided if we could find unitary rational transfer matrices $\hat{U}(s)$, $\hat{V}^H(s)$ for any plant $G(s)$ such that:

$$G'(s) = \hat{U}(s)G(s)\hat{V}^H(s) \text{ is diagonal dominant, } \forall s \epsilon D_R$$

i.e. if the diagonal elements of $G'(s)$ represent approximations of singular values of $G(s)$ with bounds specified by the off-diagonal elements of $G'(s)$. We would then be able to meet the design requirements with a method similar to the INA method. Therefore the problem is to find in a systematic way $\hat{U}(s)$ and $\hat{V}^H(s)$ for any plant $G(s)$. This requires a characterization of unitary rational transfer matrices and

further insight in transformations of the plant by unitary matrices. Research on these topics is necessary and in the author's opinion, it should prove fruitful to derive a useful frequency domain design method.

CHAPTER 4: LINEAR QUADRATIC METHODS OF DESIGN

4.1 Introduction

The purpose of this chapter is to study the linear quadratic methods of design. Recall from our presentation in Section 2.5 that the main feature of the LQ method is that we obtain automatically a stable closed-loop system. Furthermore, the closed-loop system has some guaranteed gain and phase margins of ± 6 dB and ± 60° at the plant input. Hence, if we let the design requirements be as specified in Section 2.3, we need only to consider the requirements imposed by the performance and eventually by the robustness if the guaranteed robustness properties associated to the LQ methodology are not sufficient. This simplifies the design significantly since we no longer have to worry about the stability requirement. The problem is therefore to examine how the LQ method allows us to shape the singular values.

In Section 4.2, we will study how the choice of the quadratic weights in the LQ methodology influences the singular values of the open-loop transfer function. This presentation is not original and relies on the work of Doyle and Stein in [1]. However, we will show clearly that the singular value shpaing in the LQ methodology is constrained by the lack of dynamics in our compensation.

In Section 4.3 we present an alternative approach due to Shahjahan [29] that will be more satisfactory. It consists of an adaptation of the Gupta's method presented in Section 2.5 where the frequency dependent weighting matrices are chosen so that the singular value shaping

becomes systematic, easy to perform and almost arbitrary. We will then conclude this chapter by some remarks in Section 4.4.

The results of this chapter have not been, to some extent, generated by the author's research effort. However, these are included in our presentation for the sake of completeness, that is, in order to offer a complete treatment of the multivariable feedback design from the point of view of singular value shaping.

4.2 Singular Values Shaping with the LQ Method

In this section, we restrict our attention to the LQ method since it is, as shown in Section 2.5, the key element of time domain design methods. Thus, we consider the system:

$$\dot{\underline{x}} = A\underline{x} + B\underline{u} \tag{4.1}$$

where $\underline{x} \in \mathbb{R}^n$, $\underline{u} \in \mathbb{R}^m$. The cost criterion to be minimized is

$$J(u) = \int_0^\infty (\underline{x}^T(t)\, Q\underline{x}(t) + \underline{u}^T(t)\, R\underline{u}(t))\, dt \tag{4.2}$$

where R is positive definite and Q non-negative definite. We obtain an optimal control law $\underline{u}(t) = -G\underline{x}(t)$ where G is given by (2.39). The problem is to examine how the choice of the quadratic weighting matrices Q and R influences the singular values of the open-loop transfer function.

For convenience, we will assume that the control weighting matrix is in the form $R = \rho I$, $\rho > 0$. This is consistent with the implicit assumption in our design specifications that the model uncertainties charaterized by $\ell_m(\omega)$ are uniform in all directions. Moreover, non identity R matrices can be incorporated in the LQ gain G as $GR^{1/2}$.

Also, it can be assumed with no loss of generality [10], that the state weighting matrix Q is in the form

$$Q = C^T C \tag{4.3}$$

where C is a m x n matrix of full row rank. We have then the following lemma:

Lemma 4.1 Denote by $\sigma_i(j\omega)$, $i = 1,\ldots,m$, the m singular values of the transfer function $C(sI-A)^{-1}B$ evaluated along the $j\omega$ axis. Then, the singular values of the return difference matrix $I + L(s) = I + G(sI-A)^{-1}B$ are such that

$$\sigma_i\,[I + L(j\omega)] = \sqrt{1 + \frac{\sigma_i^2(j\omega)}{\rho}}\,, \quad \forall\omega\,. \tag{4.4}$$

Proof: Let us consider the SVD of $C(sI-A)^{-1}B$;

$$C(sI-A)^{-1}B = U(s)\ \text{diag}\,[\sigma_1(s)\ldots,\sigma_m(s)]\ V^H(s)$$

where U(s) and $V^H(s)$ are unitary matrices. Then for $s = j\omega$ the Kalman equality (2.41) yields

$$[I + L(j\omega)]^H\,[I + L(j\omega)] = I + \frac{1}{\rho}\ V(j\omega)\ \text{diag}\,[\sigma_1^2(j\omega),\ldots,\sigma_m^2(j\omega)]V^H(j\omega)$$

$$= V(j\omega)\ \text{diag}\,[1 + \frac{\sigma_1^2}{\rho}(j\omega),\ldots,\ 1 + \frac{\sigma_m^2}{\rho}(j\omega)]\ V^H(j\omega)\ ,$$

so that, the singular values of $I + L(j\omega)$ are:

$$\sqrt{1 + \frac{\sigma_i^2(j\omega)}{\rho}} \qquad i = 1,\ldots,m, \quad \forall\omega$$

and there exists a unitary matrix W(jω) such that

$$I + L(j\omega) = W(j\omega)\ \text{diag}\left[\sqrt{1 + \frac{\sigma_i^2(j\omega)}{\rho}}\ ;\ i = 1,\ m\right]\ V^H(j\omega)\ . \qquad (4.5)$$

Q.E.D.

The exact value of W(jω) cannot be deduced from the Kalman equality. In fact the only information about W(jω) that we have is that the eigenvalue structure of W(jω) insures P (number of unstable open-loop poles) anticlockwise encirclements of the origin by the locus det [W(jω) V^H(jω)] as we go along the Nyquist contour. In other words, W(jω) is a unitary matrix insuring the closed-loop stability. More precise knowledge of W(jω) would require more insight into the structure of the solution of the Algebraic Riccati equation (2.40). However, the Lemma 4.1 gives us some insight on the ability to use the LQ methodology to shape the loop singular values. L(s) constitutes the open-loop transfer function of the LQ regulator for the breaking point (1) represented in Fig. 2.8. Using the inequality:

$$-1 + \sigma_i(L(s)) \leq \sigma_i(I + L(s)) \leq 1 + \sigma_i(L(s)) \quad i = 1,\ldots m$$

the relation (4.4) gives us almost exactly the singular values $\sigma_i(L(s))$ whenever these are large, since in this case we have

$$\sigma_i(L(j\omega)) \simeq \frac{\sigma_i(j\omega)}{\sqrt{\rho}} \quad i = 1,\ldots m\ . \qquad (4.6)$$

This exposes a clear relation between the choice of C and ρ and the high loop gain requirement imposed by the performance of the system (condition 2.13). Namely, the designer will have to choose C and ρ in such a way that $\frac{\sigma_i(j\omega)}{\sqrt{\rho}}$ $i = 1,\ldots,m$ are large enough in the frequency range where high loop gains are required. We note also that these gains can be made arbitrarily large by choosing ρ sufficiently small.

Unfortunately, the relation (4.14) do not give us directly the singular values of $L(j\omega)$ whenever these are small. It only allows us to derive the inequality:

$$\underline{\sigma}(I + L(j\omega)) > 1 \qquad \forall\ 0 < \omega < \infty \tag{4.7}$$

which further implies [17] that:

$$\underline{\sigma}(I + L^{-1}(j\omega)) > \frac{1}{2} \qquad \forall\ 0 < \omega < \infty \ . \tag{4.8}$$

The property (4.8) leads to the afore-mentioned guaranteed robustness margins of ± 6 dB and $\pm 60°$ (2.42) of the LQ regulator. However these margins can be insufficient. Thus, we need to find a way to satisfy the high frequency requirement imposed by the robustness constraint. The high frequency behavior of the regulator can be derived from known asymptotic properties as the scalar ρ tends to zero. If $C(sI-A)^{-1}B$ is assumed to be minimum phase, it is shown in [15], that the LQ gain G behaves as

$$\sqrt{\rho}\ G \to WC \tag{4.9}$$

when $\rho \to 0$ and where W is a unitary matrix. Hence, the asymptotic loop transfer function is [1]:

$$L(s) = G(sI-A)^{-1}B \to \frac{WCB}{\sqrt{\rho}s} \tag{4.10}$$

where CB is assumed to have full rank. Based on (4.10) we get

$$\sigma_i(L(j\omega)) \to \frac{\sigma_i(CB)}{\sqrt{\rho}\ \omega} \quad . \tag{4.11}$$

The relation (4.11) gives the high frequency behavior asymptotically as ρ becomes small. As a consequence, the maximum (asymptotic) crossover frequency is given by:

$$\omega_{c_{max}} = \frac{\bar{\sigma}}{\sqrt{\rho}}[CB] \quad , \tag{4.13}$$

Since the stability robustness requirement imposes an upper-limit on the crossover frequencies, our choices of C and ρ to achieve the performance objectives via relation (4.6) is constrained. Moveover, the asymptotic loop transfer function behaves like $\frac{1}{\omega}$ in the high frequency range. This relatively slow attenuation rate may impose further reduction of the crossover frequencies thus impairing the achievable performance. This is the price that we pay for the lack of dynamic compensation in the LQ regulator since the constant LQ gain cannot introduce any additional rolloff. Relations (4.6) and (4.11) are the key relations that intervene in a design based on the LQ methodology. Assuming that ρ is chosen small enough so that the asymptotic high frequency behavior holds approximately, the designer will choose C and by using the insight given by (4.11) and (4.6). However, it is unclear how the choice of C affects the singular values of CB in (4.11) and of $C(sI-A)^{-1}B$ in (4.11). This means that we may have to use a "trial and error" procedure in order to choose C and ρ adequately.

Furthermore, the robustness constraint of our design is a prime requirement. Due to the slow attenuation rate at high frequencies, we may be forced to reduce excessively the bandwidth of the controlled system, thus constraining the performance of our design. This could happen whenever the growth rate of uncertainties at high frequencies is larger than the attenuation rate of the singular values. In this case, the lack of dynamic compensation in the LQ regulator seems to be critical. However, for designs whose robustness requirements are not too demanding, the LQ methodology appears to be a good method since it allows us to meet the design requirements.

4.3 Singular Value Shaping with an LQ Dynamic Regulator.

The discussion of the previous section motivates the need for an LQ methodology where some dynamics are introduced in order to shape the singular values. The method that we will discuss in this section exploits the systematic approach to the synthesis of dynamic LQ regulators described by Gupta in [12]. This method's original ideal is due to Shahjahan [29]. We present the main features of this method. Some detail and proofs will be left out for the sake of brevity.

Recall from our presentation in Section 2.5 that the design method proposed by Gupta allows us to choose the state and the control weighting matrices to be frequency dependent. This means that we have to apply the LQ method to the augmented system (2.50). We will use in this section the same notations as in Section 2.5.

Assume that the control weighting matrix is in the form $R = \rho I$,

$\rho > 0$. The state weighting matrix is $Q(s) = P_1^T(-s)\, P_1(s)$ where $P_1(s)$ has the state space relization (2.49.a). The augmented state space becomes then:

$$\begin{bmatrix} \dot{\underline{x}} \\ \dot{\underline{z}}_1 \end{bmatrix} = \begin{bmatrix} A & 0 \\ G_1 & F_1 \end{bmatrix} \begin{bmatrix} \underline{x} \\ \underline{z}_1 \end{bmatrix} + \begin{bmatrix} B \\ 0 \end{bmatrix} \underline{u} \tag{4.14}$$

and the cost criterion:

$$J(\underline{u}) = \int_0^\infty [\underline{x}^T,\ \underline{z}_1^T] \begin{bmatrix} D_1^T D_1 & D_1^T H_1 \\ H_1^T D_1 & H_1^T H_1 \end{bmatrix} \begin{matrix} \underline{x} \\ \underline{z}_1 \end{matrix} + \rho\, \underline{u}^T(t)\underline{u}(t)\ dt\ . \tag{4.15}$$

The relations (4.14) and (4.15) define a LQ regulator problem. Denote by $\underline{x}_a(t)$ the augmented state vector by A_a and B_a the corresponding augmented state space matrices in (4.14), and by Q_a the augmented state weighting matrix in (4.15). The solution of this LQ problem is:

$$\underline{u}(t) = -\,[C_1,\ C_2]\ \underline{x}_a(t) = -\,\frac{1}{\rho}\ B_a^T P_a\ \underline{x}_a(t) \tag{4.16}$$

where P_a is the positive definite solution of the augmented ARE

$$A_a^T P_a + P_a A_a + Q_a - \frac{1}{\rho} P_a B_a B_a^T P_a = 0\ . \tag{4.17}$$

The closed-loop configuration of the augmented system is shown in Fig. 4.1. Let us consider the open-loop transfer function $L_a(s)$ when we break the loop at the plant input (point (1) in Fig. 4.1).

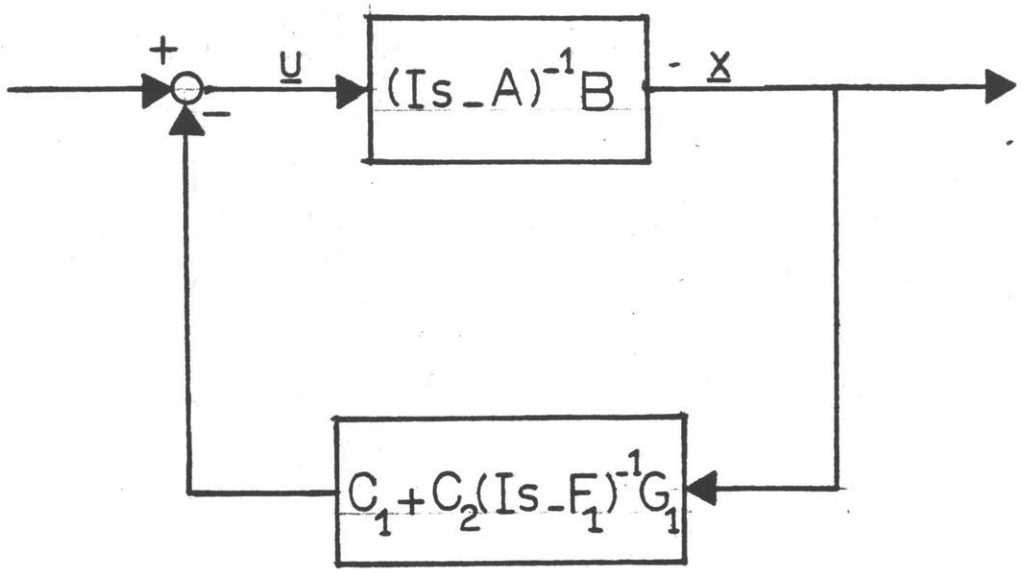

Fig. 4.1: LQ regulator with dynamic compensation and $R = \rho I$.

Straightforward calcuations allow to derive from the A.R.E. (4.17) a Kalman equality such that:

$$[I + L_a^T(-s)]\,[I + L_a(s)] = I + \frac{1}{\rho}\,\{B^T(-sI-A^T)^{-1}\,Q(s)\,(sI-A)^{-1}B\}\ . \tag{4.18}$$

This result simply shows that the Kalman equality of the regular LQ problem can be generalized to the case where the weighting matrices are frequency dependent. In view of Lemma 4.1, the fact that we have a Kalman equality where the state weighting matrix is allowed to be frequency dependent suggests that more freedom will be obtained to shape the singular values. Indeed, for values of s along the jω-axis, the relation (4.18) implies that:

$$\sigma_i^2(I + L_a(j\omega)) = 1 + \frac{1}{\rho}\,\lambda_i\,(B^T(-j\omega-A^T)^{-1}\,Q(j\omega)\,(j\omega-A)^{-1}B) \tag{4.19}$$

This means that the singular values of $\sigma_i(I + L_a(j\omega))$ can be shaped almost arbitrarily by choosing $P_1(s)$ or equivalently $Q(s)$. These choices must be such that the eigenvalues of $[B^T(-sI-A^T)^{-1}\,Q(s)\,(sI-A)^{-1}\,B]$ are easily identifiable. Among a number of possibilities, two natural choices are:

$$\text{(i)}\quad Q(s) = \frac{n(s^2)}{d(s^2)}\,Q_o = \frac{a(s)\,a(-s)}{b(s)\,b(-s)}\,Q_o \tag{4.20}$$

where Q_o is a constant matrix, and where a(s), b(s) are polynomials of s. This choice of Q(s) reduces to consider a regular LQ problem with a state weighting matrix Q_o and where each state of the system is passed separately through the same shaping filter $\frac{a(s)}{b(s)}$. This choice of Q(s)

can be considered as a good approach in order to improve the performance characteristics of a design obtained by the LQ method.

(ii) Without loss of generality it can be assumed that B, the input matrix of our system has full column rank. In this case, we can construct a symmetric matrix Q_o such that the eigenvalues of $B^T Q_o B$ have a small spread, by considering for instance the singular value decomposition of B. Hence $Q(s)$ can be selected such that:

$$Q(s) = \left[\frac{a(s)\ a(-s)}{b(s)\ b(-s)}\right] (-sI-A^T)\ Q_o (sI-A) \quad . \tag{4.21}$$

Then the singular values of $I + L_a(j\omega)$ become:

$$\sigma_i^2(I + L_a(j\omega)) = 1 + \frac{a(j\omega)\ a(-j\omega)}{b(-j\omega)\ b(j\omega)}\ \lambda_i(B^T Q_o B) \quad . \tag{4.22}$$

The MIMO design is thus reduced to a sequence of SISO design problems. Also, by making the eigenvalues of $B^T Q_o B_o$ identical we can further reduce the MIMO design problem to a single SISO design problem.

It is clear that different choices of $Q(s)$ could be made. In fact, the only requirement that will guide the choice of $Q(s)$ is that the eigenvalues of $B^T(-sI-A^T)^{-1}\ Q(s)\ (sI-A)^{-1}B$ are easily identifiable and can be modified in a simple way. The latter can be achieved by considering a shaping filter $\frac{a(s)}{b(s)}$ as in (4.20) and (4.21) which affects each state. Thus the actual choice of the state control matrix will certainly depend on the specific design problem that we are considering. However, the two systematic choices (4.20) and (4.21) show that the

singular values of $[I + L_a(j\omega)]$ can be shaped almost arbitrarily. In terms of our design requirements, the singular values of $[I + L_a(j\omega)]$ are very useful whenever they are large, since in this case they constitute a good approximation of the singular values of $L_a(j\omega)$. This means that our choices of $Q(s)$ in (4.20) and (4.21) give us a good insight on how to achieve the performance requirement of our design.

On the other hand little is known on the robustness constraint of the configuration of Fig. 4.1. The relation (4.19) implies:

$$(I + L_a(j\omega)) \triangleright 1 \tag{4.23}$$

which yields some guaranteed robustness margins of ±6 dB, ±60° as for the usual LQ regulator. This may be insufficient and this motivates the study of the high frequency behavior of our system. As in Section 4.2 this behavior can be derived from known asymptotic properties as the scalar ρ tends to zero. The only difference with the results of Section 4.2 is that the results have to be applied to the augmented system described by (4.14) and (4.15). Straightforward calculations show

$P_1(sI-A)^{-1}B$ is minimum phase, when ρ tends to zero the LQ gain $[C_1, C_2]$ behaves as:

$$[C_1, C_2] \to W[H_1, D_1] \tag{4.24}$$

where w is a unitary matrix. Hence, the asymptotic loop transfer function $L_a(s)$ becomes:

$$L_a(s) = [C_1, C_2]\ (sI - A_a)^{-1} B_a$$

$$\rightarrow W[D_1, H_1]\ (\sqrt{\rho}\, sI - A_a)^{-1} B_a$$

$$\rightarrow W P_1(\sqrt{\rho}\, s)\ (\sqrt{\rho}\, sI - A)^{-1} B \qquad (4.25)$$

Obviously, the asymptotic behavior of the loop transfer funtion depends on the choice of $Q(s)$. Let us consider respectively the choices (4.20) and (4.21) where we assume that $a(s)$ is of degree α and $b(s)$ is of degree β. For the sake of realizability, we will have $\beta \geq \alpha$ for (4.20) and respectively $\beta \geq \alpha + 1$ for (4.21). The relation (4.25) implies then

$$\text{For } Q(s) = \frac{a(s)\ a(-s)}{b(s)\ b(-s)}\ Q_o: \sigma_i(L_a(j\omega)) \rightarrow \frac{\sigma_i(Q_o^{1/2}B)}{[\sqrt{\rho}\ \omega]^{1+\beta-\alpha}} \qquad (4.26)$$

$$\text{For } Q(s) = \frac{a(s)\ a(-s)}{b(s)\ b(-s)}\ (-sI - A^T)\ Q_o(sI - A): \sigma_i(La(j\omega)) \rightarrow \frac{\sigma_i(Q_o^{1/2}B)}{[\sqrt{\rho}\ \omega]^{\beta-\alpha}} \qquad (4.27)$$

where $Q_o^{1/2}B$ have been assumed to have full rank. (4.26) and (4.27) give the asymptotic crossover frequencies. They show that the relatively slow attenuation rate of the singular values at high frequencies in the LQ methodology is improved by an adequate choice of the degrees of the polynomials $a(s)$ and $b(s)$. Moreover they give us the insight necessary to satisfy the robustness constraints. Thus, assuming that ρ is chosen small enough so that the asymptotic behavior holds approximately, the designer can choose $a(s)$, $b(s)$, Q_o, ρ by using the relations (4.19) - (4.26) for the first choice of $Q(s)$ and (4.22) - (4.27) for the second choice of $Q(s)$. In each case it appears that the design methodology

leaves us a lot of freedom for shaping the singular values. Sharp rolloff at high frequencies can be obtained by introducing poles in the shaping filter having an effect only in the high frequency range. This can be done without impairing the low frequency shape of the singular values. This shows a valuable "decoupling" between the satisfaction of the performance and robustness requirements of our design and may come as a simplication in the construction of $\frac{a(s)}{b(s)}$.

The discussion which precedes has shown how our design approach constitutes an improvement with respect to the regular LQ methodology. However, we concentrated our attention on the choice of $Q(s) = P_1^T(-s)P_1(s)$, while little has been said about the choice of $P_1(s)$. Indeed, since the dynamic approach to LQ compensation defined by Gupta [12] imposes to choose $Q(j\omega)$ to be a rational function of ω^2, we chose $Q(s)$ such that:

$$Q^T(-s) = Q(s) \quad . \tag{4.29}$$

The theory of spectral factorization [18] tells us that matrices satisfying the relation (4.29) can always be written as:

$$Q(s) = P_1^T(-s)\ P_1(s) \quad . \tag{4.30}$$

The problem arising is that $P_1(s)$ is not unique (even worse, there exists an infinite number of $P_1(s)$ satisfying (4.30) for a given $Q(s)$). However, the state space realization of $P_1(s)$ determines the exact dynamics of the compensation. In order to find the optimal control law (4.16), we made the implicit assumption that the LQ problem for the augmented state space (4.14) - (4.15) is such that (A_a, B_a) is stabilizable and

and $(Q_a^{1/2}, A_a)$ is detectable. It can be shown by studying the controllable and observable modes of the augmented system, that (A_a, B_a) is stabilizable and $(Q_a^{1/2}, A_a)$ is detectable under the following sufficient conditions:

(i) If (A,B) is stabilizable, it suffices to choose $P_1(s)$ such that $P_1(s)$ has no poles and no zeroes in the right-half plane.

(ii) If A is stable matrix, it suffices to choose $P_1(s)$ such that $P_1(s)$ has no poles in the right-half plane (stable transfer function).

The weakest sufficient condition is that the system should be stabilizable. This is not surprising since we are applying an LQ methodology in the degenerate case where Q(s) is a constant matrix. For the choice of the control weighting matrix as in (4.20), it is clear how $P_1(s)$ should be determined. The polynomials a(s) and b(s) can always be chosen such as they have no roots in the right-half plane since it is $\frac{a(s)\ a(-s)}{b(s)\ b(-s)}$ which appears in Q(s). Thus $P_1(s)$ can simply be taken as:

$$P_1(s) = \frac{a(s)}{b(s)}\ Q_o^{1/2} \tag{4.31}$$

where $Q_o^{1/2}$ is a square root of Q_o. Moveover, this square root can always be choosen such that $\frac{a(s)}{b(s)}\ Q_o^{1/2}\ (sI-A)^{1}B$ is minimum phase. This minimum phase condition allows the asymptotic high frequency analysis to hold.

In the case where the control weighting matrix is as in (4,21), the determination of $P_1(s)$ remains simple whenever the system to be controlled is stable since a satisfactory choice of $P_1(s)$ is:

$$P_1(s) = \frac{a(s)}{b(s)} \; Q_o^{1/2} \; (sI-A) \tag{4.32}$$

where $a(s)$, $b(s)$ have no roots in the right half plane. When A is only such that (A,B) is stabilizable, $P_1(s)$ could be determined by a spectral factorization algorithm [19]. But when $P_1(s)$ has no poles and zeroes in the right half plane and A is unstable, $P_1(s)\ (sI-A)^{-1}B$ can never be minimum phase. The asymptotic high frequency analysis will not hold. Therefore, in this case, the first choice of $Q(s)$ as in (4.20) seems simpler.

Our present analysis shows how simple choices of $P_1(s)$ or $Q(s)$ allow us to meet the design requirements. In particular it appears that the design method leaves a lot of freedom for shaping the singular values using the shaping filter $\frac{a(s)}{b(s)}$ to generate a large class of loop dynamics without affecting the closed-loop stability. However, let us examine the effect of the design approach on the pole placement. The relation (4.18) implies that:

$$\det [I + L_a(s)] \det [I + L_a(-s)] = \det [I + \frac{1}{\rho} \; B^T(-sI-A^T)^{-1} \; Q(s) \; (sI-A)^{-1}B] \tag{4.33}$$

but

$$\det [I + L_a(s)] = \frac{\gamma_{CL}(s)}{\gamma_{OL}(s)} \tag{4.34}$$

where $\gamma_{CL}(s)$ is the characteristic polynomial of the closed-loop system and $\gamma_{OL}(s)$ is the characteristic polynomial of the open-loop augmented system. The augmented system dynamics (4.14) implies

$$\gamma_{OL}(s) = \det (sI-A) \det (sI-F_1) . \tag{4.35}$$

In the case of the second choice of $Q(s)$ as in (4.21), i.e.

$Q(s) = \frac{a(s)\, a(-s)}{b(s)\, b(-s)} (-sI-A^T) Q_o (sI-A)$, we have

$$\det (sI-F_1) = [b(s)]^n \tag{4.36}$$

Hence based on (4.33) we get

$$\gamma_{CL}(s)\, \gamma_{CL}(-s) = \det(sI-A) \det(-sI-A) [b(s)\, b(-s)]^n$$

$$\det \left[I + \frac{a(s)\, a(-s)}{b(s)\, b(-s)} B^T Q_o B\right] \tag{4.37}$$

This shows that respectively the stable modes and the mirror image with respect to the imaginary axis of the unstable modes of the plant $(sI-A)^{-1}B$ are closed-loop poles. The second choice of $Q(s)$ as in (4.21) imposes a strong constraint in terms of pole placement. This is the price we pay for the pole zero cancellations in $B^T(-sI-A^T)^{-1} Q(s) (sI-A)^{-1}B$.

The first choice of $Q(s)$ as in (4.20) does not possess this undesirable feature. Indeed, since there is no pole zero cancellation in $B^T(-sI-A^T)^{-1} Q(s) (sI-A)^{-1}B$, the term $\det [-sI-A] \det [sI-A]$ will be cancelled out in the expression of $\gamma_{CL}(s)\gamma_{CL}(-s)$. Root locus techniques could also be derived from the actual form of $\gamma_{CL}(s)\, \gamma_{CL}(-s)$. Therefore, in terms of pole placement the first choice of $Q(s)$ as in (4.20) is more satisfactory. The pole zero cancellation in $B^T(-sI-A^T)^{-1} Q(s) (sI-A)^{-1}B$ for the second choice of $Q(s)$ as in (4.21) allows us to have more insight for shaping the singular values. But it imposes a strong pole placement

constraint.

4.4 Concluding Remarks

The developments of this chapter have shown how time-domain based design methods can be used in order to satisfy the design requirements. The LQ methodology has been first presented and was seen to be efficient for a certain class of design problems where the robustness requirement is not too demanding. In order to lift this constraint, we introduced an alternative design approach where some dynamics could be introduced in the feedback loop to shape the singular values. This was done by allowing the state weighting matrix to be frequency dependent and we showed how this weighting matrix could be chosen in order to satisfy the design requirements. This choice is easy to perform and is quite systematic. Finally the order of the compensators obtained by this design seems to be relatively low. This is particularly true for the LQ methodology itself (constant gain) and for our alternative approach where $Q(s)$ is chosen as in (4.20). However, one should remember that the LQ methods with or without dynamics in the feedback loop assume that the state vector of the system in directly available to measurements. This is not the case for most practical systems and a Kalman filter has to be introduced in the loop to estimate the state vector. A robustness recovery procedure can then be applied to retrieve asymptotically the loop transfer function obtained by the LQ methodology. However, the Kalman filter will be actually present in our compensator and increases sensibly the order of the compensator. For very large systems this could result in

unacceptably high order compensations. This constitutes a restriction of the LQ methods of the type discussed in this chapter.

Also, though the LQ dynamic compensation approach allows us to satisfy a proper robustness constraint at the plant input, little is known on how this robustness can be achieved at the plant output. The problem arises from the state augmentation. The robustness recovery methods only allow us to recover the LQ robustness properties at the output of the augmented system which does not correspond to the physical output of the plant. This may constitute a major weakness of our LQG dynamic compensation approach.

CHAPTER 5: BASIC DESIGN PROCEDURE; AN APPLICATION

5.1 Introduction

In this chapter we will present an application of the basic design procedure introduced in Section 3.4. Recall that this design method was obtained by using an approximation procedure named ALiGN(.) which allows us to find real frame matrices approximating complex frame matrices at prescribed values of complex frequencies. Then given a plant G(s) and a set of design requirements, the design proceeds in three steps:

(i) a high frequency compensation is conducted to provide adequate robustness margins by reducing the loop gains at high frequencies,

(ii) an intermediate frequency compensator is selected to guarantee the stability of the closed loop system,

(iii) a low frequency compensation insures good performance by using high loop gains at low frequencies.

Thus the overall compensation takes the form:

$$G_c(s) = G_h G_m(s)\left[I + \frac{G_\ell}{s}\right]$$

where G_h, G_m, G_ℓ are the high frequency, intermediate frequency and low frequency compensators constructed according to constraints developed in Section 3.4.2.

In the following sections, we will illustrate the basic design procedure by considering an example. In Section 5.2 we present the system to be controlled and its associated design requirements. Then in Sections 5.3 and 5.4, the successive steps of our design procedure are described. Throughout this development, we will focus our attention on different issues coming up in our design approach. Our design example does not intend to provide a "real life" controller for a specific control design problem. Rather the example aims at providing an illustration of the applicability of our design procedure.

5.2 Presentation of Design Problem

The example used here to illustrate the use of the design technique is based on a slightly modified version of a longitudinal-axes design problem for the CH.47 helicopter introduced by G. Stein and J.C. Doyle in [1] and [2]. The objective is to control two measured outputs, vertical velocity and pitch attitude, by using collective and differential collective rotor thrust commands. A nominal model for the system dynamics at 40 knot airspeed is:

$$\frac{d}{dt}\,x = \begin{bmatrix} -.02 & .005 & 2.4 & -32 \\ -.14 & -.44 & -1.3 & 30 \\ 0 & .18 & -1.6 & 1.2 \\ 0 & 0 & 1 & 0 \end{bmatrix} x + \begin{bmatrix} .14 & -.12 \\ .36 & -8.6 \\ .35 & .009 \\ 0 & 0 \end{bmatrix} u$$

$$y = \begin{bmatrix} 0 & 0 & 1 & 0 \\ 0 & 0 & 0 & 57.3 \end{bmatrix} x \cdot$$

The set of poles for this nominal system is

$$\{1,405;\ -1,5996.10^{-1};\ -1,6525+j(1,1783);\ -1,6526-j(1,1783)\}.$$

Since there is one pole in the right half plane, the stability criterion requires a net sum of one anticlockwise encirclement in the multivariable Nyquist criterion.

In the sequel, we will denote by G(s) the transfer function of the nominal system. Since G(s) is a 2x2 transfer matrix, it has two singular values $\bar{\sigma}[G(s)]$ and $\underline{\sigma}[G(s)]$. For convenience, we will denote with subscript 1 (respectively 2) all quantities revering to the channel corresponding to the largest singular value $\bar{\sigma}[G(s)]$ (respectively $\underline{\sigma}[G(s)]$), i.e.; $\bar{\sigma}[G(s)] = \sigma_1(s)$ corresponds to channel 1 and $\underline{\sigma}[G(s)] = \sigma_2(s)$ corresponds to channel 2. The values of $\sigma_1(s)$ and $\sigma_s(s)$ along the jw-axis are represented in Fig. 5.1.

Major uncertainties associated with this model are due to neglected rotor dynamics and uncertain rate limit nonlinearities. For our purpose, it suffices to assume that these uncertainties impose uniformly in both control channels a loop gain reduction at high frequencies as shown in Fig. 5.1. In particular, the controller bandwidth should be

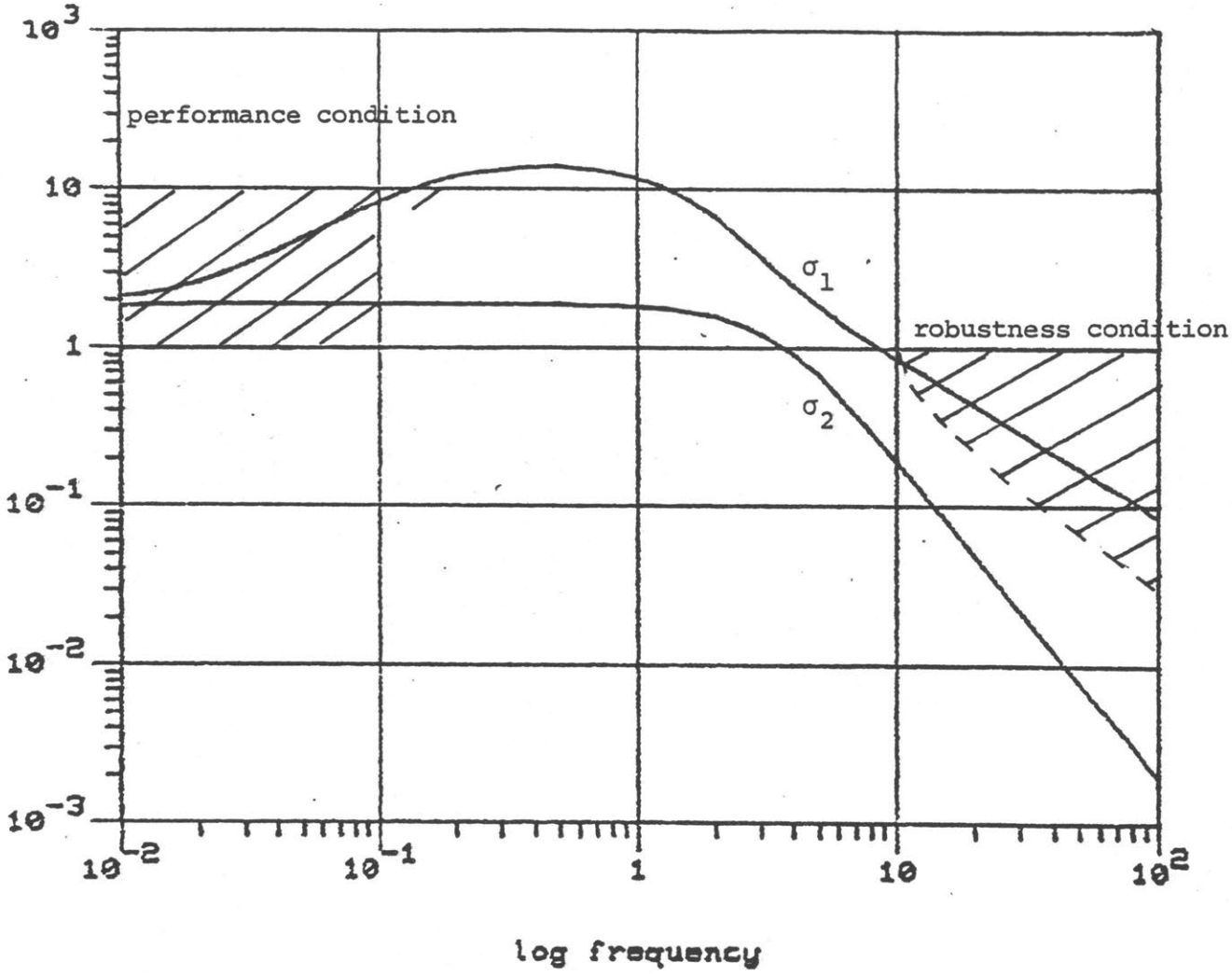

Figure 5.1: Singular Values of G(s) with Performance and Robustness Requirements

constrained to be less than 10 rd.S^{-1}. A thorough discussion in [2] of the robustness requirements of this system shows that our robustness constraint is physically reasonable. We will also assume that the system's performance requires that we achieve loop gains greater than or equal to 10 in the largest frequency range possible and at least for the frequencies less than .1 rd.S^{-1}. This somewhat loose statement about the performance condition of the controlled system translates the fact that high loop gains cannot be achieved deliberately and are constrained by the robustness constraints of the controlled system. The Fig. 5.1 which represents the singular values of G(s) together with the robustness and the performance conditions shows that our design problem is:

(i) To achieve nominal closed-loop stability

(ii) To reduce the loop gain in channel 1 at frequencies $\omega \geq 10$ rd.S^{-1}

(iii) To increase the loop gains in channel 1 and 2 for frequencies $\omega \leq 10^{-1}$ rd.S^{-1} and possibly greater than 10^{-1} rd.S^{-1}.

We then proceed to construct a controller using our design procedure.

5.3 Intermediate Frequency Range Compensation

5.3.1 Introduction

A detailed study of the limitations imposed by the robustness requirement shows that no modification at high frequencies is required in channel 2. On the other hand loop gains in channel 1 must be reduced at high frequencies. For example, at $\omega = 10^2$ rd.S^{-1} this gain

must be reduced from 9.10^{-2} to 4.10^{-2}. This gain reduction is small enough to be handled directly by intermediate frequency compensation. We will thus avoid the construction of a high frequency compensator that would have been necessary with a more constraining high loop gain reduction requirement. However, this approach will be valid only if we do not require the intermediate frequency range compensation $G_m(s)$ to approach a unitary matrix at high frequencies, this in order to be able to modify the singular values of our plant G(s) at high frequencies.

Therefore, our intermediate frequency compensation $G_m(s)$ will be chosen in order to:

(i) insure proper robustness margins,

(ii) guarantee the closed-loop nominal stability.

In particular, if we consider the Nyquist stability criterion (Theorem 3.3) since G(s) is a strictly proper transfer function with no open loop poles on the imaginary axis, we need only to consider the values of s along the imaginary axis and the singular values in a decreasing order satisfies the condition imposed on the singular value decomposition considered for our basic design procedure.

5.3.2 Approximation of Singular Vectors

The controller design process starts by finding real frame matrices A and B which approximate respectively the singular vector matrices U(s) and V(s) given by the singular value decomposition of $G(s) = U^H(s)\Sigma(s)V(s)$ at some suitably chosen frequency value. The intermediate frequency range controller will have the form

$$G_m(s) = B^T K_m(s) A$$

where the diagonal elements of $K_m(s)$ are selected in order to provide an adequate compensation. The approximation is done by using the ALiGN algorithm to approximate the complex columns of U(s) and V(s) by the real columns of A and B at the frequency ω_m. An investigation of the intermediate frequency range showed that the best results were obtained at $\omega_m = 10$ rd.S^{-1}. We have for this value:

$$U^H(10j) = \begin{bmatrix} .70124-j.70494 & -.10641+j7.4358.10^{-4} \\ -.086392+j.062126 & -.982-j.15606 \end{bmatrix}.$$

$$\text{and } V^H(10j) = \begin{bmatrix} .041361 & .99914 \\ -.74199+j.66913 & .030716-j.0.0277 \end{bmatrix}$$

We then found

$$A \simeq \begin{bmatrix} 1 & 0 \\ 0 & -1 \end{bmatrix} \qquad B \simeq \begin{bmatrix} 0 & -1 \\ +1 & 0 \end{bmatrix}$$

Where the sign ambiguity on the columns of A and B yielded by the ALiGN algorithm has been removed by considering the dominant entries of U(10j) and V(10j) respectively. As discussed in Section 3.4.1 the coefficients:

$$\Phi_{ai} = \frac{|u_i^H(10j)a_i|^2}{\sum_{\substack{j=i \\ j\neq i}}^{2} |u_j^H(10j)a_i|^2} \quad \text{and} \quad \Phi_{bi} = \frac{|v_i^H(10j)b_i|^2}{\sum_{\substack{j=i \\ j\neq i}}^{2} |v_j^H(10j)b_i|^2} \quad \text{for } i = 1,2$$

give us a measure of the "quality" of the approximation performed, i.e., the larger they are, the better is the alignment between the pair of vectors $(a_i, u_i(10j))$ and $(b_i, v_i(10j))$. We represented in Figures 5.2.a and 5.2.b the different values taken by these coefficients for frequencies around 10 $rd.S^{-1}$. A first observation is that these coefficients have the same values for i=1 and i=2. This is a consequence of the fact that we approximate 2x2 unitary matrices. The misalignment plots show also clearly the coefficients Φ_{a_i} and Φ_{b_i} become large for frequencies $\omega \geq 10$ $rd.s^{-1}$ while they become small for frequencies $\omega < 5$ $rd.s^{-1}$. This means simply that the approximations of U(s) and A and V(s) by B will remain valid for frequencies $\omega \geq 10$ $rd.s^{-1}$ and become poor for frequencies $\omega < 5$ $rd.s^{-1}$. Thus the choice of a diagonal compensation $K_m(s)$ will allow us to modify the loop gains for frequencies $\omega \geq 10$ $rd.s^{-1}$ in a predictable way. This justifies our ap-

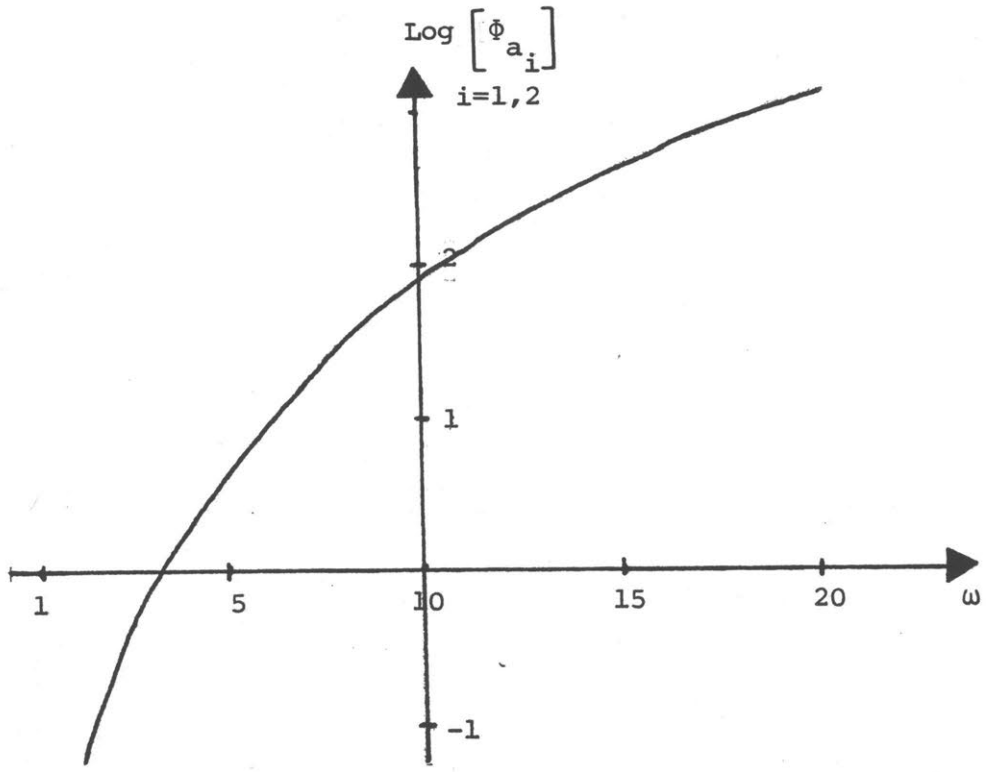

Figure 5.2.a: Misalignment Plot for A at ω = 10 rd.s^{-1}

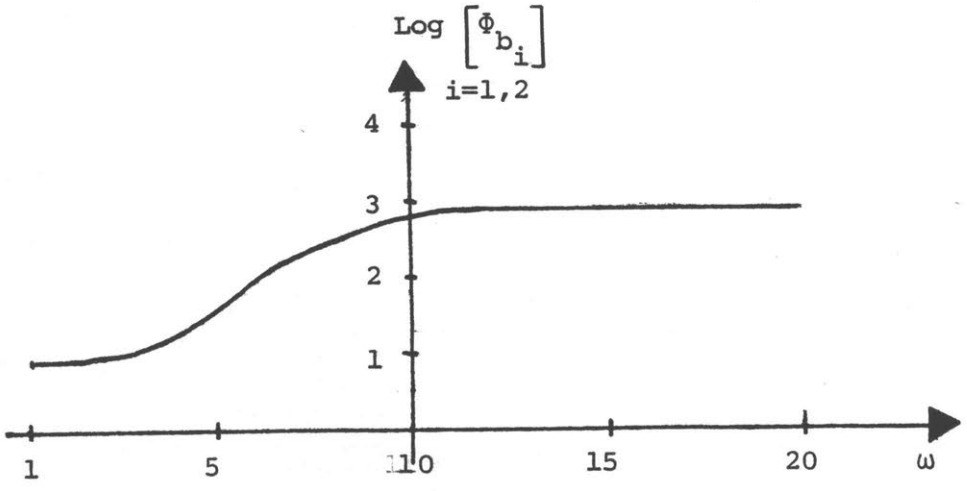

Figure 5.2.b: Misalignment Plot for B at ω = 10 rd.s^{-1}

proach of constructing directly on intermediate frequency range controller without using high frequency compensation. On the other hand, we can expect that the loop gains for frequencies $\omega < 5$ rd.s^{-1} will be modified in a very unpredictable way.

As a result of our approximation, the intermediate frequency range controller $G_m(s)$ will have the form:

$$G_m(s) = \begin{bmatrix} 0 & 1 \\ -1 & 0 \end{bmatrix} \begin{bmatrix} k_{m_1}(s) & 0 \\ 0 & k_{m_2}(s) \end{bmatrix} \begin{bmatrix} 1 & 0 \\ 0 & -1 \end{bmatrix}$$

where $k_{m_1}(s)$ and $k_{m_2}(s)$ are the controllers for channels 1 and 2 respectively. We proceed now to choose these two controllers.

5.3.3 Choice of the Diagonal Compensation

We must choose $k_{m_1}(s)$ and $k_{m_2}(s)$ such that the closed loop system becomes stable and such that the loop gain reduction imposed by the robustness requirement is satisfied. Since only the gain in channel 1 needs to be reduced, our approach for selecting $k_{m_1}(s)$ and $k_{m_2}(s)$ will be to use $k_{m_1}(s)$ to obtain an adequate gain reduction in channel 1 and to use $k_{m_2}(s)$ to obtain the required number of anticlockwise encirclements of -1.

Compensation in channel 1:

A natural choice for the controller $k_{m_1}(s)$ is a lag compensator of the form $\frac{1}{\alpha} \times \frac{s + \frac{1}{T}}{s + \frac{1}{\alpha T}}$ with $\alpha > 1$. This compensator will provide a gain reduction of 20 log α db at high frequencies. Furthermore, it will not introduce any encirclement of the point -1 in the Nyquist stability criterion since the phase associated to this compensator stays between 0 and $-\frac{\pi}{2}$. Inspection of the robustness requirement represented in Fig. 5.1 leads us to choose $\alpha = 4$, so that, the values of σ_1 for $\omega \geq 10$ rd.s^{-1} will be divided by 4, and $\frac{1}{T} = 25$, i.e., the crossover frequency in channel 1 stays close to 10 rd.S^{-1}. Thus, the compensation in channel 1 will be given by:

$$k_{m_1}(s) = .25 \frac{s + 25}{s + 6.25} .$$

Compensation in channel 2

In order to obtain a stable closed-loop system, compensation in channel 2 must introduce one anticlockwise encirclement of the point -1 in the Nyquist stability criterion. A way to do that is to choose the controller $k_{m_2}(s)$ to be a lead compensator dephased by π, i.e., to be of the form: $-\frac{1 + Ts}{1 + \alpha Ts}$ with $\alpha < 1$. Such a compensator will not affect the gain at low frequencies, and will increase it at high frequencies. Thus we must take care of choosing α large enough in order to preserve the robustness in channel 2. Inspection of the robustness

requirement represented in Fig. 5.1 leads us to choose $\alpha = 0.5$, so that, the values of σ_2 for $\omega \geq 10$ rd.s^{-1} will be multiplied by 2. We also choose $\frac{1}{T} = 3$ so that the crossover frequency will be slightly augmented and so that we will obtain a good phase margin in channel 2. Thus, the compensator in channel 2 will be:

$$k_{m_2}(s) = -2\,\frac{s+3}{s+6}$$

Result of the Compensation

With our choice of $k_{m_1}(s)$ and $k_{m_2}(s)$, the intermediate frequency range controller $G_m(s)$ will be:

$$G_m(s) = \begin{bmatrix} 0 & 1 \\ -1 & 0 \end{bmatrix} \begin{bmatrix} .25\,\frac{s+25}{s+6.25} & 0 \\ 0 & -2\,\frac{s+3}{s+6} \end{bmatrix} \begin{bmatrix} 1 & 0 \\ 0 & -1 \end{bmatrix}.$$

In order to check the success of our compensation, we must first verify that the system is closed loop stable. Indeed, as shown in Figure 5.3 where we represented the Nyquist plots of $\sigma_1(s)k_{m_1}(s)$ and $\sigma_2(s)k_{m_2}(s)$, the compensations in channel 1 and channel 2 introduce a net sum of anticlockwise encirclements of the point -1 equal to one. Thus the system is expected to be closed-loop stable. The computation of the

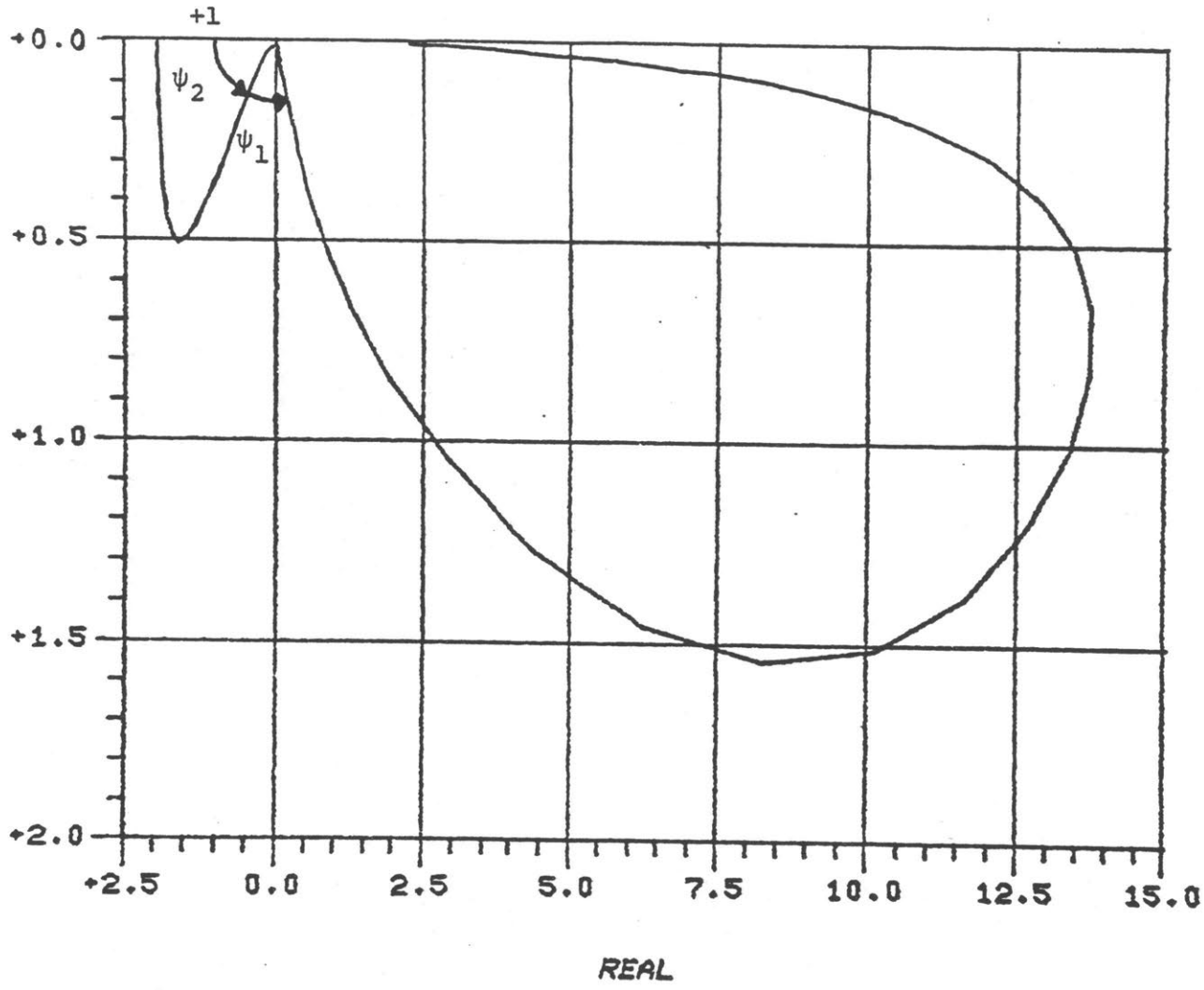

Figure 5.3: Nyquist Plot of $\sigma_1(s)k_{m_1}(s)$ and $\sigma_2(s)k_{m_2}(s)$

closed-loop poles of the controlled system yield the following set of poles:

$$\{-1,1896.10^{-2};\ -2,2552\pm j5,5152;\ -3,2463;\ -4,3457\pm j6,0094\}.$$

Therefore, the closed-loop system is stable as expected.

The singular values of $G(s)G_m(s)$ and $G_m(s)G(s)$ are represented in Fig. 5.4 and 5.5. These plots show that the robustness requirement has been satisfied with our compensation. Furthermore, they show that the singular values of $G_m(s)G(s)$ and $G(s)G_m(s)$ are almost identical. This was expected from the very nature of our design approach. This shows clearly that our method of design yields the same robustness conditioning at the plant input and output.

Thus the controller $G_m(s)$ appears to be satisfactory since it yields a stable closed loop system with the required robustness properties.

5.3.4 Discussion

The intermediate frequency compensator described above does not attempt to increase the loop gains for intermediate frequencies smaller than the crossover frequencies in order to improve the performance or the system. This would be needed in particular in channel 2 corresponding to the smallest singular value. However, we have seen that the approximations of U(s) by A and V(s) by B become poor for frequencies $\omega < \text{rd.s}^{-1}$. This means that the loop gains for frequencies

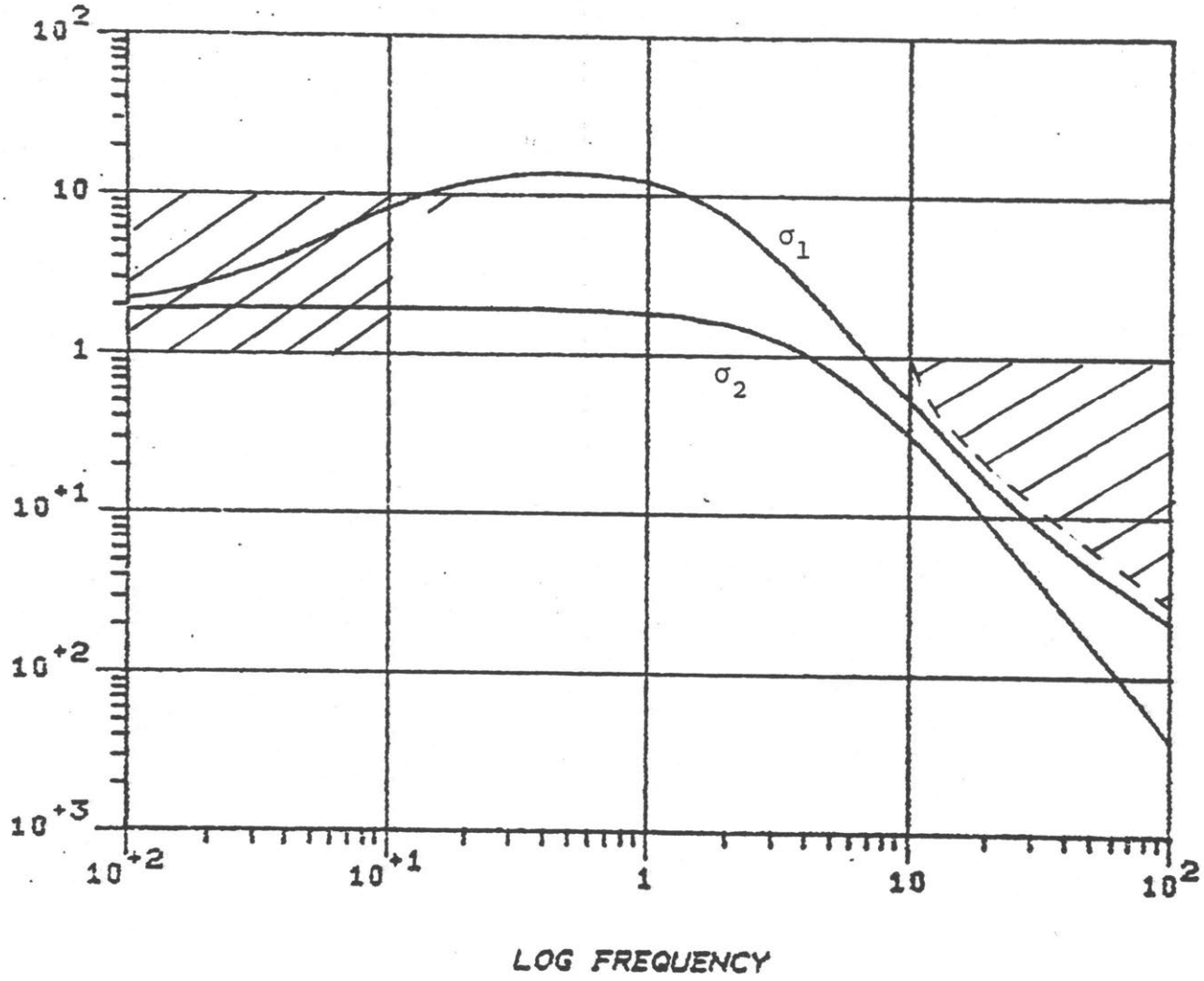

Figure 5.4: Singular Values of $G(s)G_m(s)$ with Robustness Requirement

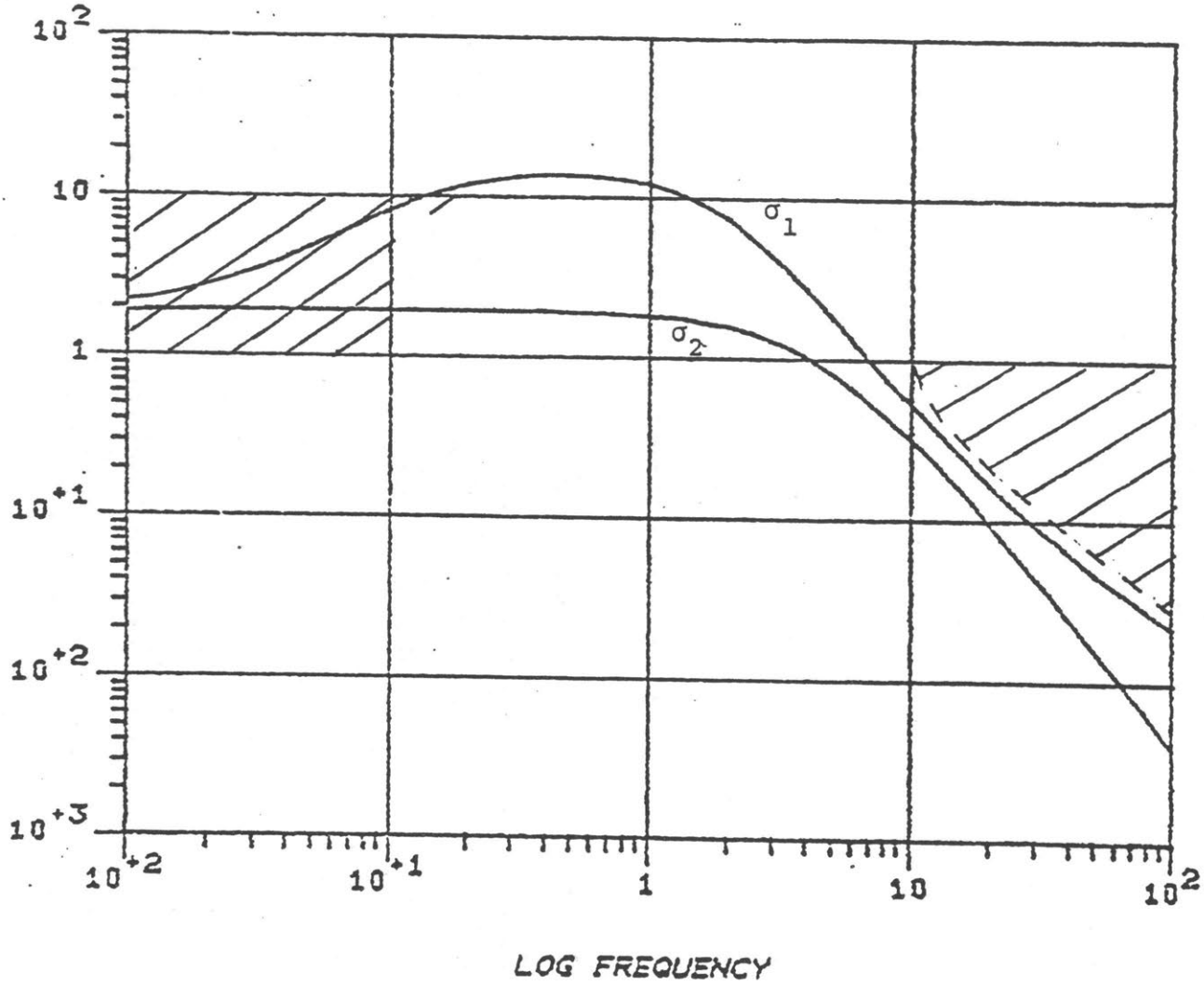

Figure 5.5: Singular Values of $G_m(s)G(s)$ with Robustness Requirement

$\omega < 5$ rd.s^{-1} cannot be modified in a predictable way. This problem turns out to be of little concern with our choice of controller $G_m(s)$ since $G_m(s)$ tends to a unitary matrix for the frequencies $\omega < 1$ rd.s^{-1}. Hence $G_m(s)$ does not affect the loop gains at low frequencies. Nevertheless, one could try to improve the performance of the system in the intermediate frequency range by increasing the loop gains in channel 1 and 2 provided that a low frequency compensator can still be used to adjust the loop gains at low frequency.

In particular, one could cascade a lag compensator $\alpha > 1$, $\dfrac{s + \frac{1}{T}}{s + \frac{1}{\alpha T}}$ to our controller $k_{m_2}(s)$ in channel 2, acting on a frequency range just below the crossover frequency. Such a compensator would increase the loop gain in the intermediate frequency range just below the crossover frequency. However this compensator would also provide a certain amount of phase delay in channel 2. This phase delay could dangerously impair the closed-loop stability by reducing excessively the angle ψ_2 represented in Fig. 5.3. This observation corresponds to the fact that as the slope of the singular values plot around crossover frequencies gets steeper and steeper, the closer we will be from unstability [1]. Thus, one cannot hope to obtain good performances in the intermediate frequency range without dangerously impairing closed-loop stability.

The actual computation of the principal phases associated to the largest and smallest singular values of $G(s)G_m(s)$ shows that the "true" values of ψ_1 and ψ_2 are given by

$$\psi_1 = 65° \quad \text{and} \quad \psi_2 = 32°$$

Thus a further reduction of ψ_2 will make the system close to unstability. We will therefore proceed to construct a low frequency compensator assuming an intermediate frequency controller $G_m(s)$ as previously designed.

5.4 Low Frequency Compensation

5.4.1 Introduction

The goal of the low frequency compensator is to insure good performance by increasing the loop gains in the low frequency range. As shown in Figure 5.1, we want the gains to be larger than 10 in both channel 1 and 2 for frequencies $\omega \leq 10^{-1}$ rd.s^{-1}. The intermediate frequency compensator does not satisfy this requirement as the loop gains tends to 2 for $\omega = 10^{-2}$ rd.s^{-1}. Following our design procedure, we will choose a controller $G_c(s)$ of the form:

$$G_c(s) = G_m(s) \left[I + \frac{G_\ell}{s} \right]$$

where G_ℓ is a constant gain matrix that acts on the transformed plant $G(s)G_m(s)$ at low frequencies. The procedure to be followed in order to choose G_ℓ is similar to the one that we used when choosing $G_m(s)$ with the only difference that G_ℓ is constant and controls the transformed plant $G(s)G_m(S)$.

5.4.2 Choice of the Low Frequency Controller

As we did in Section 5.3.2, we approximate the singular vector matrices $\tilde{U}(s)$ and $\tilde{V}(s)$ given by the singular value decomposition of $G(s)G_m(s)$, by real matrices $\tilde{A}$ and $\tilde{B}$ using the ALiGN algorithm. We found that the best results were obtained for the low frequency $\omega = 10^{-2}$ rd.s^{-1} for this value we have:

$$\tilde{U}^H(10^{-2}j) = \begin{bmatrix} -.67616+j.063639 & -.86305-j.039761 \\ .6587-j.55922 & -.44481+j.236 \end{bmatrix}$$

and

$$\tilde{V}^H(10^{-2}j) = \begin{bmatrix} -.43851+j.63545 & -.36097+j.52308 \\ .63554 & -.77207 \end{bmatrix},$$

and we found:

$$\tilde{A} \simeq \begin{bmatrix} -0.67 & 0.74 \\ 0.74 & 0.67 \end{bmatrix} \text{ and } \tilde{B} = \begin{bmatrix} -.81 & .58 \\ -.58 & -.81 \end{bmatrix}$$

where the sign ambiguity on the columns of $\tilde{A}$ and $\tilde{B}$ yielded by the ALiGN algorithm is removed by considering the sign of the entries of $\tilde{U}(10^{-2}j)$ and $\tilde{V}(10^{-2}j)$.

Similarly as in Section 5.3, we plot the successive values of the coefficients $\Phi_{\tilde{a}_i}$ and $\Phi_{\tilde{b}_i}$ for frequencies around $\omega = 10^{-2}$ rd.s^{-1}. These plots give us a measure of the quality of the approximations performed and are represented in Figures 5.6.a and 5.6.b. They show clearly that the quality of approximations at $\omega = 10^{-2}$ rd.s^{-1} is not as good as what we obtained while constructing $G_m(s)$. Moreover, these approximations seem to be valid only for a small frequency region around 10^{-2} rd.s^{-1} as the coefficients $\Phi_{\tilde{a}_i}$ and $\Phi_{\tilde{b}_i}$ decrease rapidly. We are faced here with a case where the rate of change of the singular vector directions is large enough for the approximation to hold only in a small frequency range. However, it turns out that the design of the low frequency controller is flexible enough to allow us to choose adequately the gain matrix G_ℓ by using our design approach.

As a result of the approximation step, the gain matrix G_ℓ will have the form:

$$G_\ell = \begin{bmatrix} -.81 & -.58 \\ .58 & -.81 \end{bmatrix} \begin{bmatrix} k_{\ell_1} & 0 \\ 0 & k_{\ell_2} \end{bmatrix} \begin{bmatrix} -.67 & .74 \\ .67 & .67 \end{bmatrix}$$

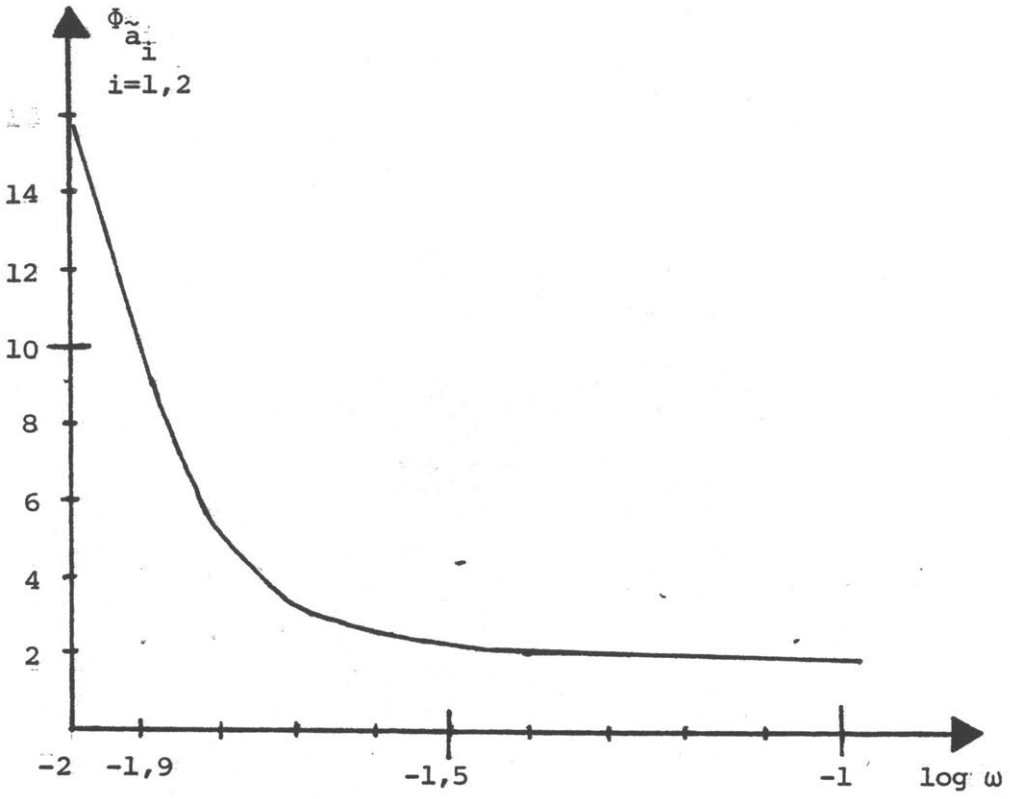

Figure 5.6.a: Misalignment Plot for $\tilde{A}$ at $\omega = 10^{-2}$ rd.s^{-1}

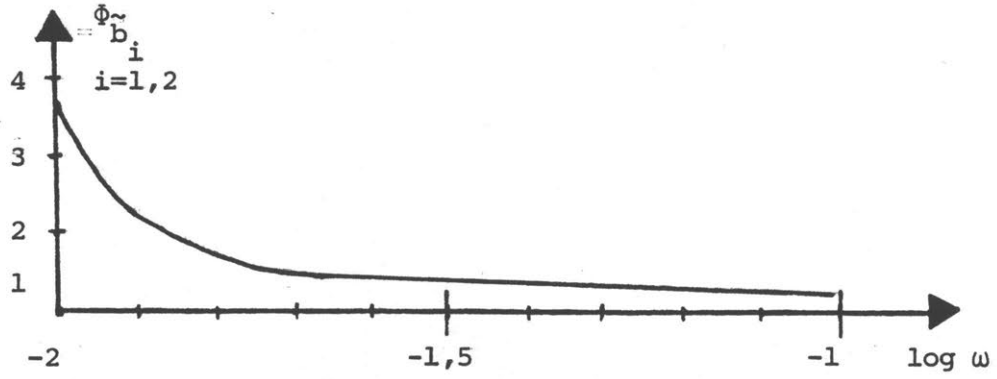

Figure 5.6.b: Misalignment Plot for $\tilde{B}$ at $\omega = 10^{-2}$ rd.s^{-1}

where k_{ℓ_1} and k_{ℓ_2} are suitable gains applied to integrators in channel 1 and 2. These gains must be chosen such that

(i) The closed-loop stability obtained by intermediate frequency compensation is preserved,

(ii) The loop gains satisfy the performance requirements at low frequencies.

The closed-loop stability will be preserved if the integrators acting in the low frequency range in both channel 1 and 2 do not change the number of encirclements of the point -1 in the Nyquist stability criterion. This reduces to choose the signs of k_{ℓ_1} and k_{ℓ_2}, that is, to determine whether we should apply negative or positive feedback in the low frequency range. Inspection of the Nyquist plots represented in Figure 5.3 suggests that a choice of $k_{\ell_1} > 0$ and $k_{\ell_2} < 0$ will not change the number of encirclements of the point -1 in both channel 1 and 2. We will therefore apply a negative feedback in channel 1 while in channel 2 a positive feedback will be used at low frequencies. At the same time, the performance requirements impose the loop gains to be greater or equal to 10 for $\omega \leq 10^{-1}$ rd.s^{-1}. As shown in Figures 5.4 and 5.5, the loop gain in channel 2 is equal to 2 for $\omega = 10^{-1}$ rd.s^{-1} and therefore need to be multiplied by at least 5. This suggests to choose $|k_{\ell_2}| = +.5$, that is:

$$k_{\ell_2} = -.5$$

Obviously, the gain to be applied in channel 1 does not need to be as large as in channel 2. However since the approximation performed in the low frequency range are not very accurate, the loop gains will be modified in an unpredictable way by G_ℓ. One way to avoid this difficulty is to choose G_ℓ to be a scaled identity matrix times a unitary matrix. Since a scaled identity commutes with every matrix, the scalar coefficient will allow us to predict almost exactly how the loop gains are modified. This leads us to choose k_{ℓ_1} to have the same absolute value than k_{ℓ_2}, that is:

$$k_{\ell_1} = .5.$$

Then the loop gains in both channel 1 and 2 will be multiplied by 5 at $\omega = 10^{-1}$ rd.s^{-1} almost exactly and this fully justifies our choice for k_{ℓ_2}. On the other hand, we can expect that the loop gains will be augmented more than necessary in channel 1 at low frequencies.

More generally, for frequencies where the approximation algorithm ALiGN does not yield very good results, we can always choose a compensator to be of the form of a product of a unitary matrix by a scaled identity in order to predict almost exactly how the loop gains will be modified. This alternative procedure can prove to be very useful particularly when selecting the low frequency and high freqeuncy controllers of our design procedure.

5.5 Final Design Results and Concluding Remarks

As a result of our low frequency compensation, our final controller will have the form:

$$G_c(s) = \begin{bmatrix} 0 & 1 \\ -1 & 0 \end{bmatrix} x \begin{bmatrix} .25\,\frac{s+25}{s+6.25} & 0 \\ 0 & -2\,\frac{s+3}{s+6} \end{bmatrix} x \begin{bmatrix} 1 & 0 \\ 0 & -1 \end{bmatrix} x$$

$$\left[I + \frac{1}{s} \begin{bmatrix} -.81 & -.58 \\ .58 & -.81 \end{bmatrix} x \begin{bmatrix} .5 & 0 \\ 0 & -.5 \end{bmatrix} \begin{bmatrix} -.67 & .74 \\ .74 & .67 \end{bmatrix} \right].$$

The closed-loop system will have then the set of poles:

$\{-1.795.10^{-2}; -2.914; -5.0826.10^{-1} \pm j1.9361.10^{-1}; -2.173 \pm j5.3848; -4.0787 \pm j6.1934\}$.

Thus, the closed loop system remains stable after low frequency compensation. Comparison of the set of poles after and before low frequency compensation shows that the low frequency compensator has the effect of introducing a pair of complex conjugate poles $\{-5.0826.10^{-1} \pm j1.9361.10^{-1}\}$ while slightly shifting the other poles. This illustrates

the frequency decoupling between the low and intermediate frequencies compensators. Furthermore, the computation of the principal phases associated to the largest and smallest singular values of $G(s)G_m(s)$ shows that the values of the phase angle ψ_1 and ψ_2 at the crossover frequencies are reduced respectively from 65° to 59° and from 32° to 29°. This means that the low frequency compensator does not impair the closed loop stability obtained by the intermediate frequency compensator.

We represented in Figures 5.7 and 5.8 respectively the singular values of $G(s)G_c(s)$ and $G_c(s)G(s)$. These plots show that the robustness requirement is still satisfied without affecting the bandwidth after the low frequency compensation. Moreover, the singular values are now greater than 10 for frequencies $\omega \leq 10^{-1}$ rd.s^{-1}, so that our performance requirement is satisfied. Thus the compensator $G_c(s)$ meets all the design requirements.

Thus we have been able to devise an adequate and simple compensator $G_c(s)$ by using our basic design procedure. At each step of the procedure controllers have been selected in a systematic way. However, since the choice of the controllers for the low frequency range as well as the high frequency range seems to be very flexible even in the case where the results of the approximation algorithm are not very good, the success of our design procedure seems to depend on the quality of the approximation performed in the intermediate frequency range. This suggests that our design approach will be successful for systems such that

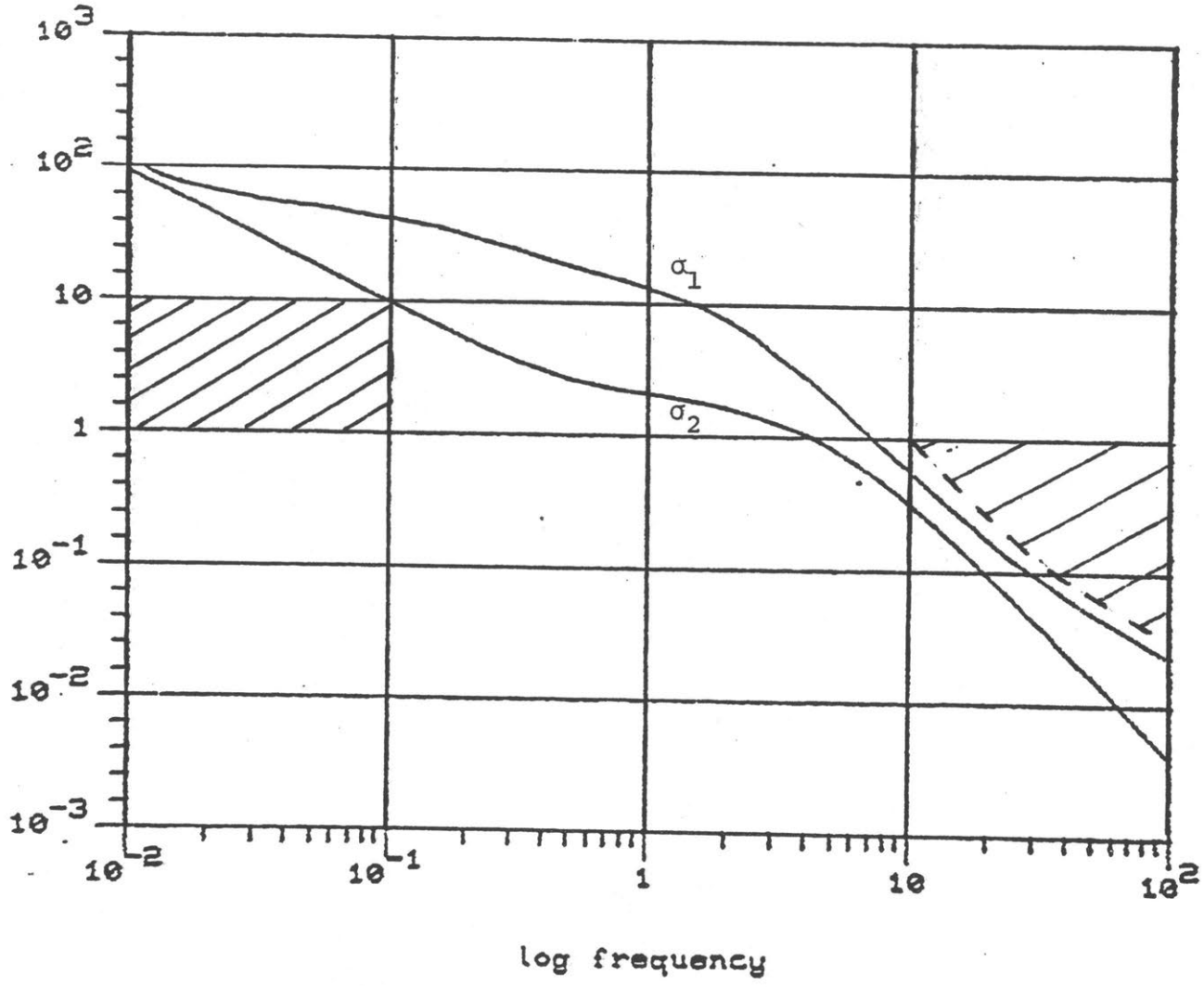

Figure 5.7: Singular Values of $G(s)G_c(s)$

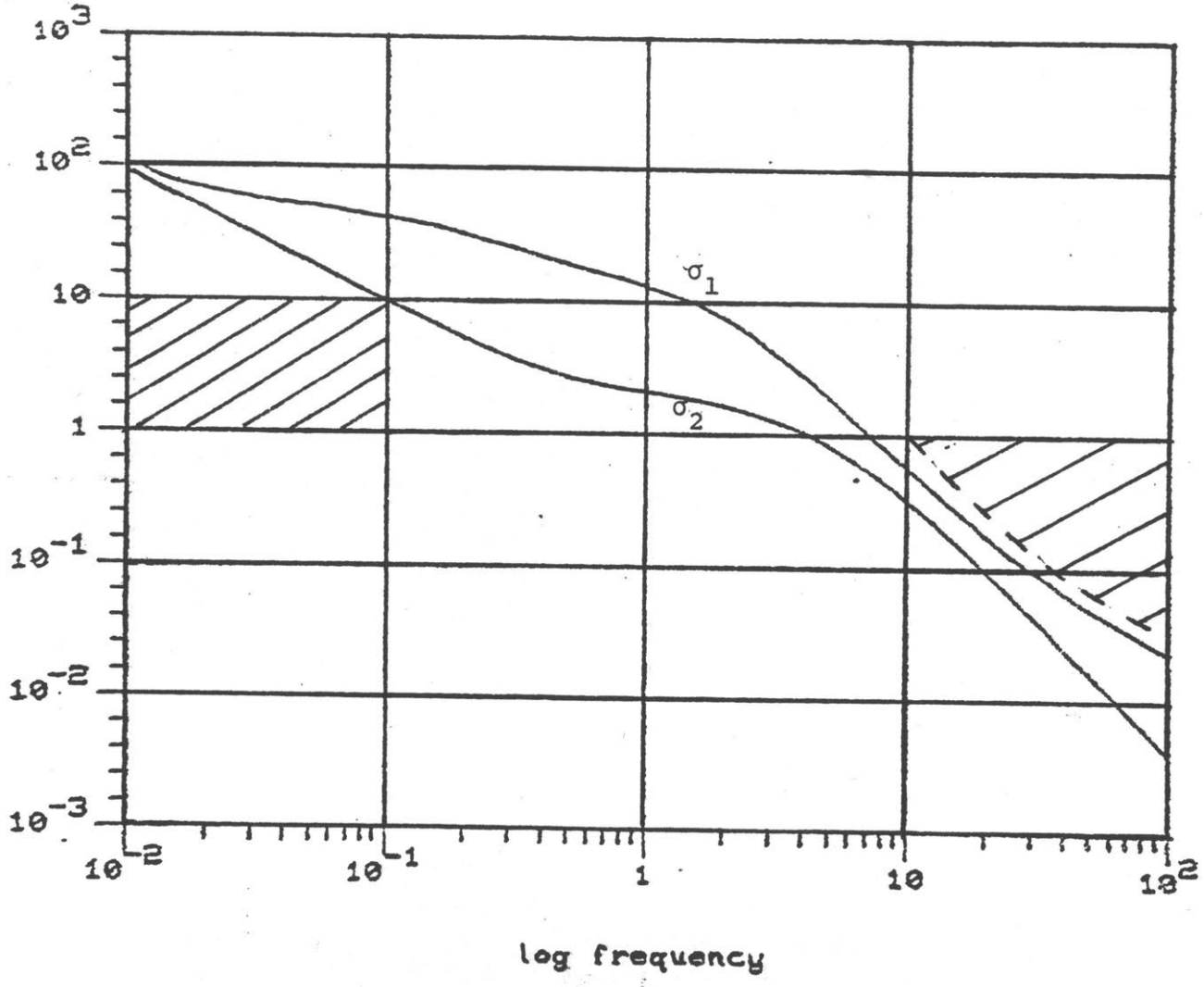

Figure 5.8: Singular Values of $G_c(s)G(s)$

the singular vectors can be approximated accurately around the cross-over frequencies by using the ALiGN algorithm. This was the case in the example considered and this explains primarily why our design procedure proved to be successful.

On the other hand, the final results of our design shows that we were not able to achieve a very large bandwidth for tight loop controls. This translates the fact that one cannot achieve too tight loop controls without damaging dangerously the stability of the system. Hence, the frequency transitions between low frequencies and intermediate frequencies are limited and cannot be too large.

CHAPTER 6: SUMMARY, CONCLUSIONS AND SUGGESTIONS FOR FUTURE RESEARCH

6.1 Summary

We have examined in this thesis the problem of designing multivariable feedback loops by shaping singular values. The importance of singular values in control systems design stems from the robustness issue since robustness criteria can be defined in terms of singular values. Moreover, since the largest singular value of a matrix corresponds to a matrix norm, it also allows to express the high loop gain usually required for performance in terms of singular values. Thus, as shown in Chapter 2, a typical design problem is to find a controller such that:

(i) The nominal closed-loop system is stable

(ii) The singular values of the open-loop transfer function are small enough at high frequencies to satisfy the robustness requirement (2.15).

(iii) The singular values of the open-loop transfer function are sufficiently large at low frequencies to satisfy the performance requirement (2.13).

In other words, the multivariable feedback design method that we use should guarantee the nominal closed-loop stability and should shape the singular values of the open-loop transfer function. This constitutes the approach to MIMO feedback design taken in this thesis. With this point of view, we have concentrated our analysis on several existing design methods and derived some new ones.

In Chapter 3, we have investigated diagonalization design methods in the frequency domain. Two diagonalization (exact or approximate) methods, i.e. the CL and INA methods of design were analysed. Even though these methods offer the simplifying feature of reducing the MIMO design problem to a sequence of SISO design problems, we found that they do not preserve the stability against a sufficiently large class of errors. This stems from the fact that the transformation matrices that diagonalize (exactly or approximately) the plant are not unitary matrices. This motivated a new diagonalization approach where by considering the SVD of the plant, we were able to choose unitary transformation matrices. This led to a control system structure (Fig. 3.2) allowing us to shape exactly the singular values and to meet the performance and robustness requirements in a loop by loop fashion. Moreover, further analysis of the SVD of the plant (Theorems 3.1 and 3.2) allowed us to derive (Theorem 3.3) a Nyquist stability criterion for the control system structure. The design requirements could then be satisfied by an adequate choice of a diagonal compensator reducing the MIMO design problem to SISO problems. However, the transformation matrices of this compensation structure do not generally correspond to finite dimensional LTI systems. We were thus confronted with the problem of implementing these transformation matrices. This reduces to an approximation problem requiring to approximate the transformation matrices by finite-dimensional LTI systems. A trivial approximation procedure, the ALIGN algorithm, approximating the frequency dependent matrices by constant real matrices led to the

development of a simple design procedure (Section 3.4). This design procedure is systematic and yields some simple compensators which are adequate to meet the design requirements. However, the simplicity of the ALIGN algorithm imposes some restrictions on the applicability of the design procedure. We then examined the approximation problem in its full generality. Some desirable features of the approximation algorithm were described and we found that, to our knowledge, no approximation procedure presently availabe was satisfactory since existing methods do not provide a closed-form solution with respect to the L_∞ norm. Adopting a pragmatic point of view, we then proposed an approximation procedure which consists of an interpolation step (the Nevanlinna algorithm) followed by an optional model order reduction step. This solves the problem of implementing the transformation matrices once the design has been performed.

Design methods based on a time-domain description of linear systems are considered in Chapter 4. Since the key element of these methods is the LQ methodology we turned first our attention to this method. Since the LQ methodology allows us to obtain automatically a nominally stable closed-loop system, we investigated its ability to shape the singular values. The asymptotic properties of the loop transfer function at high frequencies as the control weighting matrix $R = \rho I$ tends to zero were used to obtain some insight on the robustness constraint for the control system. The Lemma 4.1 shows also how the high loop gain requirement can be satisfied. These results help the designer to choose

the weighting matrices. However, the shaping of singular values when one use the LQ methodology is constrained by the lack of dynamics in the feedback loop since we must have a $\frac{1}{\omega}$ attenuation rate of the singular values at high frequency. This is remedied by considering the systematic LQ dynamic compensation introduced by Gupta in [12]. Special choices of the weighting matrices, $R = \rho I$ and a frequency dependent state weighting matrix yield a nominally stable closed-loop system where some dynamics have been introduced in the feedback loop. With two particular choices of the state weighting matrix we investigated the effect of this method on singular values. The asymptotic high frequency behavior of the structure as ρ tends to zero shows that the attenuation rate restriction of the LQ methodology can be avoided. Furthermore, the singular values can be shaped very easily by a shaping filter affecting each state of the system. A simple choice of this shaping filter allows the design requirements to be satisfied. Thus the LQ dynamic compensation approach improves the singular values shaping properties of the LQ methodology.

The Chapter 5 provides an application example of the design procedure developed in Section 3.4. We follow the succesive steps of our design procedure. It is shown that the success of our design procedure depends merely on the quality of the approximations performed in the region of the crossover frequencies. The high frequency and low frequency compensation are much more flexible with respect to the quality of approximations. The results of Chapter 5 prove the applicability of our basic design procedure.

6.2 Conclusions and Suggestions for Future Research

By using a physically based design perspective we have been able to evaluate in a common framework several existing design methodologies. The results of this study shows that:

(i) The existing diagonalization methods (CL and INA) do not apply to the most general cases. More precisely, they only yield good results for normal or approximately normal systems.

(ii) The LQ methodology is constrained by the lack of dynamic compensation in the feedback loop.

These results have already appeared in the literature and they have been used here to motivate the need for the introduction of new multivariable feedback design methods. These constitute the major contribution of this thesis and are basically of two kinds. The first contribution concerns the development of a new frequency domain based design method using a diagonalization approach. This was achieved by considering the SVD of the plant to be controlled and results include:

(i) A special controller structure allowing us to meet the performance and robustness requirements using the properties of the singular values.

(ii) A Nyquist stability criterion for the closed-loop system.

(iii) Approximation algorithms for the actual implementation of the controller.

The main interest of this design method besides that it could be useful to solve some design problems is that it proves that there

exists a diagonalization method that takes into account the robustness constraint. Furthermore, the strength of our design approach with respect to robustness is demonstrated in that it allows to build a control system which is robust both at the plant input and at the plant output. However, it is clear that the implementation issue of our controller introduces some complexities in the design approach. In some cases, our design procedure with its associated trivial approximation algorithm will be successful, but unless new and simple closed-form solution techniques for the approximation problem are found, the computational aspects of approximations may be too cumbersome for the design approach to be simple.

The second contribution deals mainly with the improvement of the singular values shaping properties of the LQ methodology. This is achieved by introducing some dynamics in the feedback loop by using the approach introduced by Gupta [12]. Special choices of weighting matrices show that the singular values can be shaped very easily and that this design approach is very simple. However, due to the possible need of a Kalman filter in the feedback loop, our LQ dynamic compensator may have a high order. This aspect may be a justification for using a frequency-domain based design technique. Furthermore, although the LQ dynamic compensation approach allows us to satify robustness constraints at the plant input, it is not clear how robustness constraints can be satisfied at the plant output. One of the problems arising from the state augmentation procedure is that robustness recovery methods will recover

the loop robustness only at the output of the augemented system which does not correspond to the physical output of the plant. This may constitute a major weakness of the LQ dynamic compensation approach.

The multivariable feedback methods described in this thesis suggest several directions of further research. The most useful direction of research would be to derive a diagonalization method avoiding the complexities introduced by approximations. Indeed, as Mac Farlane and Al for the CL design, we have derived in this thesis an exact diagonalization method of design using the SVD properties of the plant. But, as Rosenbrock showed in the INA method of design, exact diagonalization may be too restrictive and moreover, introduces implementation problems. The approximation problem would be avoided if we could find some rational unitary matrices $\hat{U}(s)$, $\hat{V}(s)$ for any plant $G(s)$ such that:

$$G'(s) = \hat{U}(s)\, G(s)\, \hat{V}(s) \text{ is diagonal dominant, } \forall\, s \in D_R \,.$$

Then, the diagonal elements of $G'(s)$ will represent approximations of the singular values of $G(s)$ with bounds specified by the off-diagonal elements of $G'(s)$. We would then be able to meet the design requirements with a method similar to the INA method. Therefore, the problem lies in how to find in a systematic way $\hat{U}(s)$ and $\hat{V}(s)$ for a given plant $G(s)$. More precisely, this requires the characterization of efficient algorithms to find $\hat{U}(s)$ and $\hat{V}(s)$.

However, the major limitation of this thesis is associated with the representation of uncertainties in section 2.2. A single magnitude

bound on matrix perturbations is a worst-case representation which is often too conservative. The problem of representing more structured uncertainties would require the notion of directionality of the perturbations, thus introducing principal phases in robustness tests. Methods of design taking into account these less conservative robustness tests represent in the author's opinion an interesting direction of research. This may be achieved by a diagonalization approach for the system which would allow the principal phases as well as the singular values of the plant to be modified in a simple manner.

APPENDIX: Proof of Theorem 3.2

For all s and z, the characteristic equation $\Delta_2(\Sigma, s, z) = 0$ can be written as

$$\Sigma^n + a_1(s,z)\,\Sigma^{n-1} + \ldots + a_n(s,z) = 0 \quad .$$

Each coefficient $a_i(s,z)$ is a rational function of s and z. Also since,

$$\Delta_2(\Sigma, s, z) = \det [\Sigma I - G^T(z)\, G(s)] = \det [\Sigma I - G^T(s)\, G(z)]$$

$$= \Delta_2(\Sigma, z, s)$$

the coefficients $a_i(s,z)$ are symmetric rational function of s and z. Since

$$a_i(s,z) = (-1)^i \; (\Sigma \text{ principal minors of order i of } G^T(z)\, G(s))$$

$a_i(s,z)$ is a sum of products of rational functions in s by rational functions in z and can be expressed as

$$a_i(s,z) = \frac{\sum_{j=1}^{p} P_{ij}(s)\, P_{ij}(z)}{P_o(s)\, P_o(z)} \qquad i=1,\ldots n$$

where $P_{ij}(\cdot)$ $j = 1,\ldots,p$, $i = 1,\ldots,n$, and $P_o(\cdot)$ are polynomials. Each product $P_{ij}(s)\, p_{ij}(z)$ can be decomposed as:

$$P_{ij}(s)\, P_{ij}(z) = \Pi[s+\alpha]\; [z+\alpha]\; \Pi[(s+\beta)^2 + \delta^2]\; [(z+\beta)^2 + \delta^2]$$

But $(s+\alpha)(z+\alpha) = sz + \alpha(s+z) + \alpha^2$ is a function of sz and s+z, and

$$[(s+\beta)^2 + \delta^2][(z+\beta)^2 + \delta^2] = [(s+\beta)(z+\beta)]^2 + \delta^4 + \delta^2[(s+\beta)^2 + (z+\beta)^2]$$

$$= [sz + \beta(s+z) + \beta^2]^2 + \delta^4 + \delta^2[2\beta^2 + 2\beta(s+z) + (s+z)^2 - 2sz]$$

and is a function of sz, s+z.

Therefore $a_i(s,z)$ can be viewed as a function of sz and s+z denoted by $a_i(s,z) = f_i(sz, s+z)$ $i=1,\ldots,n$.

The characteristic equation $\Delta_2(\Sigma, z, s) = 0$ can be written as

$$\Sigma^n + f_1(sz, s+z)\,\Sigma^{n-1} + \ldots + f_n(sz, s+z) = 0$$

The algebraic function $\Sigma(s,z)$ can be viewed as a function $\Sigma(sz, s+z)$ depending uniquely on the two variables sz, s+z. Therefore the branches $\Sigma_i(s,z)$ can be viewed as function of sz and s+z, i.e,

$$\Sigma_i(s,z) = f'_i(sz, s+z) \quad i=1,\ldots,n.$$

Thus, we have

$$\sigma_i^2(s) = \Sigma_i(s,z)\Big|_{z=\bar{s}}$$

$$= f'_i(s\bar{s}, s+\bar{s})$$

$$= \Sigma_i(\bar{s},z)\Big|_{z=s}$$

$$= \sigma_i^2(s)$$

Therefore $\sigma_i(s) = \sigma_i(\bar{s})$ for all s and $i = 1,\ldots,n$.

Q.E.D.

REFERENCES;

1. J.J. Doyle and G. Stein: "Multivariable Feedback Design: Concepts for a Classical/Modern Synthesis", IEEE Trans. Auto. Control. Vol. AC 26, No. 1, February 1981.

2. G. Stein and J.J. Doyle: "Singular Values and Feedback: Design Examples", L.I.D.S - R.954 Massachusetts Institute of Technology.

3. N.A. Lehtomaki: Practical Robustness Measures in Multivariable Control System Analysis, L.I.D.S. Thesis - 1093, Massachusetts Institute of Technology.

4. J.J. D'Azzo and Houpis: Linear Control System Analysis and Design: Conventional and Modern, McGraw Hill, New York, 1975.

5. D.H. Owens: "Feedback and Multivariable Systems", IEEE Control Engineering, Series 7.

6. A.G.H. MacFarlane and B. Kouvaritakis: "A Design Technique for Linear Multivariable Feedback Systems", Int. Journ. Control, Vol. 23, No. 6, June 1977, pp. 837-874.

7. A.G.J. MacFarlane and I. Postlethwaite: A Complex Variable Approach to the Analysis of Linear Multivariable Feedback Systems. Springer-Verlag, New York, 1979.

8. H.H. Rosenbrock: Computer Aided Control System Design, Academic Press, 1974.

9. H. Kwakernaak and R. Sivan: Linear Optimal Control Systems, Wiley-Interscience.

10. B.D.O. Anderson and B.C. Moore: Linear Optimal Control, Englewood Cliffs, N.J., Prentice-Hall, 1971.

11. C.A. Harvey and G. Stein: "Quadratic Weights for Asymptotic Regulator Problems", IEE. Trans. Auto. Control, Vol. AC 23, No. 3, pp. 378-387, June 1978.

12. K. Gupta: "Frequency shaped Costs Functionals: An Extension of LQG Design Methods", Systems Control, Inc. (Vt).

13. G. Stein and N.R. Sandell, Jr.: Classical and Modern Methods for Control System Design, Notes of course 6.232 offered in the spring of 1982, Dept. of Electrical Engineering and Comptuer Science, M.I.T., Cambridge, MA.

14. J.G. Doyle and G. Stein: "Robustness with Observers", IEEE. Trans. Automatic Control, Vol. AC-24, Aug. 1979.

15. H. Kwakernaak: "Optimal Low-Sensitivity Linear Feedback Systems", Automatica, Vol. 5, May 1969.

16. J.H. Wilkinson: The Algebraic Eigenvalue Problem, Clarendon Press, 1965.

17. A.J. Laub: "Robust Stability of Linear Systems-Some Computational Considerations", L.I.D.S. - R-904, Massachusetts Institute of Technology.

18. D.C. Youla: "On the Factorisation of Rational Matrices", IRE Trans. Information Theory, Vol. IT-7, pp. 172-189, July 1981.

19. M.C. Davis: "Factoring the Spectral Matrix", IEEE Trans. Automatic Control, Vol. 8, pp. 296-305, Oct. 1963.

20. C.A. Desoer and Y.T. Wang: "On the Generalized Nyquist Stability Criterion", IEEE Trans. Automatic Control, Vol. AC-25, No. 2, April 1980.

21. G.A. Bliss: Algebraic Functions, 1966, reprint of 1933 original (New York: Dover).

22. R. Hartshorne: Algebraic Geometry, New York: Springer-Verlag, 1977.

23. B.A. Francis: "On Robustness of the Stability of Feedback Systems" IEEE Trans. Automatic Control, Vol. AC-25, No. 4, August 1980.

24. L.M. Silverman and M. Bettayeb: "Optimal Approximation of Linear Systems:, Proc. 1980 JACC, San Francisco, CA.

25. S. Kung, "Optimal Hankel-Norm Model Reduction-Scalar Systems", Proc. 1980 JACC, San Francisco, CA.

26. Ph. Delsarte, Y. Genin and Y. Kamp: "The Nevanlinna-Pick Problem for Matrix-Valued Functions", SIAM J. Appl. Mathematics, Vol. 36, No. 1, February 1979.

27. S. Kung and D.W. Lin: "Optimal Hankel-Norm Model Reduction: Multi-variable Systems", IEEE Trans. Automatic Control, Vol. AC-26, No. 4, August 1981.

28. E.A. Jonckheere, M.G. Safonov, and L.M. Silverman: "Topology Induced by the Hankel-Norm in the Space of Transfer Matrices", Proc. IEEE Conference on Decision and Control, San Diego, December 1980.

29. M. Shahjahan: "Loop Shaping Methods for LQ Regulators", Ph.D. Thesis Proposal, M.I.T., Department of Electrical Engineering and Computer Science, June 1982.